UNIVERSITÀ DEGLI STUDI DI PAVIA

Dipartimento di Medicina Molecolare

“Proteomic approaches to define the protein profiles of salivary glands and ovary of the tick *Ixodes ricinus* and to investigate the relationship with its intracellular symbiont *Midichloria mitochondrii*”

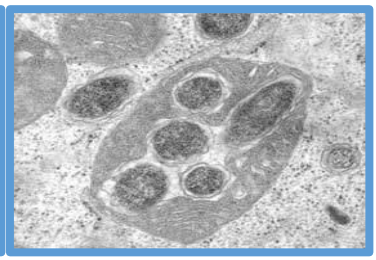

Monica Di Venere

Supervisor: Anna Bardoni

PhD in Biomolecular Sciences
XXX cycle
A.Y. 2016/2017

INTRODUCTION

MATERIALS AND METHODS

“Quanto manca alla vetta?

-Tu sali e non pensarci!”

F. Nietzsche

Introduction

1. Ticks

Ticks are obligate hematophagous arthropods that parasitize every class of vertebrates (1) and vector-borne diseases are among the leading causes of sanitary concern worldwide, being responsible for millions of deaths every year (2). Although most vectors (such as mosquitoes) mainly exert their toll on developing countries, ticks are also widespread in the Northern hemisphere and are indeed considered the most important vectors in Europe and Nord America (3). The major tick families are three: i) the Ixodidae (C.L. Koch, 1844), also called "hard ticks" because of their sclerotized dorsal plate, are the most important family in numerical terms and in medical importance, ii) the Argasidae, called "soft ticks" because of their flexible cuticle (1) and iii) the Nuttalliellidae which differ from others for a combination of characteristics including the position of the stigmata, strongly corrugated integument and form of the fenestrated plates (4). According to the most commonly used classification (5), the family Ixodidae consists of two major groups, the Prostriata and the Metastriata (Fig.1). Ticks are currently grouped with members of the subclass Acari, which is the largest subclass in the class Arachnida of the suborder Ixodida within the order Parasitiforms.

Ticks have been recognized as human parasites for thousand years and were described by ancient Greek writers, including Homer and Aristotle (1). While having been studied for a long time, the first demonstration that ticks may transmit infectious diseases were made at the end of 19th century (3). Lyme disease, caused by Borrelia burgdorferi (6), was described in 1975 and is currently one of the most important vector borne disease in Europe and the United States. Ticks may also act as reservoirs of tick-transmitted bacteria. In these cases, bacteria are transmitted trans-stadially (from stage to stage) and/or trans-ovarially (from one generation to the next one). Given that each tick species requires optimal environmental conditions, this determines their geographic distribution and the risk areas of tick borne diseases.

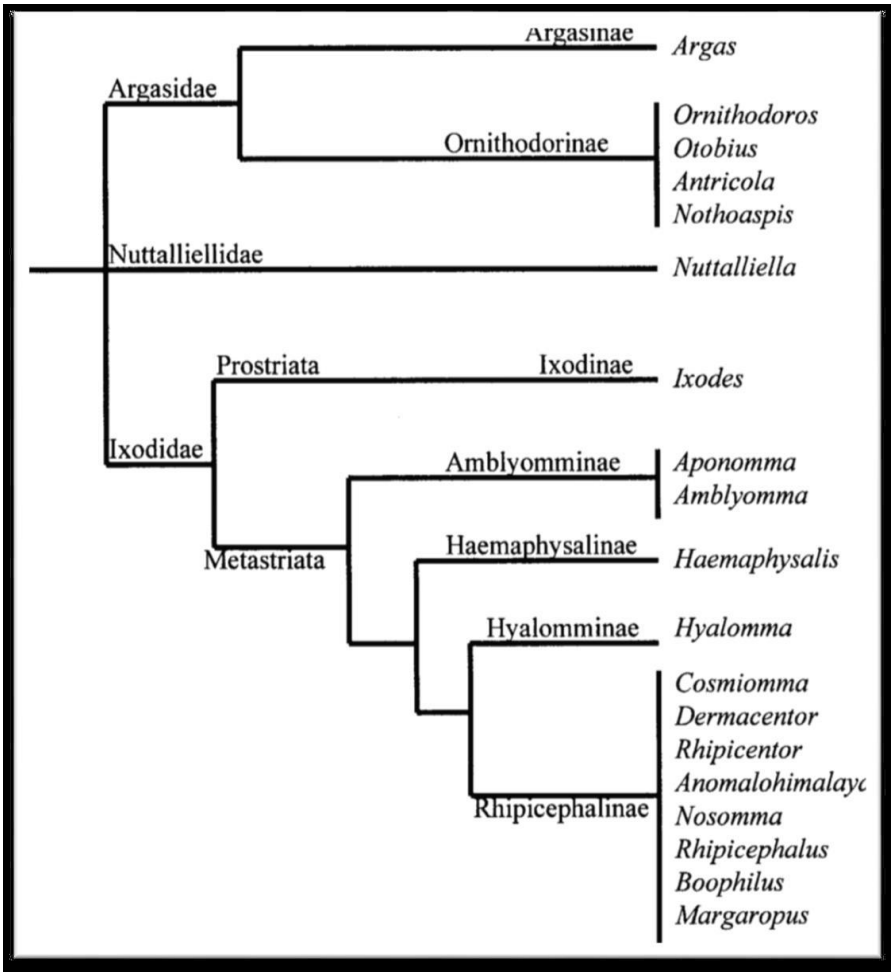

Figure 1. Hoogstraal classification

2. Ixodes ricinus

Approximately 900 tick species have been described (7), nearly 10% of which have an impact on human and animal health (8). The Ixodidae are capable of transmitting numerous viral, bacterial and protozoan pathogens through the blood meal. Hard ticks, in particular, are dangerous vectors and, among them, the sheep tick Ixodes ricinus (Fig. 2) is one of the most relevant species. It has an XX: XY sex determination system (9).

Figure 2. *Ixodes ricinus*

The importance of Ixodes ricinus is due to its wide area distribution (i.e. Europe and Northern Africa), to its low host specificity and capacity to parasitize humans and to its central role in the transmission of multiple infectious agents (10). Borrelia spp, the causative agent of Lyme disease, is possibly the most important microorganism vectored by I. ricinus. This bacterium is responsible for hundreds of thousands of novel infections each year and its role in multiple chronic pathogenesis is currently being investigated (11). Requiring a relative humidity of at least 80%, I. ricinus is sensitive to climatic conditions, and is restricted to areas of moderate to high rainfall. While being primarily observed in deciduous woodland and mixed forest, it can be found in a range of habitats that support its blood hosts and a moist microclimate. The prevalence of ticks is on the rise throughout Europe due to environmental changes including climate (12), forestry and wildlife management (e.g. increasing deer population) (13). Nowadays, I. ricinus is found at higher latitudes and altitudes than just a few decades ago (14) and it is also increasingly found in urban parks, recreational areas, private garden and cemeteries (15). Therefore, I. ricinus represents a considerable hazard not only for specific

risk groups such as foresters, agricultural workers and livestock, but also for the general population and companion animals (16). Moreover, I. ricinus is capable of transmitting numerous other bacteria, such as Rickettsia spp. and Ehrlichia spp., but also the flavivirus responsible for Tick Borne Encephalitis and the etiological protozoan agents of babesiosis (17). In addition to the before mentioned pathogens, I. ricinus harbours a recently described bacterium named Midichloria mitochondrii (18), although the biological role of this new endosymbiont is not understood yet.

2.1 Anatomy of *I. ricinus*

Ticks are large-body-size (2-30 mm) acarines. Adults and nymphs have four pairs of walking legs, and larvae have three. All stages have no antennae and, unlike insects, their bodies are not divided into a distinct head, thorax, and abdomen (19). The anterior part of the body, the capitulum, bears the mouthparts, including sensory organs, cutting organs, and a median immobile organ (the hypostome) with numerous recurved teeth that anchor the tick to the host skin. The ixodides are characterized by the presence of a sclerotized plate, the scutum, on the dorsal surface of the body, and the remainder of the body is able to expand during feeding (Fig. 3). Ticks possess a circulatory system and a circulating fluid, the haemolymph, wets all organs and tissues. Ticks have a variety of peripheral sensory organs which include hair-like structures on the body, legs, mouthparts and a sensory complex located on the dorsal surface of the tarsus of leg I that contains a cluster of olfactory and gustatory receptors, the Haller's organs. These sensory organs are evidently important in enabling ticks to locate their hosts and to communicate with other ticks.

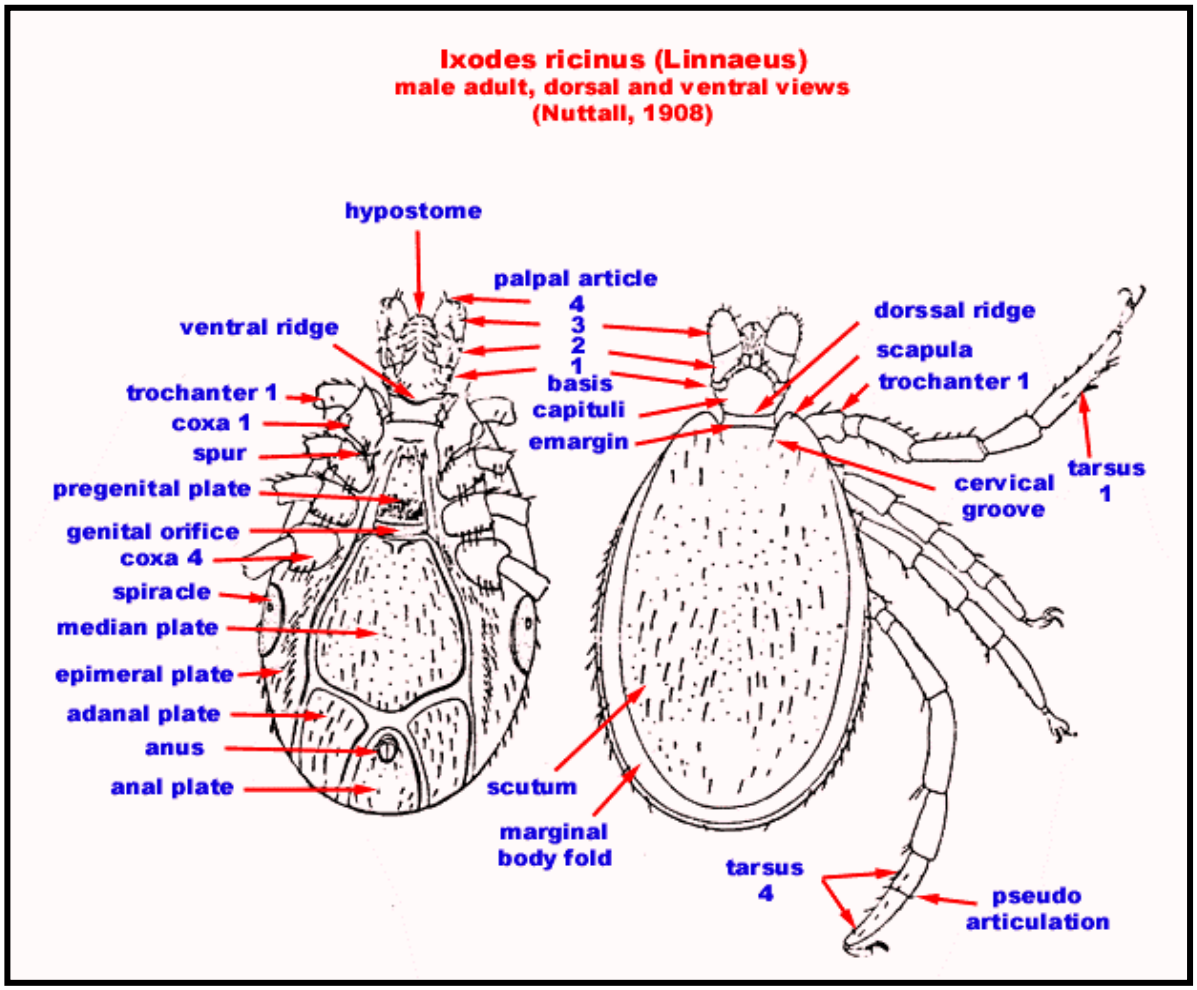

Figure 3. Anatomy of *I. ricinus*

2.2 Life cycle and feeding

The lifecycle of the tick includes three instars: larva, nymph and adults, which all require a blood meal from a vertebrate host before progressing to the next instar or laying eggs. The blood host of larvae are typically small rodents, for nymphs, medium sized mammals and birds, while the adult female feed of larger ungulates (20-23). One replete, the tick detaches and, after dropping from the host, finds a resting place where digests blood meal and molts to the next feeding stage, or enter in diapause, a state characterized by reduced metabolism and delayed development (Fig. 4).

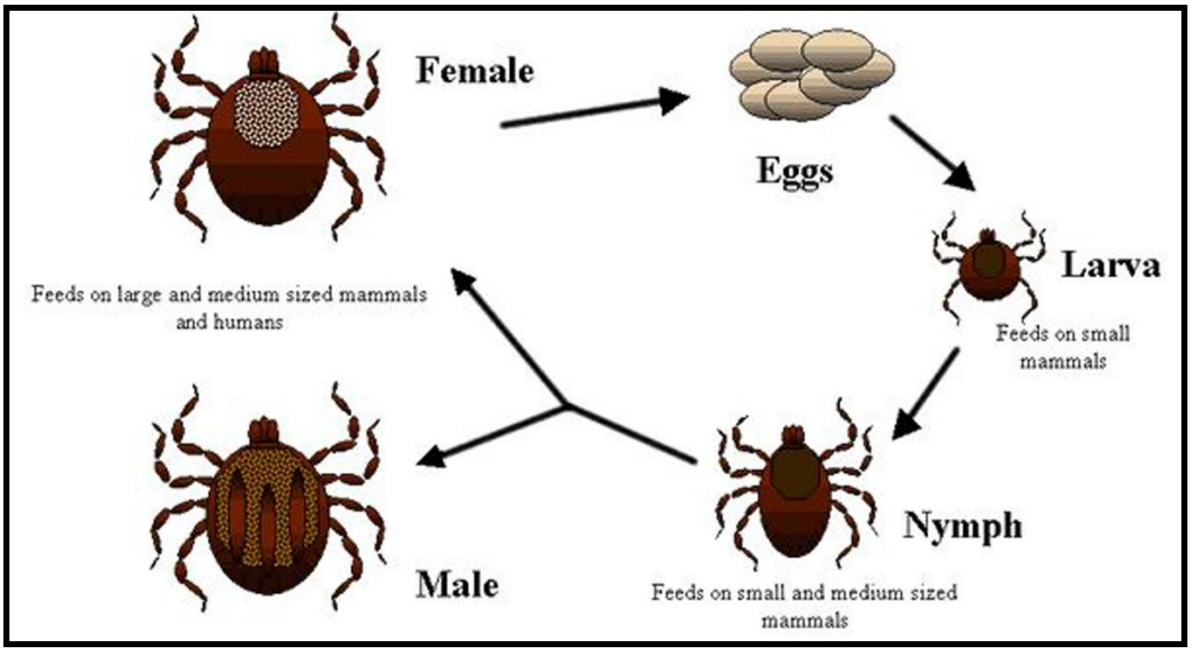

Figure 4. Schematic view of the life's cycle of *I. ricinus*

Mating generally occurs on the host; thereafter the females detach and drop off the host to digest their blood meal. They then lay their eggs (from 400 to > 20,000 depending on the species), in a sheltered environment and die (24). The life cycle of ixodid ticks is usually completed in 2-3 years, although it may take 6 months to 6 years, depending on environmental conditions, including temperature, relative humidity, and photoperiod. There is no or little ingestion of blood during the first 24-36 hours of attachment and penetration and attachment are the predominant activities. The salivary secretions produced by ixodid ticks include a cement to anchor the mouthparts to the skin of the host; enzymes; vasodilators; anti-inflammatory, antihemostatic and immunosuppressive substances. These facilitate successful blood feeding and an anaesthetic present in the saliva makes the bite of ixodid ticks usually painless. Ixodid ticks feed for extended period, and 2-15 days are required for a complete blood meal to be ingested, depending on the feeding stage, species of tick, type of host, and site of attachment. An initial slow feeding period (3-4 days) is followed by a period of a rapid engorgement (1-3 days) when ticks, particularly females, may increase their body weight up to 120-fold.

3. Diseases caused by *Ixodes ricinus* bite

The characteristics of the tick bite such as absence of pain, rarity of immediate symptoms and misinformation in the population, make estimating the actual health impact of this parasite difficult. While the impact on human health of these occult infections is a matter of debate, most authors agree in considering the tick bite as a risk factor for the development of various chronic degenerative diseases. The most discussed correlation is between tick bite and Amyotrophic Lateral Sclerosis (ALS), for which several lines of evidence have been reported (25).

The tick-borne diseases associated with the bite of *I. ricinus* with major impact on public health in Europe and the United States were recognized with the emergence of *B. burgdorferi* as the etiological agent of Lyme disease. To follow, *Francisella tularensis* as the agent of Tularemia, *Babesia microti* as the agent of Babesiosis, the Flavivivus as agent of TBE (Tick Borne Encephalitis) and *Erhlichia caffeensis* as the agent of Ehrlichioses (Fig. 5).

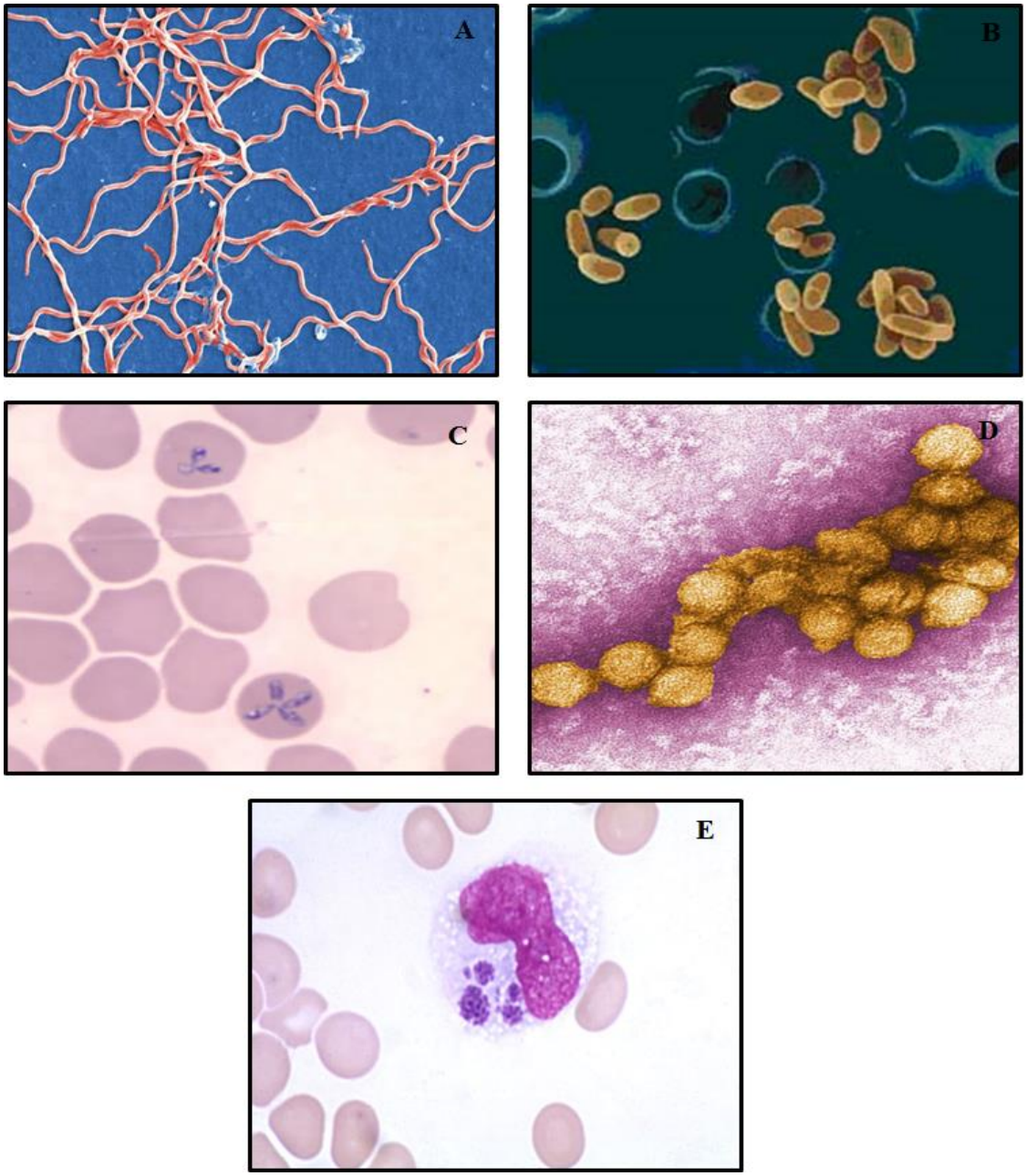

Figure 5. A) *Borrelia burgdorferi*. **B)** *Francisella tularensis* **C)** *Babesia microti* **D)** *Flavivirus* **E)** *Erhlichia caffeensis*

3.1 Lyme disease

Lyme disease was first recognized in 1975 in the city of Lyme, Connecticut (USA). The disease is caused by *Borrelia burgdorferi, B. garinii, B. afzelii,* gram-negative microaerophilic mobile spirochetes (26). The course of Lyme disease presents three stages: i) in the first stage infection is localized and the erythema migrans occurs; ii) in stage two infections become disseminated with lesions that involve skin, eyes, heart and nervous system; iii) in the third stage skin abnormalities may be observed, intermittent attacks of joint swelling and pain, fatigue, ocular and neurological signs (27). The diagnosis is made on the basis of clinical and epidemiological findings and serological testing. Specific antibodies against *Borrelia* can be detected by ELISA (28) or by applying PCR to amplify *B. burgorferi* DNA in blood, skin, synovial fluid and urine samples from infected patients (29). In the early stages, doxycycline is the recommended treatment. Nowadays is also available the vaccine against the Lyme disease (30). Liguria, Veneto, Friuli-Venezia Giulia and Trentino Alto Adige are the Italian regions mainly affected by this disorder.

3.2 Tularemia

Francisella tularensis is the causative agent of Tularemia. It is a small, aerobic, gram-negative coccobacillus. The incubation period of Tularemia averages 4-5 days (31). The onset of the disease is variable and depends on the involved organism. The most common characteristic form is the ulcero glandular one, in which a papule develops at the tick bite site, becomes pustular and then ulcerated, and is associated with regional lymphadenopathy. Although mortality has been estimated to be ~7%, it was probably much higher (around 33%) before the introduction of antibiotics (31). The disease is diagnosed by use of a serological test and doxycycline is the conventional drug.

3.3 Babesiosis

I. ricinus is able to transmit *Babesia microti*, a protozoan parasite that infects red blood cells causing a special type of anaemia called haemolytic anaemia. The infected people develop nonspecific flu-like symptoms, such as fever, chills, headache and loss of appetite, nausea and fatigue. The disease is diagnosed by examining blood specimens under microscope.

3.4 Tick borne encephalitis

Tick borne encephalitis (TBE) is a human viral infectious disease involving the central nervous system. The causative agent is a member of the family *Flaviviridae*, which was isolated in 1937. The incubation period is usually between 7 and 14 days and is asymptomatic. The most common clinical abnormalities are low white blood cell count and a low platelet count. There is no specific drug therapy for TBE.

3.5 Ehrlichioses

Erlichiae are obligate intracellular small gram-negative cocci, and are the agent of human granulocytic Ehrlichiosis (HGE). The symptoms include fever, headache, muscle aches and general feeling of weakness and fatigue. In some cases, the symptoms may progress to include nausea, vomiting, cough, diarrhoea, loss of appetite and confusion. If the disease is left untreated, kidney failure and respiratory problems may develop. A specific diagnosis of ehrlichiosis may be made by observing morulae in leukocytes, by serological tests or by molecular methods (32,33).

4. Midichloria mitochondrii

The numerous tick-associated bacteria have been called symbiont, microsymbiont or endosymbiont (34). The bacteria may have a negative, positive, or no effects on their arthropod hosts, and prediction of whether symbionts found in ticks may be human pathogens is not possible yet (3). *Midichloria mitochondrii* is one of the "unknown" endosymbiont present in *I. ricinus* and the basis of the symbiosis is not well understood.

"*Candidatus* Midichloria mitochondrii" belongs to the phylum *Proteobacteria*, to the class *Aphaproteobacteria* and to the order *Rickettsiales*. It is assigned on the basis of the 16S rRNA (AJ566640) and gryB (girase B) gene sequences (AM159536) (Fig. 6).

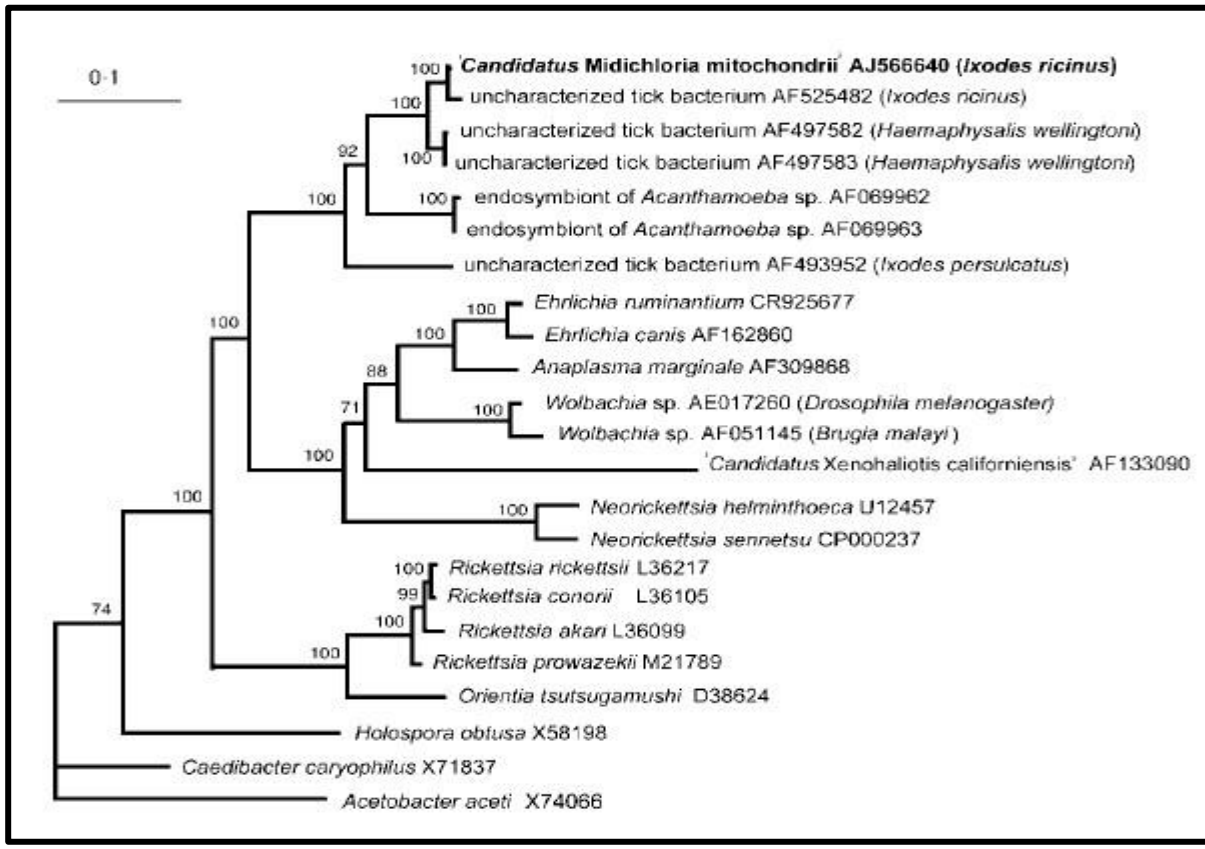

Figure 6. Phylogenetic tree based on near full-length 16S rRNA gene sequences showing the position of "*Candidatus* M. mitochondrii". The tree was generated using MrBaye (18).

The genus name *Midichloria* is derived from the midichlorians, organisms within the fictional Star Wars universe. Midichlorians are microscopy symbionts that reside inside the cells of living things and "communicate with the force" (18). *Midichloria mitochondrii* is a Gram-negative bacterium with a bacillus shape of ≈ 0.45 μm in diameter and 1.2 μm in length. It is observed within lumenal cell, funicular cell and oocytes of the tick *I. ricinus*. The bacterium appeared for the first time during an electron microscopy (EM) study on the ovary of *I. ricinus* in England (35) and it was found inside the mitochondria as well as in the cytoplasm. In a further EM study using engorged female ticks collected in Italy, bacteria were seen colonizing mitochondria in the periplasmic space between the inner and outer membranes (36). The bacteria seem to consume the inner part of the mitochondria and multiply therein, as the

development of the oocytes proceeds. This results in the reduction of mitochondrial matrix and some mitochondria appear as sacs full of bacteria, from a single bacterium to over 20 (36) (Fig. 7).

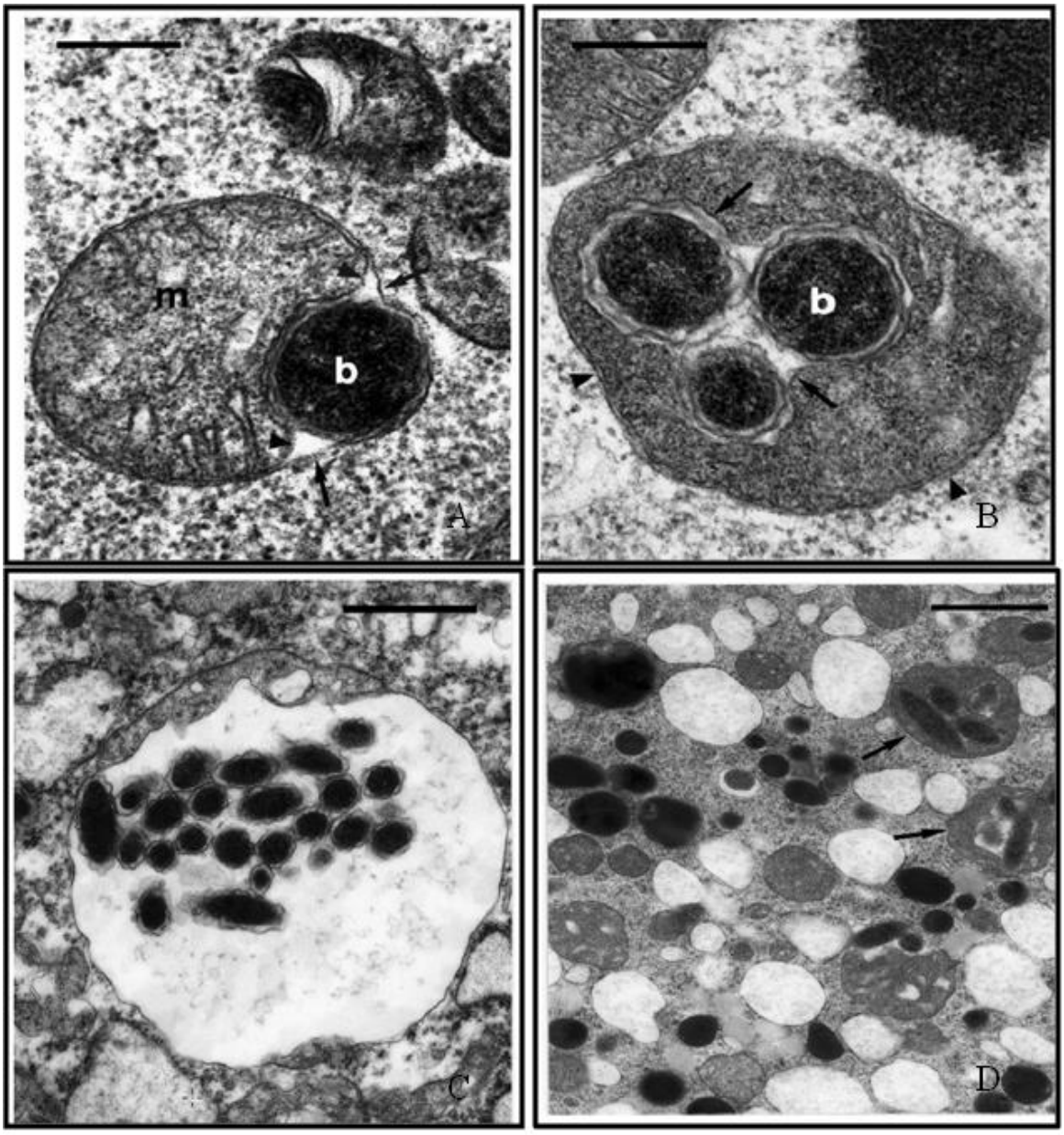

Figure 7. **A**) An infecting bacterium (b) can be observed between the outer and the inner membranes of mitochondria (m). **B**) Transverse section of an infected mitochondrion with three bacteria (b) encircled by the inner mitochondrial membrane. **C**) The end of the parasitic activity: the mitochondria are transformed in a swollen empty sac containing a rich population of bacteria. **D**) A vitellogenic oocyte rich of bacteria (36).

Despite the high number of mitochondria consumed by the bacterium, the eggs of the tick develop normally. The symbiont seems to be widespread in the female of *I. ricinus* with a prevalence of 100%, while a lower prevalence is observed in male ticks (44%) (18, 37). Furthermore, *M. Mitochondrii* is vertically transmitted to the progeny, as indicated by PCR evidence in eggs and larvae (18, 36), but also to the humans during the blood meal (38). Sybr green real time qPCR protocols allowed to examine the dynamic population of the symbiont during the host's cycle life. The increase in the *gyrB* copy numbers following engorgements of each three stages indicated that the bacterial growth is, most likely, linked to the blood meal (39).

The genome of *M. mitochondrii* consists of a single 1,183,732 bp circular chromosome with a Gb C content of 36.6% (Fig. 8).

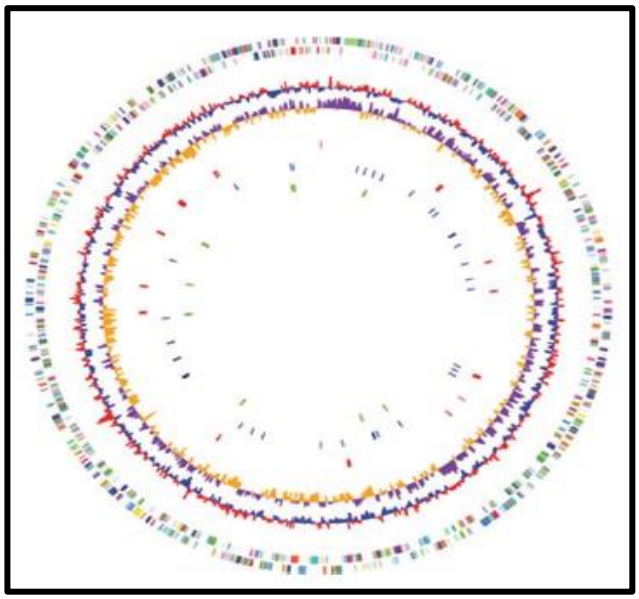

Figure 8. The genome of *M. mitochondrii*. The two outermost circles show all predicting coding regions; the fifth circle shows the location of the flagellar genes in red (40).

Among the identified genes, 26 (i.e. fliC, fliD, flgL, flgK, flgE and others) encode a flagellum which include all key components, such as the hook, filament and basal body. The function of these genes is therefore unclear. The hypothesis is that the flagellum might be assembled in as-yet-unexplored stages of the bacterium cycle and may also play a role in the invasion of tick mitochondria. A second set of genes is predicted to encode a cytochrome cbb_3. The presence of the cytochrome may enable *M. mitochondrii* to synthesize ATP at oxygen concentrations that are suboptimal for the mitochondrion (40).

Materials and Methods

1. Tick collection, DNA and protein extraction

One hundred and twenty semi-engorged *I. ricinus* ticks were collected from roe dears (*Capreolus capreolus*) of the Chize forest (Northern France) in February 2014. Semi-engorged ticks were selected as, at this stage, they present the highest development of the two organs investigated e.g. ovaries (OV) and salivary glands (SG), and also a high concentration of *Midichloria mitochondrii* symbiont (39). Ticks were manually dissected under Leica stereomicroscope (Wentzler, Germany) to collect organs. In particular, twenty ticks were pooled in 100 µl PBS containing 1.5 µl of 1X protease inhibitor (Sigma). After mechanical disruption of tissues, 20 µl of lysate were recovered for subsequent DNA extraction. The remaining volume was subjected to sonication (Digital Sonifier 450, Branson Ultrasonic Corporation, USA) applying three five-second treatments in a row. Each sample was then centrifuged at the maximum speed (14,000 rpm) for 10 min and the supernatants were stored at -80°C until use. DNA from each sample was extracted using the Quiagen DNeasy Blood and Tissue Kit (Hilden, Germany) following manufacturer instructions. DNAs were eluted in 50 µl of sterile water and stored at -20°C until molecular analysis.

2. PCR

The presence of common tick-borne pathogenic bacteria (41) in the extracted DNA was screened using previously described PCR protocols for *Borrelia burgorferi* (42), *Anaplasma spp.*, *Ehrlichia spp*. and *Rickettsia spp*. (43). Samples negative for the presence of pathogens were subsequently analysed for absolute quantification of *M. mitochondrii*. Sybr green real-time qPCR protocols were designed for the following: (i) the gyrB gene (coding for the protein gyrase B) of *M. midichloria* (primers CTTGAGAGCAGAACCACCTA [forward] and CAAGCTCTGCCGAAATATCTT [reverse]; amplifying 125 bp); (ii) *the I. ricinus* nuclear gene cal (coding for the protein calreticulin) (primers ATCTCCAATTTCGGTCCGGT and TGAAAGTTCCCTGCTCGCTT; amplifying 109 bp). PCR cycling for gyrB and cal was as follows: 95°C for 2 min, 40 cycles at 95°C for 15 s and at 60°C for 30 s, and melt curve from 55 °C to 95 °C with increasing increments of 0.5 °C per cycle. All reactions were performed in 25 µl of Milli-Q water containing 400 nM of each primer, 12, 5 µl of iQ Sybr green supermix, and 1 µl of DNA. PCR products were sequenced to confirm PCR specificity and

then ligated into the pGEM-T Easy vector and cloned. Purified plasmids containing the desired fragments were serially diluted to evaluate the efficiency and detection limit of each PCR protocol (10 copies in each case) (39). Results were expressed as ratio of *gyrB/cal* copy numbers.

3. Protein assay

The Bicinchoninic Acid (BCA) assay was applied to obtain the exact concentration of each pool of proteins extracted from SG and OV (44). Bovine serum albumin was the standard protein used for the production of calibration curves in the range of concentration between 2,5 and 25 µg/mL.

4. 2-DE

About 250 µg of extracted proteins were dissolved in 125 µl of rehydration buffer (8M urea, 4% CHAPS (w/v), 65 mM DTE, 0,8% carrier ampholytes (v/v), 0,5% bromophenol blue) and loaded onto 7 cm IPG strips, with nonlinear (NL) pH 3-10 or linear pH 4-7 gradient range (GE Healthcare, UK). Strips were rehydrated without applying voltage for 1h at 20°C. The first dimensional IEF was carried out at 15°C using an Ettan IPGphor 3 system (GE Healthcare, UK) (Table 1).

Table 1. Isoelectrofocusing steps

Time	*Current*	*Temperature*
8h	30 V	16°C
1h	120 V	16°C
30 min	500 V	16°C
30 min	1000 V	16°C
ON (>7h)	Constant 5000V (to reach a total of 25-27 kV/h)	16°C

Three hours after the start, the IEF run was stopped to allow positioning of small pieces of paper between the IPG strip and electrodes. Reduction and alkylation steps were performed between the first and the second dimension. The focused IPG strips were incubated for 15 min at room temperature in 6M urea, 2% (w/v) SDS, 50 mM Tris pH 6.8, glycerol 30%, containing 2% (w/v) DTE, followed by a second incubation step of 15 min in the same buffer containing 2,5% (w/v) iodoacetamide and 0,5% bromophenol blue. At the end of the IEF step, strips were hold in place with 0,4% low melting temperature agarose and loaded onto 8 x 6 cm slabs, 12,5% SDS polyacrylamide gels. Electrophoresis was carried out at a constant current of 10 mA per gel in a PROTEAN II xi 2-D BioRad Cell equipment (Berkeley, California), until the buffer front line was 1 mm from the bottom of the gel.

5. Protein detection

The 2-DE gels were stained with "Blue silver" (colloidal Coomassie G-250 staining) (45). This staining method has a sensitivity of 5-10 ng per spot and is compatible with mass spectrometry detection.

In the first step, proteins were fixed in the gel by treatment for one hour with 40% methanol and 7% acetic acid. Then, gels were incubated overnight in the staining solution (10% orthophosphoric acid, 10% ammonium sulphate, 20% methanol and 0,12% Coomassie

Brilliant Blue G-250). Gels were bleached initially with 5% acetic acid and then with water until a transparent background was obtained.

6. Reproducibility of study

To verify the reproducibility of the study, 2-DE maps were obtained in triplicate for each of the analysed SG and OV pools. Those presented in this report are the best representative gels among all generated that showed spots consistently present. Experimental steps concerning sample preparation, electrophoretic run and gel staining were performed "in parallel" on both pools.

7. PD- quest analysis

Digital image of stained gels was acquired using the VersaDoc Imaging Model 3000 (Bio Rad) equipment and then subjected to qualitative and quantitative analysis using the PD-Quest version 8.0.1 software (Bio Rad). Thanks to the advanced algorithm of the software, the scanned images were filtered and smoothed to remove background noise, vertical or horizontal streaking and gel artefacts. They were also normalized to eliminate the variability of each sample. The software determined the number of spots present and calculated their intensity by applying the following algorithm: peak value (ODs/image units) *σx*σy (standard deviations in x and y). The following step was the creation of a "Match Set" necessary to compare all the gels of a single group and to match the spots present. A synthetic image (called Master Gel) containing the information about all the spots of Match Set was created. The Master Gels of every group were finally compared each other through a Higher Master Set to create a Higher Master Gel (HGM) that contained all information about the whole analysis.

The HGM gives the chance to observe the presence/absence of a given spot and to determine the intensity value of common ones that can later be submitted to statistical analysis.

8. Western Blotting

Western blot analysis was performed starting from 100 µg of proteins from the OV and SG pool that exhibited the highest concentration of M. mitochondrii based on GryB/cal gene ratio. Separated proteins were transferred onto a PVDF membrane by using a Trans-Blot Turbo Transfer System that applied a current of 1.3 A up to 25 V for 7 min. To verify the transfer of proteins, the membrane was stained with Ponceau Red and washed with PBS (10 ml) for 10 min. After 1h incubation in 5% milk (10 ml) diluted in PBS and three additional washes with PBST (0,1% Tween, 10 ml), the membrane was incubated overnight with the polyclonal antibodies against the M. mitochondrii flagellar protein FliD (38) at a dilution 1: 5000 in 2% milk. After washing the membrane three times with PBST (10 ml), incubation was carried out for 1h at room temperature with the secondary antibody (polyclonal goat anti-rabbit immunoglobulin, Dako, Glostrup, Denmark) diluted 1:2000 in 1% milk in PBST. The membrane was finally washed three times with PBS and incubated in ECL Prime Solution (GE Healthcare). Immunoblots were acquired with the ImageQuant LAS 4000 analyzer (GE Healthcare).

9. In situ enzymatic digestion

The gels pieces containing the selected spots were carefully excised, placed into Eppendorf tubes and broken into smaller snippets. This material was then washed twice with aliquots (200 µl) of 100 mM ammonium bicarbonate buffer pH 7.8, 50% acetonitrile (ACN) and kept under stirring overnight, until complete destaining. Gels were dehydrated by addition of ACN (100 µl). After removal of the organic solvent, reduction was performed by addition of 50 µl of 10 mM Dithiothreitol (DTT) solution (40 min at 37°). DTT was replaced by 50 µl of 55 mM iodoacetamide that was incubated for 45 min at 56°C. This solution was removed and the gel pieces were washed twice with 200 µl of 100 mM ammonium bicarbonate for 10 min, while vortexing. The washing solution was removed and gel dehydrated by addition of 200 µl of ACN until the gel pieces became an opaque-white colour. ACN was finally removed and gel pieces were dried under vacuum. Gels were rehydrated by addition of 75 µL of 100 mM ammonium bicarbonate buffer pH 7.8, containing 20 ng/µl sequencing grade trypsin (Promega, Madison, WI, USA) and digestion was performed by incubating the mixture overnight at 37°C. The resultant peptides were extracted from gel matrix by a three-step treatment (each step at 37°C for 15 min) with 50 µl of 50% ACN in water, 5% trifluoroacetic acid (TFA) and finally

with 50 µl of 100% ACN. Each extraction involved 10 min of stirring followed by centrifugation and removal of the supernatant. The original supernatant and those obtained from sequential extractions were pooled, dried and stored at -80°C until mass spectrometry analysis. At the moment of use, the peptide mixture was solubilized in 100 µl of 0,1% formic acid (FA) for MS analysis.

10. LC-MS/MS

Identification of the protein(s) under the spots was carried out on an LC-MS/MS (Thermo Finnigan, USA) system consisting of a thermostated column oven Surveyor autosampler controlled at 25°C, a quaternary gradient surveyor MS pump equipped with a diode array detector, and a Linear Trap Quadrupole (LTQ) mass spectrometer with electrospray ionization ion source (ESI) controlled by Xcalibur software 1.4. Analytes were separated by RP-HPLC on a Jupiter (Phenomenex, USA) C_{18} column (150 x 2 mm, 4 µm, 9 Å particle size) using a linear gradient (2-16% solvent B in 60 min) in which solvent A consisted of 0.1% aqueous FA and solvent B consisted of ACN containing 0.1% FA. Flow-rate was 0,2 ml/min. Mass spectra were generated in positive ion mode under constant instrumental conditions: source voltage 5.0 kV, capillary voltage 46 V, sheath gas flow 40 (arbitrary units), auxiliary gas flow 10 (arbitrary units), sweep gas flow 1 (arbitrary units), capillary temperature 200 °C, tube lens voltage -105 V. MS/MS spectra, obtained by CID studies in the linear ion trap, were performed with an isolation width of 3 Th *m/z*, the activation amplitude was 35% of ejection RF amplitude that corresponds to 1.58 V. Data processing was performed using Peaks studio software. An "ad-hoc" system database was obtained selecting from the NCBI database all the protein sequences belonging to the following taxonomic groups: *Ixodida* (taxid: 6935), *Cervidae* (taxid: 9850), *Borrelia* (taxid: 138), *Rickettsiales* (taxid: 766). The mass lists were searched against the Swiss Prot and the "ad-hoc" protein database under continued mode (MS plus MS/MS), with the following parameters: trypsin specificity, five missed cleavages, peptide tolerance at 0.2 Da, MS/MS tolerance at 0.25 Da, peptide change 1,2,3+, and experimental mass values: monoisotopic.

11. Protein extraction and nanoflow liquid chromatography electrospray ionisation tandem mass spectrometry

To solubilise proteins after protein extraction, the pellets were sonicated on ice in 5 mM ammonium bicarbonate (Sigma) and 0.05% (w/v) Rapigest (Waters, UK). Proteomic-grade trypsin was added at a protein: trypsin ratio 50:1, and samples were incubated at 37° overnight before removal of Rapigest by TFA precipitation. Peptide mixtures (2 ul) were analysed by online nanoflow liquid chromatography using the nanoACQUITY-nLC system (Waters) coupled to an LTQ-Orbitrap Velos (ThermoFisher Scientific, Germany) mass spectrometer equipped with the manufacturer's nanospray ion source. The analytical column was maintained at 35°C and a flow-rate of 300 nl/min. The gradient consisted of 3-40% ACN in 0,1% FA for 90 min, followed by a ramp of 40-85% ACN in 0.1% FA for 3 min. Full scan MS spectra (m/z range, 300-2000) were acquired by the Orbitrap. Identification of peptides was obtained using Mascot (v.2.2.03, Matrix Science). Thermo RAW files were imported into Progenesis LC-MS (version 4.1, Nonlinear Dynamics, UK), and runs were time-aligned using default settings. Tandem MS data were searched against Swiss-Prot and the "ad-hoc" database.

12. Bioinformatic analysis

To perform a bioinformatic analysis of data, different gene function prediction programs were utilized. The first databases that were exploited were UniProtKB (http://www.uniprot.org/), a free accessible resource of protein sequence and functional information (that contains the Swiss-Prot section where a knowledgebase is present) and NCBI (The National Center for Biotechnology Information, http://www.ncbi.nml.nih.gov/) for obtaining information about gene and their related nomenclature, maps, pathways, variations, phenotypes and links to worldwide resource. To integrate the information obtained with UniProt, other bioinformatic tools were employed. One of them was the STRING database (Search Tool for the Retrieval of Interacting Genes, http://string-db.org), an online database resource that provides predicted protein to protein interaction information. In this database, interaction and accessory information such as protein domains and 3D structure are provided with a confidence score. The input proteins are presented in the context of a graphical network interaction partner that provides also accessory information on a protein or on the evidence behind a proposed connection. Then the network display can be modified by adding or removing proteins,

changing the required confidence level and by selecting or de-selecting evidence types. STING is a database of known and predicted protein interactions. The interactions include direct (physical) and indirect (functional) associations derived from four sources: genomic context, high-throughput experiments, co-expression (conserved) and previous knowledge (46,47).

PANTHER (Protein Analysis Through Evolutionary Relationship, http://pantherdb.org) was used to categorize the identified proteins. It a comprehensive database of functional information about protein-coding genes. Functional annotations are updated using the models generated by the Gene Ontology Phylogenetic Annotation Project (48).

Kyoto Encyclopedia of Genes and Genomes (KEGG, http://www.genomejp/kegg/ or http://www.kegg.jp/) was also used. This system develops large metabolic pathway databases and it can be considered an integrated database resource for deciphering the genome. Experimental knowledge on systemic functions of the cell and the organism is represented in terms of molecular networks using KEGG pathway. The KEGG pathway maps are graphical diagrams representing molecular interaction and reaction networks for metabolism, genetic information processing, environmental information processing, cellular process, organism systems, diseases and drug developments (49-51).

Aim

The main purpose of my PhD project was to develop a serological test to detect whether a human or animal subject has been parasitized by *I. ricinus*. The setting up of an innovative serological method for the diagnosis of the *I. ricinus* bite will allow to achieve future important results in medicine and veterinary.

To obtain this goal, I started widening the knowledge of *I. ricinus* protein profiles by applying "in gel" analysis. Two-dimensional electrophoresis and protein identification by LC-MS/MS wee the tools applied to compare the protein pattern of the ovary, the principal tissue that contains *M. mitochondrii*; with that of salivary glands, where the presence of the symbiont has also been observed.

To improve the "in gel" results and to understand more in depth the relation between the tick and its endosymbiont, a high-resolution shotgun proteomics approach was also performed. This part of my work was done at the University of Liverpool (UK) where I spent three months. The "off gel" technique offered the opportunity to: i) identify thousand tick and symbiont proteins; ii) compare differential expressed proteins in five different stages of engorgement and iii) make a comparison between the proteomic profile of field ticks and pathogen free (without *M. mitochondrii*) ticks.

In addition, immunoproteomic experiments using the sera from patients parasitized by *I. ricinus* and those from infested experimental rabbits were performed. This procedure allowed to detect tick and symbiont markers potentially able to produce antigenic molecules. Work is in progress to set-up an ELISA assay for a first application and validation of a serological test to study the immunology of tick bite.

Chapter I

Detection and identification of proteins in different organs/tissues, with the aim of understanding whether they represent an attractive tool for monitoring alterations in these districts is currently an area of increased interest. Recently, studies have been focused on the characterization of *I. ricinus* ovary and salivary gland proteomes, to better understand the role of these organs, fundamental in the tick bite and metabolism (52, 53). The first goals of this study were the following: i) obtain the proteomic profile of *I. ricinus* ovary and salivary glands; ii) identify the differentially expressed proteins between these tissues and iii) provide clues on the symbiotic relationship between the tick and its endosymbiont.

Results

1. PCR

Concentration of *M. mitochondrii* and presence of tick-borne pathogens was assessed in all the ovary (OV) and salivary gland (SG) pools by performing PCR on the DNA extracted from the samples. Two out of six OV and SG pools were positive to tick-borne pathogens and were thus excluded from subsequent analysis. PCR for the detection on *M. mitochondrii* was performed on the remaining samples and all OV and SG pools resulted, as expected, positive to the symbiont (Table 2).

Table 2. GyrB and Cal gene copy numbers, GyrB Cal gene ratio and PCR positivity to *Borrelia burgdorferi*, *Anaplasma spp.*, *Ehrlichia spp.*, and *Rickettsia spp*.

Pool code	*GyrB* copies	*cal* copies	*gyrB/cal* ratio x 1000
OV1	373899,9594	37,66598829	9926726,373
SG1	13880,81163	34,89770488	397757,1499
OV2	1872603,455	1500,759257	1247770,718
SG2	168,2698052	9,937737539	16932,40585
OV3	3738999,594	1060,761728	3524825,128
SG3	2437,79344	487,6015747	4999,560228
OV4	1265223,304	328,3030099	3853827,916
SG4	116,9799564	88,44119687	1322,686265

2. Two-dimensional electrophoresis with nonlinear pH 3-10 gradient range

To identify proteins of *I. ricinus* differentially expressed between OV and SG, and proteins of the *M. mitochondrii* symbiont, 2-DE analyses were performed "in parallel" on the samples that were infected by *M. mitochondrii* but resulted free from other bacterial pathogens. Gels were scanned and spots were detected using the spot detection wizard tool, after defining and saving a set of detection parameters. The original gel scans were filtered and smoothed to clarify spots, remove vertical and horizontal streaks, and remove speckles. Three dimensional Gaussian spots were then created from filtered images. Three images were created from the process: the original raw 2-D scan, the filtered image and the Gaussian image. A match set for each pool was then created for comparison after the gel image had been aligned and automatically overlaid. If a spot was saturated, irregularly shaped, or otherwise of poor quality, then the Gaussian model was unable to accurately determine the quantity. In these cases, the spot was defined in the filtered image using the spot boundary tools. Thus, for each pool, a master gel was produced which included protein spots only if present at least in two out of the three gels. The mean spot number in Coomassie stained gels was 235±29 in SG and 221±21 in OV. A few spots chosen from the two master gels were excised, destained, digested with

trypsin, and peptides were submitted to LC-MS/MS. The MS fragmentation data were searched against the SwissProt studio 4.5 software. In total, 47 proteins (20 from SG and 27 from OV) were identified. (Supplementary Materials Table S1).

The master gel from both SG and OV pools showed similar patterns of proteins such that they could be matched each other. This facilitated the correlation of the gels and the creation of a virtual image, indicated as high master gels (HMG), comprehensive of all matched spots derived from master gels (Fig. 9).

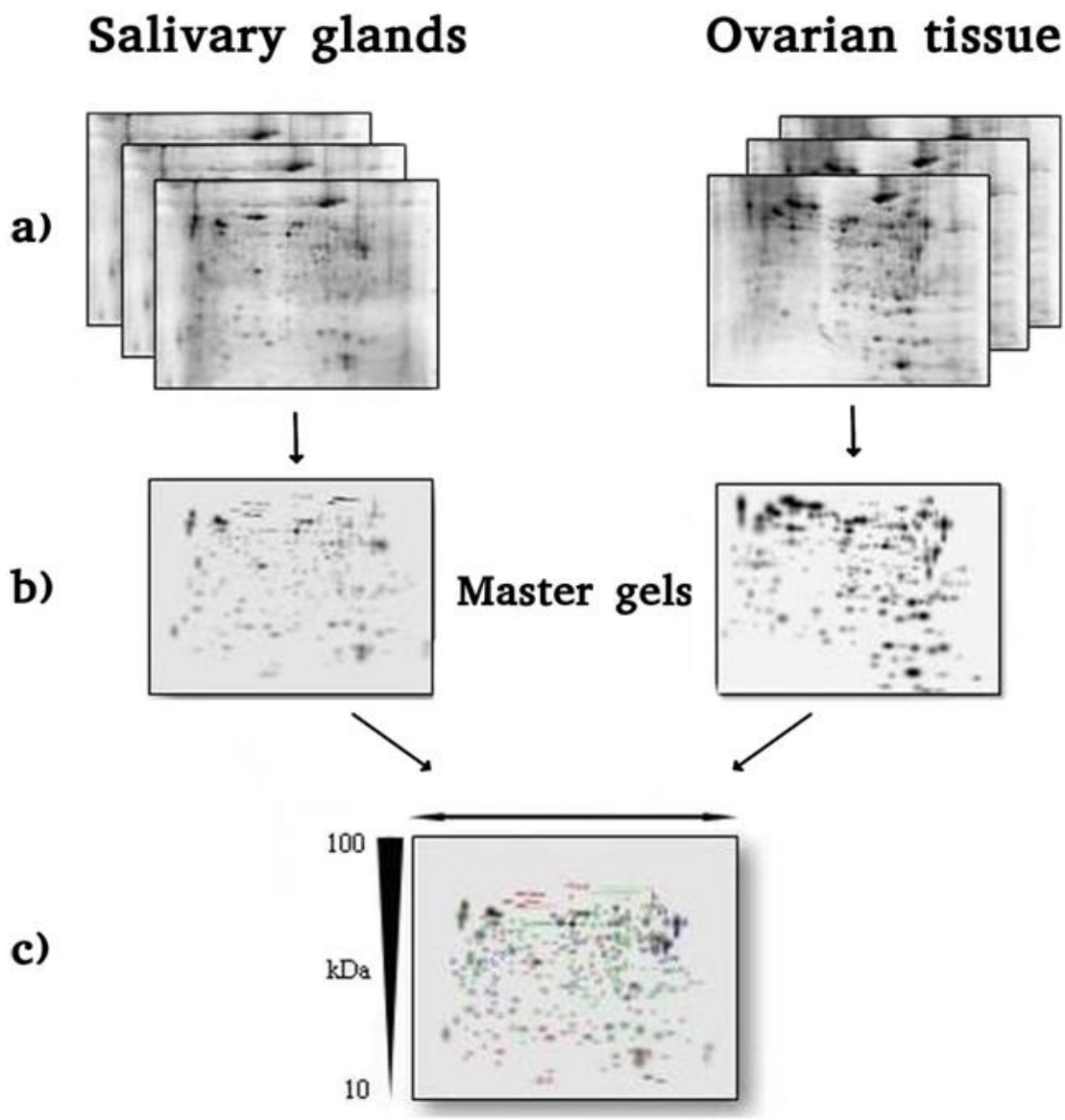

Figure 9. **A**) 2-DE maps of three different pools of SG and OV of *I. ricinus*, obtained by performing IEF on 7 cm IPG strips with 3-10 NL pH range and SDS-PAGE in the second dimension on 12.5% T gels. **B**) SG and OV master gels produced by merging the three gels for each sample type. **C**) High Master Gels created comparing the SG and OV.

3. Differentially expressed proteins

Comparison of 2-DE patterns for SG and OV revealed several qualitative and quantitative differences between the two sets of pools. In terms of presence/absence of spots, qualitative differences are represented in Fig.10. As shown, while the majority of spots was common to both SG and OV (170±25, evidenced in green), some protein spots present in SG profile were absent in the OV and vice versa. In particular, 81 spots (marked in red) were exclusive of SG and 57 spots (labeled in blue) were detected solely in OT.

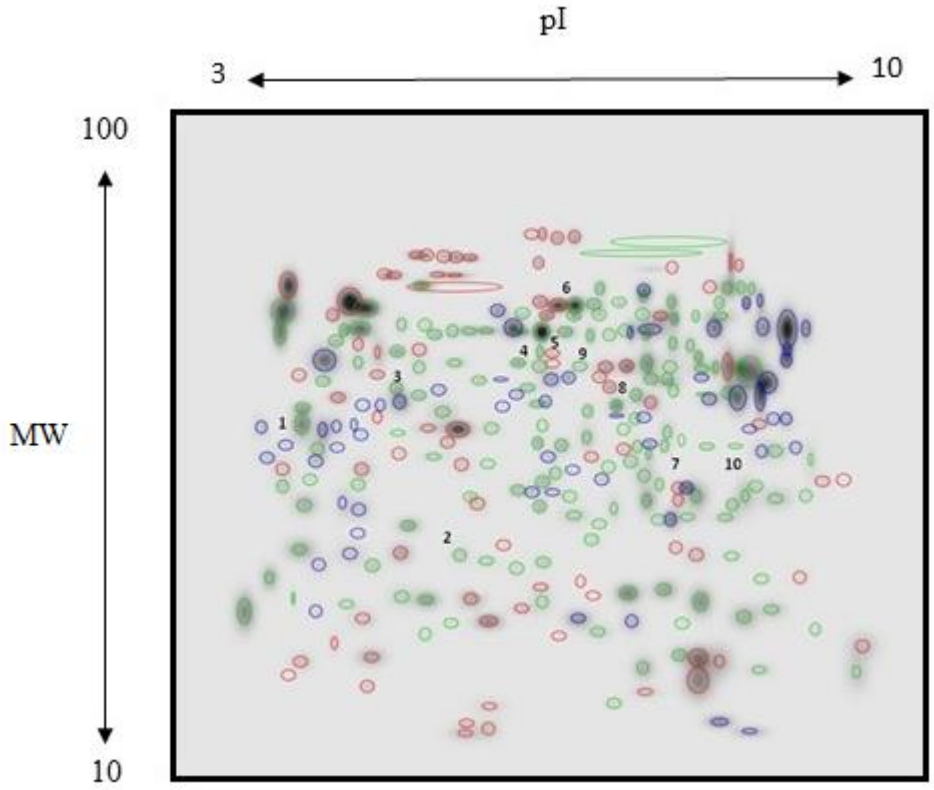

Figure 10. High Master Gel, showing qualitative differences between the SG and OV. Labelled in green: spots (n= 170±25) common to both SG and OV. Labelled in red: spots (n= 81) exclusive of SG. Labelled in blue: spots (n= 57) detected solely in OV.

Spots quantities of all gels were normalized to remove non-expression-related variations in spot density and data were exported as clipboard for further statistical analysis. The raw amount of each protein in a gel was divided by the total quantity of all proteins that were included in the gel. The results were evaluated in terms of spot optical density (OD). Statistical analysis of PDQuest data allowed to assess differences in protein abundance on a protein-by-protein basis. Only the spots that showed a change in density at p value<0.01 (by Student's t-test) were considered "differentially expressed" in the two pools of samples. Using these criteria, 21 spots differed by the ratio indicated above and were selected by the statistical program as spots having a significant difference in the relative abundance between SG and OV. Ten among these spots, indicated by numbers 1 to 10 in Fig.10, showed 4- to 18-fold increase/decrease in density. A set of panels, shown in Fig.11, was generated to highlight density variances of these spots between the pools.

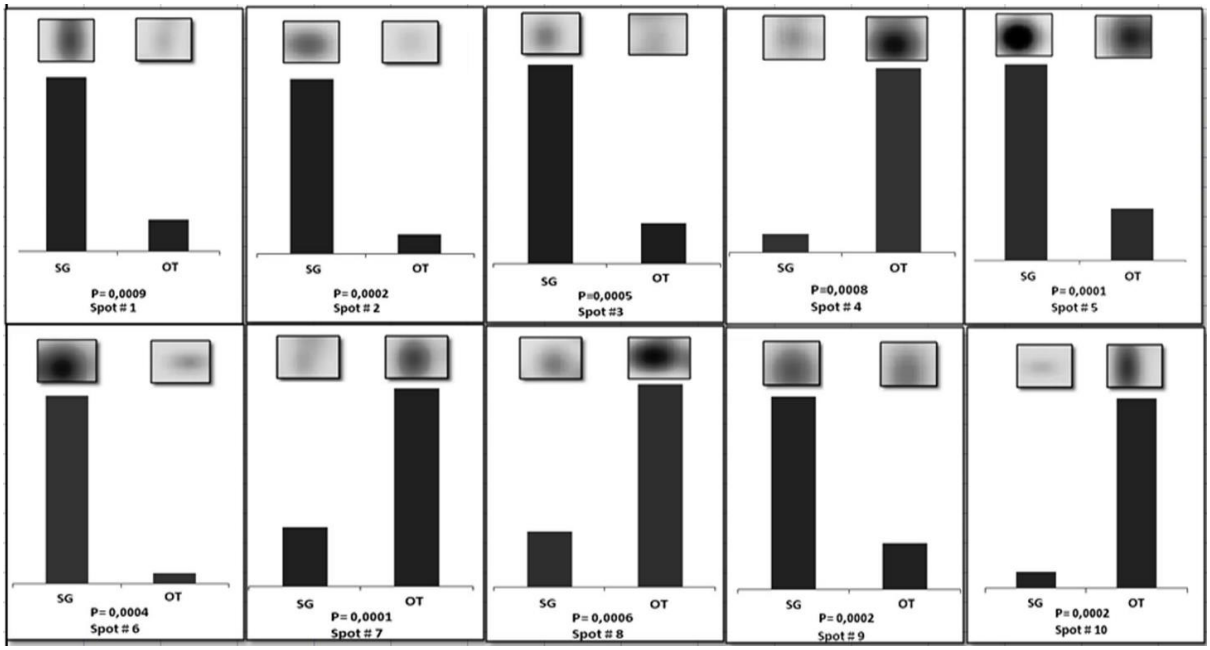

Figure 11. Set of panels showing the density variances between SG and OV pools for spots 1 to 10 excised from 2-DE gel 3-10 NL pH gradient. In each panel, the region of stained gel containing the spots of interest was magnified and the up-/down-regulation graphically represented. The p value indicating statistically significant variance is reported in each panel.

Efforts have been devoted to the identification of these proteins, to understand whether they might be involved in the biological process characteristic of ovaries and salivary glands, or in the interaction between *M. mitochondrii* and *I. ricinus*. These spots were thus carefully excised from the gel, destained, proteins digested with trypsin, and peptides submitted to LC-MS/MS. The MS fragmentation data were searched against the SwissProt and the ad-hoc designed protein database, and the queries were performed using Peaks studio 4.5 software. All but two (spots 2 and 9) of the proteins were identified (Table 3). The low abundance of proteins included in spots 2 and 9 most likely determined the poor quality of their MS signals and the failure in their identification. The fact that unique proteins were identified for all other analyzed spots suggested that, at least for these, spot overlap was minimized.

Table 3. Up and down-regulated proteins identified by LC-MS/MS. Accession number, theoretical pI, molecular mass, percent of sequence coverage and the number of peptides identified are reported.

Spot	Accession	Description	Mass	Score (%)	Coverage (%)	Query matched
1	**gi|442756551|gb|JAA70434.1|**	Putative heat shock 70 kda protein 5 [Ixodes ricinus]	72,595	99	8,05%	5
2	**/**	Not detected	/	/	/	/
3	**gi|322422107|gb|ADX01224.1|**	Beta actin [Ixodes ricinus]	16,038	90	6,94%	1
4	**gi|215497327|gb|EEC06821.1|**	Enolase, putative [Ixodes scapularis]	21,493	90	4,52%	1
5	**gi|442753241|gb|JAA68780.1|**	Putative enolase [Ixodes ricinus]	47,145	99	23,79%	6
6	**gi|215491972|gb|EEC01613.1|**	Protein disulfide isomerase, putative [Ixodes scapularis]	54,929	98	6,38%	4
7	**gi|442748259|gb|JAA66289.1|**	Putative 3-hydroxy-3-methylglutaryl-coa reductase [Ixodes ricinus]	10,741	20	22,43%	2
8	**gi|597718071|gb|AHN19768.1|**	Serum albumin, partial [Cervus nippon]	66,15	75	6,67%	4
9	**/**	Not detected	/	/	/	/
10	**gi|442754645|gb|JAA69482.1|**	Putative heat shock protein [Ixodes ricinus]	36,782	82	4,01%	2

4. Western blotting

One of the goal of my PhD project was to evaluate whether it is possible to detect proteins from the bacterial symbiont *M. mitochondrii* starting from protein extracts of ovaries and salivary glands of the hard tick *I. ricinus.* To achieve this goal, the pool that exhibited the highest concentration of *M. mitochondrii* was transferred onto PVDF membranes and incubated with the polyclonal anti-FliD antibody, followed by anti-rabbit antibody. Based on: i) its positions (pI/Mr) on the PVDF membrane and ii) its identification by the antibody, the protein spot indicated by an arrow in panel A (OV pool) of Fig.12, was tentatively assigned to FliD.

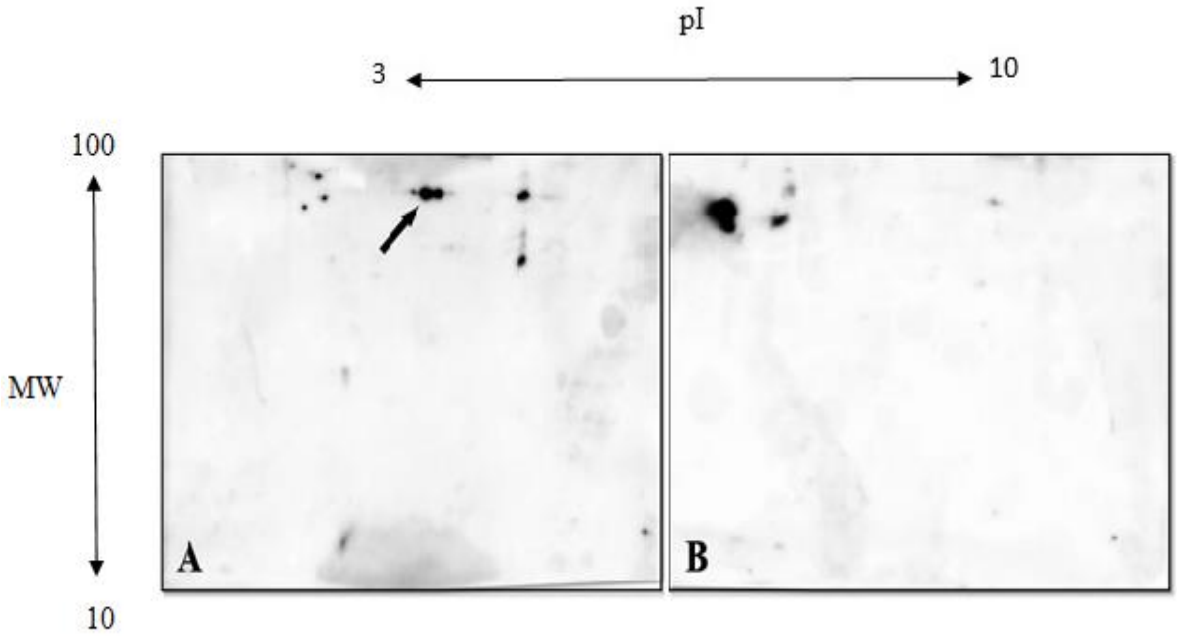

Figure 12. Immunoblotting of proteins from SG and OV profiles generated as indicated in Fig 9. PVDF membrane were incubated with the rabbit polyclonal antibody anti-FliD of *M. mitochondrii*. The spot indicated by an arrow in panel A (OV pool) was assigned to FliD. Panel B shows the SG profile in which the FliD spot is undetectable.

As shown in Panel B of Fig.12 despite the appearance of interfering spots, the hypothetical FliD spot was undetectable in the SG profile. To achieve identification, the immunoreactive protein spot was thus excised and submitted to LC-MS/MS. The results, shown in Table 4, confirmed that the analyzed spot was a mixture of at least three components, i.e. Endoplasmic reticulum protein 60, putative actin 2, and an unknown protein of *Borrelia*.

Table 4. List of proteins identified under the immunoreactive spot.

Accession	Description	Mass	Score (%)	Coverage (%)	Query matched
gi|442747467|gb|JAA65893.1|	Putative erp60 [Ixodes ricinus]	52,115	98	6,45%	3
gi|556065071|gb|JAB75571.1|	putative actin-2 [Ixodes ricinus]	36,27	89	9,79%	2
gi|6841058|gb|AAF28881.1|	unknown [Borrelia hermsii]	29,518	25	3,92%	1

We hypothesized that the failure in detecting the putative flagellar protein FliD was due to its lower abundance compared to that of other proteins present in the spot. Obviously, these results made it difficult to confirm the presence of FliD protein under the spot considered.

5. 2-DE with pH 4-7 gradient range and identification of FliD

To overcome the limitations indicated above and to definitively establish (or exclude) the presence of FliD under the spot of the OV pool examined, we worked on the optimization of the electrophoretic conditions. After performing an extensive set of trials with various electrophoretic conditions, the best option was the application of a different pH range (linear pH 4-7). This provided a better resolution of proteins, minimizing their overlapping (Fig.13).

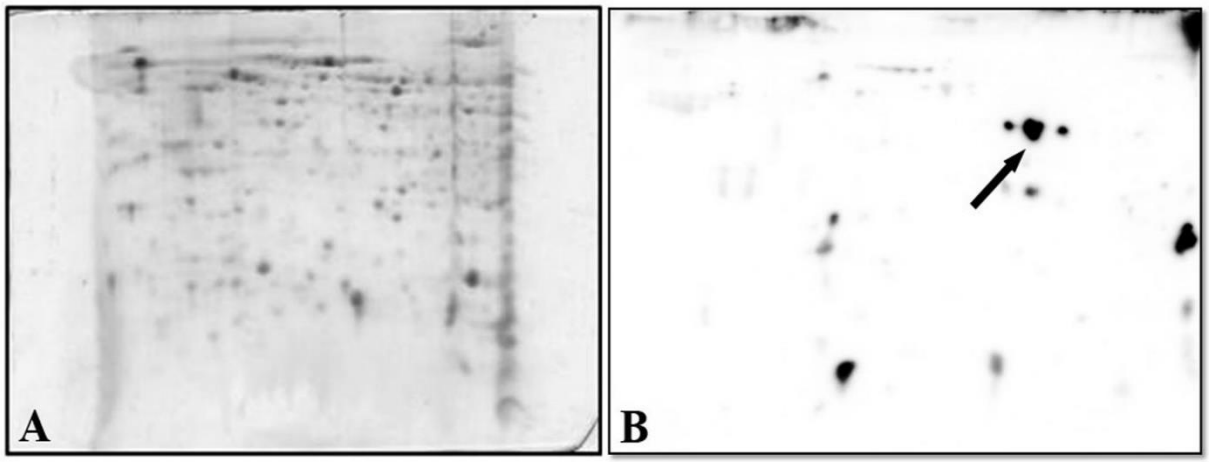

Figure 13. A) 2 DE map of OT obtained by performing IEF on a 4-7 linear pH range and SDS-PAGE on a constant 12,5%T in the second dimension, to separate proteins clustered in the apparent single spot shown in fig. 12. **B)** Immunoblotting of the gel slab indicated in Panel A.

The immunoreactive spot (indicated by an arrow in Panel B), was evidenced in OV profile obtained under the experimental conditions mentioned above. After spot excision and tryptic digestion, LC-MS identification confirmed the presence of flagellar protein FliD under this spot (Table 5).

Table 5. List of proteins identified under the spot indicated by an arrow in Fig.13 B.

Accession	Description	Mass	Score (%)	Coverage (%)	Query matched
/	Flagellar protein FLID OS=Midichloria mitochondrii	100,58	84	14,64%	13
gi|442747467|gb|JAA65893.1|	Putative erp60 [Ixodes ricinus]	52,115	98	6,45%	3

6. Functional classification of differentially expressed proteins

Using the PANTHER tool, the altered proteins identified (shown in Table 3) were categorized into different groups based on their Gene Ontology terms. In particular, 62% of the proteins have a molecular function, 25% are involved in a biological process (i.e. glycolytic process) and 13% represents a cellular component. A pie chart with the different GO Terms is shown in Figure 14.

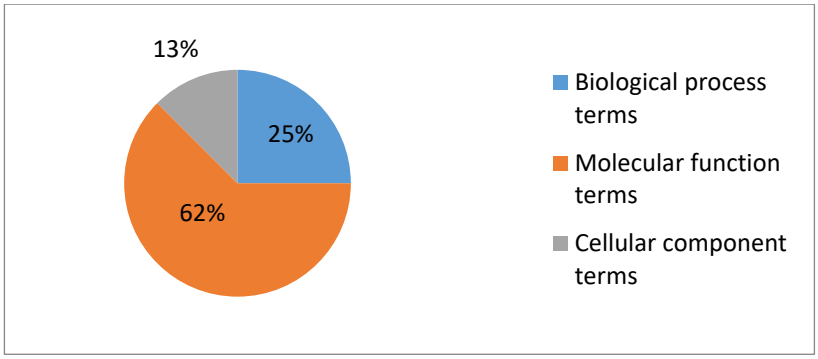

Figure 14. Pie chart built using Gene Ontology information merged with the application of the PANTHER tool. Altered protein identified were categorized into different groups based on their function.

As shown in Figure 15, the prevalent biological process (with 40 % of proteins involved) was the glycolytic pathway.

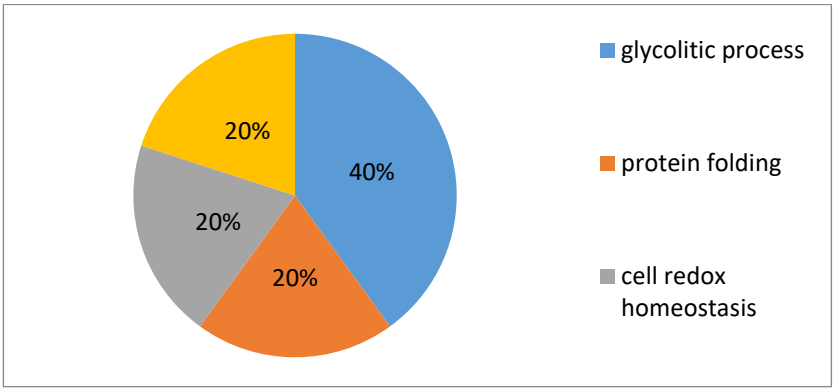

Figure 15. Pie chart of biological process associated with identified proteins, built using Gene Ontology data merged with the use of PANTHER tool.

Discussion

7. Analysis of common proteins differentially expressed

In the first part of my project, a total of 47 spots, 27 from OV and 20 from SG were selected and identified. The results were fully congruent with those previously published (54) validating the applied approach and confirming the variability in the expression level between OV and SG of a number of proteins, such as Heat shock protein, Protein disulfide isomerase, Enolase, Actin, Hemelipoglycoprotein precursor etc. This effort allowed detection of only proteins belonging to the tick proteome but did not reveal the presence of proteins belonging to the bacterial symbiont *M. mitochondrii*. To evaluate whether detection of symbiont proteins was possible, a specific immunoproteomic approach was designed.

To explore qualitative and quantitative differences between SG and OV of *I. ricinus* infected by *M. mitochondrii*, and to identify tissue-specific proteins, as well as proteins involved in the interaction between the bacterium and the tick, the proteomic profiles of these tissues were compared. The reproducible patterns generated for both tissues evidenced 170±25 spots shared between SG and OV. In addition, 81 proteins spots were exclusive of SG and 57 spots were detected solely in OV. The 10 spots that exhibited the largest changes in density were selected and investigated.

Proteins under spots 1 and 10, both identified as putative heat shock proteins (HSP), were heavily differentially expressed. Putative HSP70 detected under spot 1 was 6-fold more abundant in SG than in OV. By contrast, the putative HSP identified under spot 10 was 11-fold more abundant in OV than in SG. Heat shock proteins are chaperones that, together with other stress response, are well known to protect cells and organisms from environmental stress. HSP70 is involved in many cellular processes, including folding and refolding of nascent and/or misfolded proteins, protein translocation across membranes, and degradation of terminally misfolded or aggregated proteins (55). The role played by HSP proteins in the growth and survival of *I. ricinus* is potentially very important. Being involved in the binding and presentation of antigens to the immune system, they constitute candidate molecules that could be involved in tick immunoresponse to pathogen infection. Interestingly, a connection may exist between the pathogen infection and tick response to stress conditions. In response to heat and other stress, nearly all ticks undergo diapause. Indeed, HPSs involved in the diapause of multiple species of insects have been reported (56), suggesting that many of them play key roles in the physiological response to stress of other arthropods, such as a tick. HPS70

is more expressed in salivary glands than ovaries and its expression increase with female tick feeding, suggesting a possible role of this protein during blood ingestion and/or digestion (57). We speculated that this could be ascribed to the great changes in structure that the salivary glands of hard ticks undergo during blood feeding with an increase in size and the acceleration of protein synthesis (58). However, the fact that HSP70 was found to be down regulated in *Anaplasma phagocytophilum* infected guts and salivary glands of *Ixodes scapularis* ticks, guts and salivary glands (57), may suggest that these proteins have a different function during pathogen infection.

The protein identified under spot 3 was β-actin. The reason of its 5-fold higher expression in SG compared to OV is still a matter of speculation. First, we hypothesized that this was a consequence of the importance of SG in tick feeding. Actin is an important structural protein required for esoskeleton rearrangement during tick engorgement (59) and is a common target on many bacterial proteins. It has been shown that cellular responses induced by a variety of stimuli and pathogens involve changes in cell morphology and the polymerization state of actin (60-62). Studies in prokaryotes and eukaryotes demonstrated that nutrition and stress affect the expression of housekeeping genes (63). For example, the low expression of actin shown in the unfed first instars nymphs of *I. scapularis* is likely due to their low nutrition level. Since they have not yet taken the blood meal, the nutrients incorporated into the eggs have been depleted by larval development (64). The significant differences observed during and immediately after feeding in females are likely related to the dynamic changes that occur in the physiology of ticks preparing for reproduction. It has also been shown that silencing the expression of actin in the soft tick *Ornithodoros moubata* resulted in impairment of tick feeding by a global attenuation of tick activity unrelated to specific function associated with engorgement (63). Finally, further aspects should be taken into consideration. *I. ricinus*, as *I. scapularis*, are vectors of bacterial pathogens including *A. phagocytophilum*, and *B. burgdorferi* (64,65). To persist in their hosts, obligate intracellular bacteria have evolved a variety of mechanisms including modulating host signaling and the actin cytoskeleton (66). If this hypothesis proves correct, it may be speculated that the high concentration of actin detected in SG of *I. ricinus* could be the result of a sort of survival strategy of development by the symbiont *M. mitochondrii* to persist in the arthropods vector.

Putative enolase was identified under spots 4 and 5. Alpha-enolase, one of the most abundantly expressed proteins in human cytosol, is a key glycolytic enzyme that converts 2-phosphoglycerate to phosphoenolpyruvate (67). In blood-feeding arthropods, this protein is secreted in saliva and inoculated into the host during feeding. The finding of 4-fold higher

expression of enolase in SG compared to OV was not surprising. This result may account for one of the pivotal roles of the enzymes. Enolase, in fact, is shown to act as a plasminogen receptor (68) that promotes fibrinolysis and maintains blood fluidity during blood ingestion and distribution in the tick midgut. Fibrinolysis is the natural process of fibrin clot that might be formed during feeding, as well as preventing clotting of the ingested blood meal in its midgut (69). The higher expression level in OV (10 fold more expressed than in SG) of another enolase (spot 4) was a result apparently in contradiction with the previous one. However, the multifunctionality of this protein in both prokaryotes and eukaryotes may probably account for this founding. In fact, it has been shown in *Rhipicephalus microplus* (70) that, to support the energy intensive processes of embryogenesis, before blastoderm formation, glycogen reserves are preferentially mobilized. As a consequence, protein degradation and gluconeogenesis intensify to supply the embryo with sufficient glucose to allow glycogen re-synthesis. If glycogen is the main energy source during the early stages of *R. microplus* embryogenesis, protein degradation increases during late embryogenesis (70). Thus, the use of amino acids as a substrate for gluconeogenesis and a subsequent glycogen re-synthesis plays an important role during stages of *R. microplus* embryogenesis. Protein metabolism depends strongly on the substantial expression and activity of carbohydrate metabolism enzymes and alpha-enolase is a key glycolytic enzyme (71).

The protein identified under spot 6 was disulfide isomerase (PDI), a 55 kDa multifunctional protein that participates in protein folding, assembly, and post-translational modification in the endoplasmic reticulum (72). The fact that it was 18-fold-more expressed in SG than in OV was not surprising. This protein, together with other saliva enzymes which are putatively associated with antioxidant functions (i.e. glutathion-S-transferase, cytochrome C oxidase, oxidoreductase, NADH dehydrogenase), plays an important role in oxidative stress (73). Tick feeding, in fact, induces injuries and oxidative stress leading to production of reactive oxygen and nitrogen species (ROS and RNS) as part of the wound healing mechanism and anti-microbial defense. Several lines of research have shown that many parasites including ticks are susceptible to ROS and RNS, as revealed by high expression of anti-oxidant enzymes in these parasites or improved survival of these parasites when anti-oxidant system of their hosts are impaired (73). The production of antioxidant enzymes can be considered an evasion mechanism of the immune response used by tick-borne diseases. It is also interesting to note that, given that the tissue destroying effects of oxidative stress products are non-selective, there is a possibility that tick saliva anti-oxidants are protective to host tissue (73).

In conclusion, the results of experiments described in this chapter allowed to establish a method for the characterization of the proteome of *I. ricinus* that was applied to the detection of multiple proteins exhibiting a differential expression. Additionally, the immune-proteomic approach allowed the unambiguous identification of the protein FliD from the *M. mitochondrii* symbiont.

Chapter II

Ixodes ricinus is the most important carrier of vector-borne pathogens in Europe. To have a faster control of this disease vector, a better understanding of the tick and its endosymbiont would be necessary. In this context, genome coding sequences will indeed pave the way for comprehensive proteomic and transcriptomic studies. However, despite the high prevalence in Europe of *I. ricinus*, and the scientific potential of a complete annotated genome, the first reference genome for this species was published only recently by Cramaro et al (16, 74). Thus, in an effort to integrate the "in gel" results and to explore more in depth the relation between *I. ricinus* and *M. mitochondrii*, a high-resolution shotgun proteomic approach was performed. Aim of this chapter is to outline the "state of the art" of proteomic profile of *I. ricinus* and its endosymbiont. This work was carried out at the Institute of Infection & Global Health of the University of Liverpool (UK) where I spent three months to perform the experiments.

Results

1. Overview of protein identification

In this study, I took advantage of the remarkably close relationship between *I. ricinus* and *I. scapularis* to refine MS search database using a proteogenomic approach based on gene predictions from both species (74) (Fig. 16). I identified 2335 (59%) *I. ricinus* proteins, 1571 (39%) *I. scapularis* proteins and 92 (2%) *M. mitochondrii* proteins in 5 stages of engorgement (Fig. 17) (Supplementary materials Table S2).

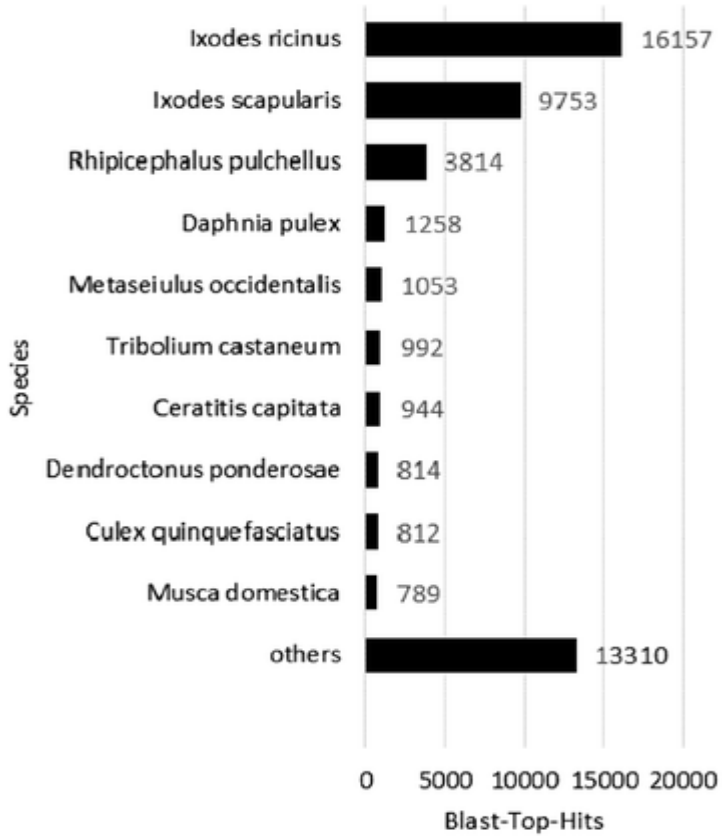

Figure 16. Species were ranked by number of transcriptome contigs with a top hit in the Blast search against NCBI Arthropoda database (74).

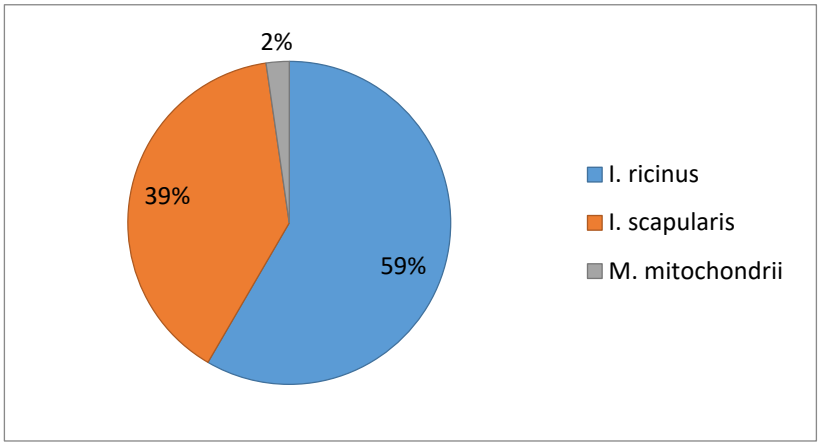

Figure 17. Pie chart of identified proteins ranked in: *I. ricinus (59%), I. scapularis (39%) and M. mitochondrii (2%).*

2. Gene ontology analysis of proteins from *I. ricinus* and *I. scapularis*

As above mentioned, the label free proteomic approach allowed the identification of 2335 *I. ricinus* proteins and 1571 proteins of *I. scapularis*. The GO analysis of these proteins led to their classification into three categories: molecular function, biological process and cellular component. The most prevalent molecular functions were: i) ATP binding, metal ion binding, metalloendopeptidase activity and RNA binding for *I. ricinus* (Fig. 18, panel A) and ii) catalytic activity, binding, hydrolase activity, protein binding, nucleic acid binding and structural molecule binding for *I. scapularis* (Fig. 18, panel B).

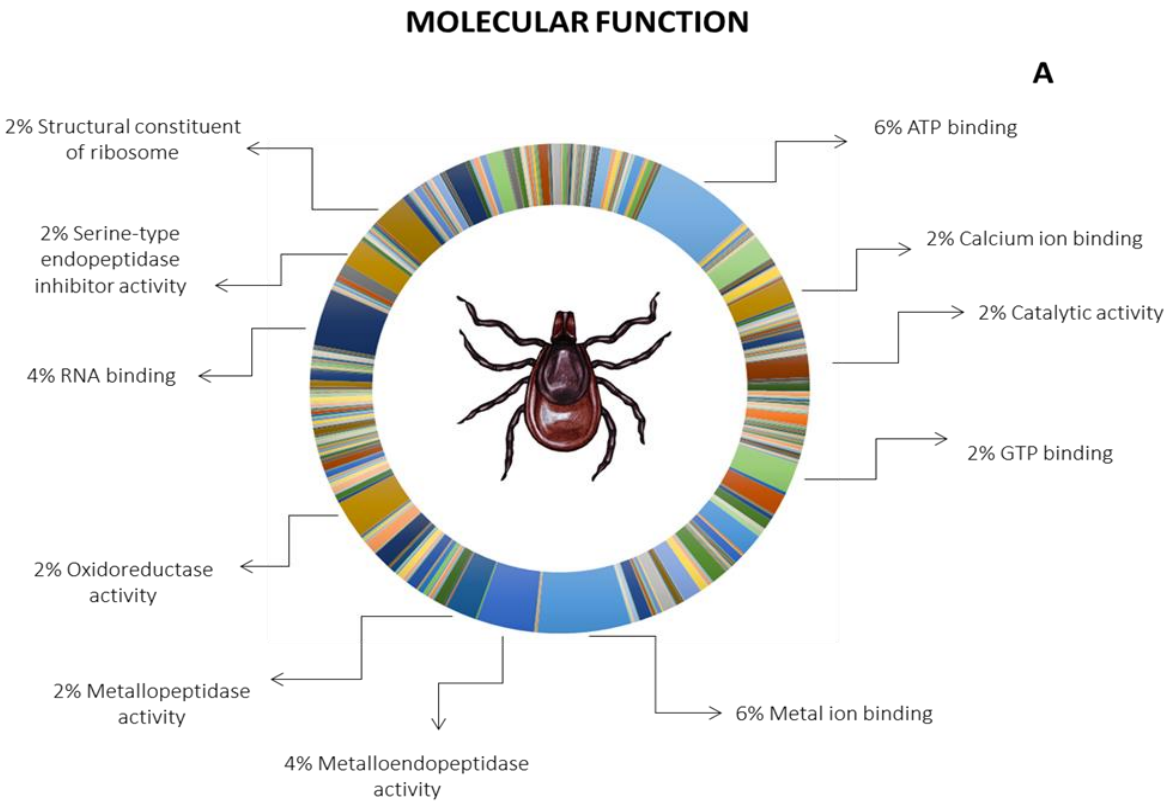
MOLECULAR FUNCTION
A
2% Structural constituent of ribosome
2% Serine-type endopeptidase inhibitor activity
4% RNA binding
2% Oxidoreductase activity
2% Metallopeptidase activity
4% Metalloendopeptidase activity
6% Metal ion binding
2% GTP binding
2% Catalytic activity
2% Calcium ion binding
6% ATP binding

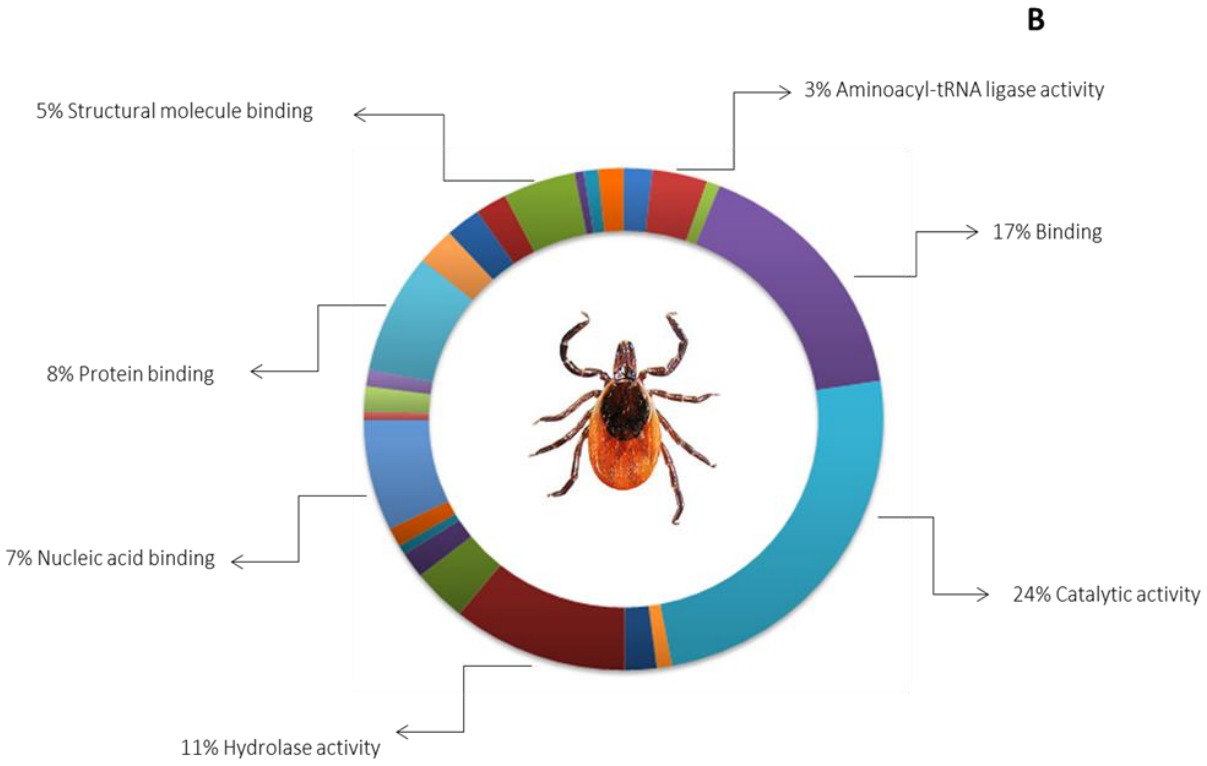

Figure 18. Pie charts of the most representative molecular functions of *I. ricinus* (panel A) and *I. scapularis* (panel B) proteins.

The most considerable biological processes were: i) carbohydrate metabolic processes, evasion of tolerance of host defense response, intracellular protein transport and metabolic processes for *I. ricinus* (Fig. 19, panel A), ii) metabolic and cellular processes, protein metabolic processes, localization and nucleobase containing compound transport for *I. scapularis* (Fig. 19, panel B).

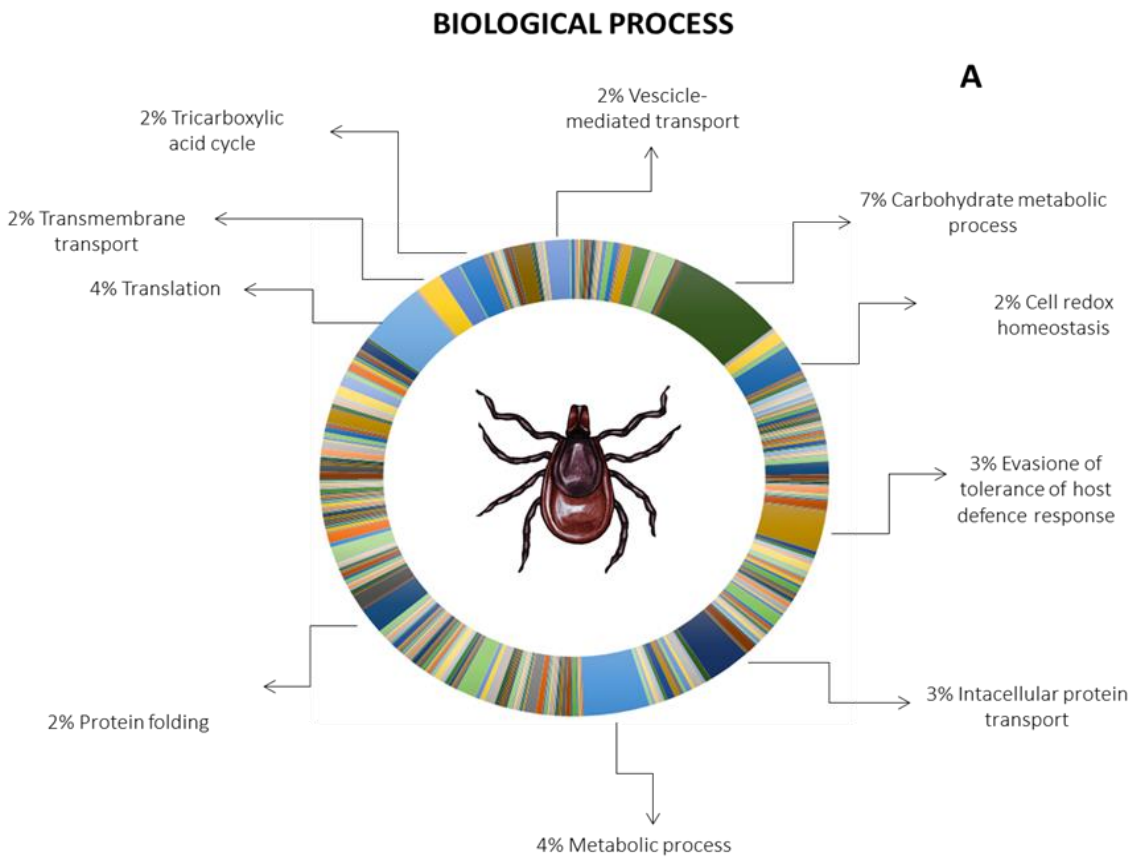
BIOLOGICAL PROCESS
A
2% Vescicle-mediated transport
2% Tricarboxylic acid cycle
7% Carbohydrate metabolic process
2% Transmembrane transport
4% Translation
2% Cell redox homeostasis
3% Evasione of tolerance of host defence response
3% Intacellular protein transport
2% Protein folding
4% Metabolic process

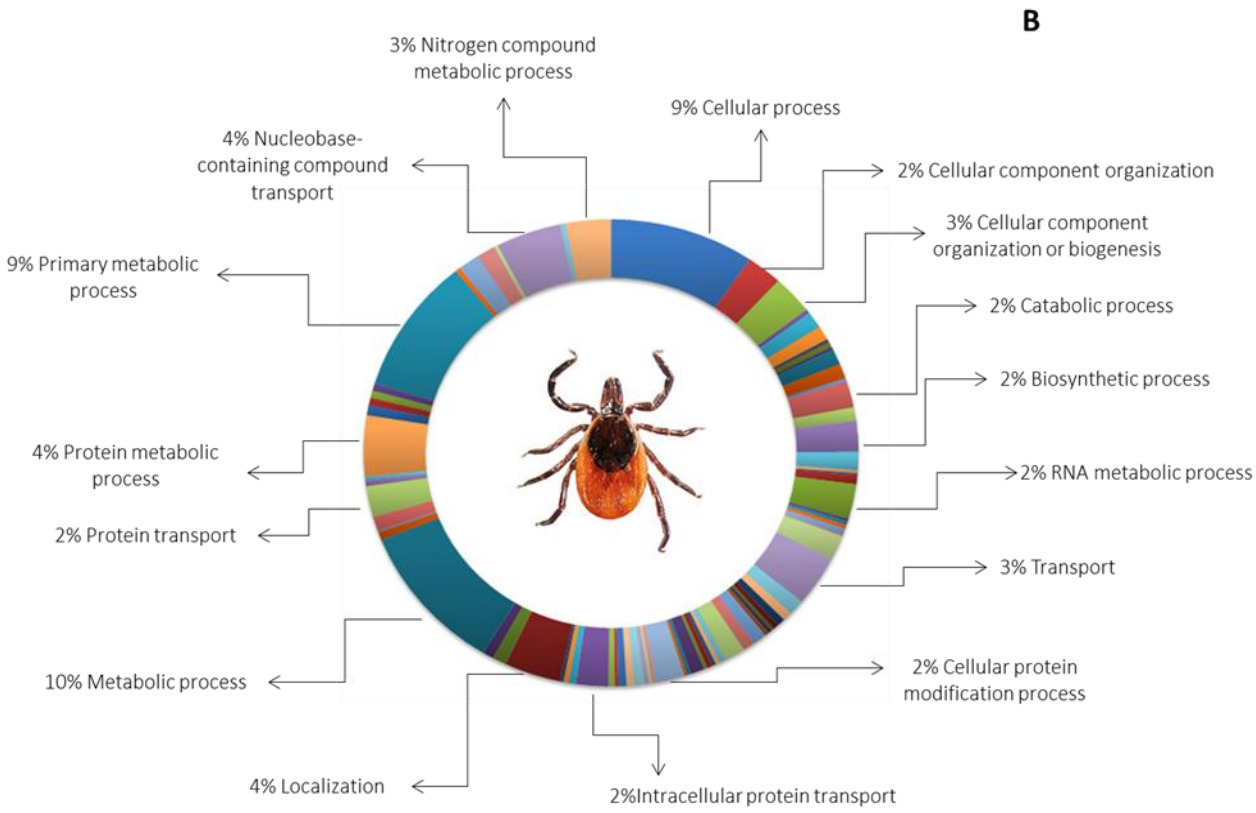

Figure 19. Pie charts of molecular functions of I. *ricinus* (panel A) and *I. scapularis* (panel B) proteins.

Lastly, the predominant cellular components were: i) integral components of membrane, cytoplasm, ribosome, nucleus and intracellular for *I. ricinus* (Fig. 20, panel A) and ii) intracellular, cell part, cytoplasm, organelle and macromolecular complex for *I. scapularis* (Fig. 20, panel B).

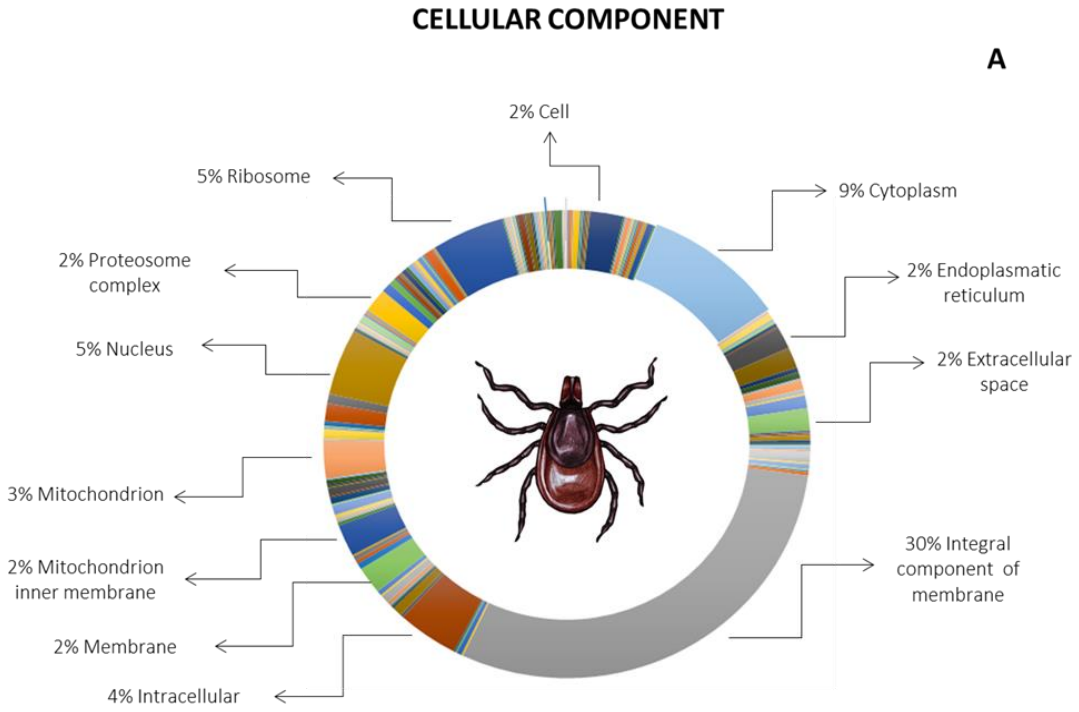
CELLULAR COMPONENT
A
2% Cell
5% Ribosome
9% Cytoplasm
2% Proteosome complex
2% Endoplasmatic reticulum
5% Nucleus
2% Extracellular space
3% Mitochondrion
30% Integral component of membrane
2% Mitochondrion inner membrane
2% Membrane
4% Intracellular

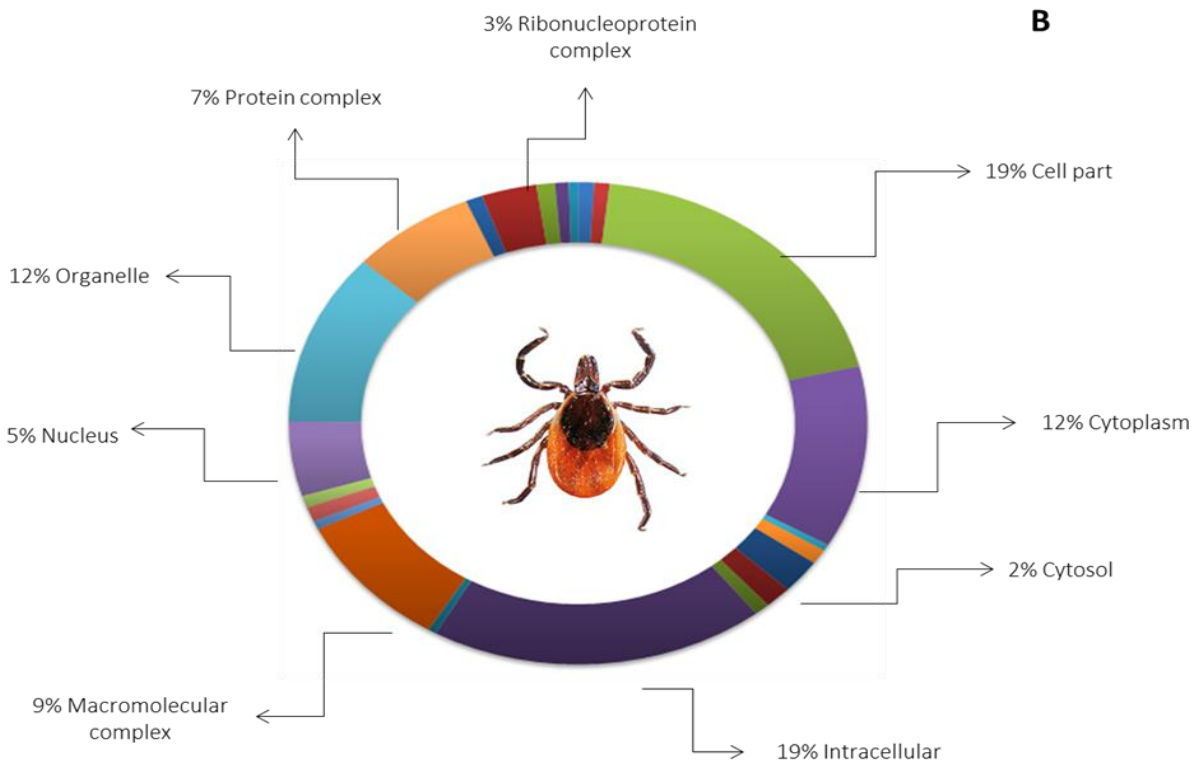

Figure 20. Pie charts of the predominant cellular components of *I. ricinus* (panel A) and *I. scapularis* (panel B) proteins.

3. Proteins of *Ixodes* differentially expressed in ovaries and salivary glands

To understand the patterns of differentially regulated proteins in OV and SG between the different stages of engorgement (from stage 1 to 3) a hierarchical clustering map was built (Fig. 21). All the differentially regulated proteins were mapped to various biological networks using GO annotation.

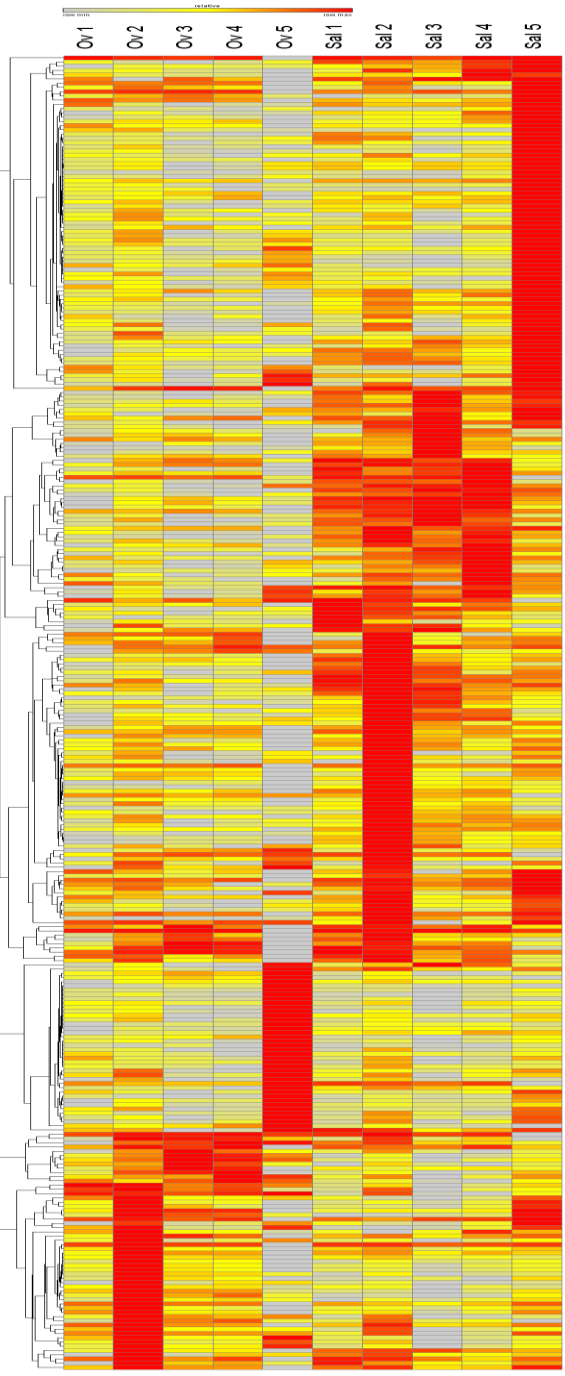

Figure 21. Heat map analysis of differential expressed *Ixodes* proteins in OV and SG in 5 different stages of engorgements, with a p value<0.05. The bar code represents the relative scale of abundance.

4. KEGG pathway analysis of *Ixodes* proteins

The KEGG pathway analysis evidenced the involvement of *Ixodes* proteins in many different pathways. The list of these pathways can be found in table S3 of Supplementary Materials. Sixteen proteins, among those detected, which belonged to a variety of pathways (oxidative phosphorylation, porphyrin metabolism, RNA degradation, DNA replication, proteasome and endocytosis), were identified for the first time. Table 6 summarizes the newly identified proteins, the respective pathways according to KEGG and their accession number.

Table 6. Newly identified proteins, their pathway according to KEGG, name and accession number of proteins.

KEGG PATHWAY	NAME OF THE PROTEIN
Oxidative phosphorylation [isc00190]	**Ndufa7**: Putative nadh: ubiquinone oxidoreductase ndufa7/b14.5a subunit [*Ixodes ricinus*]
	Ndufab1 : Putative acyl carrier protein/nadh-ubiquinone oxidoreductase ndufab1/sdap subunit [*Ixodes ricinus*, JAA71849.1]
	a : ATP synthase F0 subunit 6 (mitochondrion) [*Ixodes ricinus*, AEM23569.1]
	QCR2 : Putative ubiquinol cytochrome c reductase subunit qcr2 [*Ixodes ricinus*, JAB74170.1]
	COX4 : COX4 neighbor protein, putative [*Ixodes scapularis*, EEC00167.1]
	COX6B: cytochrome c oxidase subunit vib isoform 1, partial [*Ixodes ricinus*, JAB80661.1
	F: Putative vacuolar h+atpase v1 sector subunit f *[Ixodes ricinus*, JAA68519.1]

Porphyrin metabolism [isc00860]	**HemA**: putative glutamyl-tRNA synthetase mitochondrial, partial [*Ixodes ricinus*, JAB78034.1]
RNA degradation [isc03018]	**CNOT4**: putative ccr4-not transcription complex subunit 4-like protein, partial [*Ixodes ricinus*, JAB74316.1] **Lsm4**: putative small nuclear ribonucleoprotein snrnp, partial [*Ixodes ricinus*, JAB77406.1]
DNA replication [isc03030]	**MCM4**: putative DNA replication licensing factor mcm4 component [*Ixodes ricinus*, JAB77642.1]
Proteasome [isc03050]	**Rpt1**: Putative 26s proteasome regulatory complex atpase rpt1, partial [*Ixodes ricinus*, JAA73429.1] **Rpt4**: Putative 26s proteasome regulatory complex atpase rpt4 [*Ixodes ricinus*, JAA68966.1] **Rpn12**: Putative 26s proteasome regulatory complex subunit [*Ixodes ricinus*, JAA69645.1] **Rpt5**: putative 26s proteasome regulatory complex atpase rpt5 [*Ixodes ricinus*, JAB82925.1]
Endocytosis [isc04144	**Rab11**: Putative ras-related protein rab-11a [*Ixodes ricinus*, JAA67216.1]

5. Gene ontology analysis of *M. mitochondrii* proteins

The 92 proteins identified in *M. mitochondrii* applying the label free proteomic approach were classified into molecular function, biological process, and cellular components based on gene ontology annotation. The most prevalent molecular function was structural constituent of ribosome (23%) and other functions were: ATP binding (14%), rRNA binding (12%), DNA binding (8%), translation elongation factor activity (5%), tRNA binding (5%) and RNA binding (2%) (Fig. 22, panel A).

The biological processes were represented by: protein translation (39%), protein folding (10%), transcription DNA template (9%), cell redox homeostasis (7%) and tricarboxylic acid cycle (5%) (Fig. 22, panel B). The cellular components involved were: cytoplasm (30%), ribosome (27%), integral components of membrane (11%), cell (7%), small ribosomal subunit (7%), large ribosomal subunit (5%), plasma membrane (5%), proton transporting ATP synthase complex, catalytic core F (1) (4%) and intracellular components (4%) (Fig. 22, panel C).

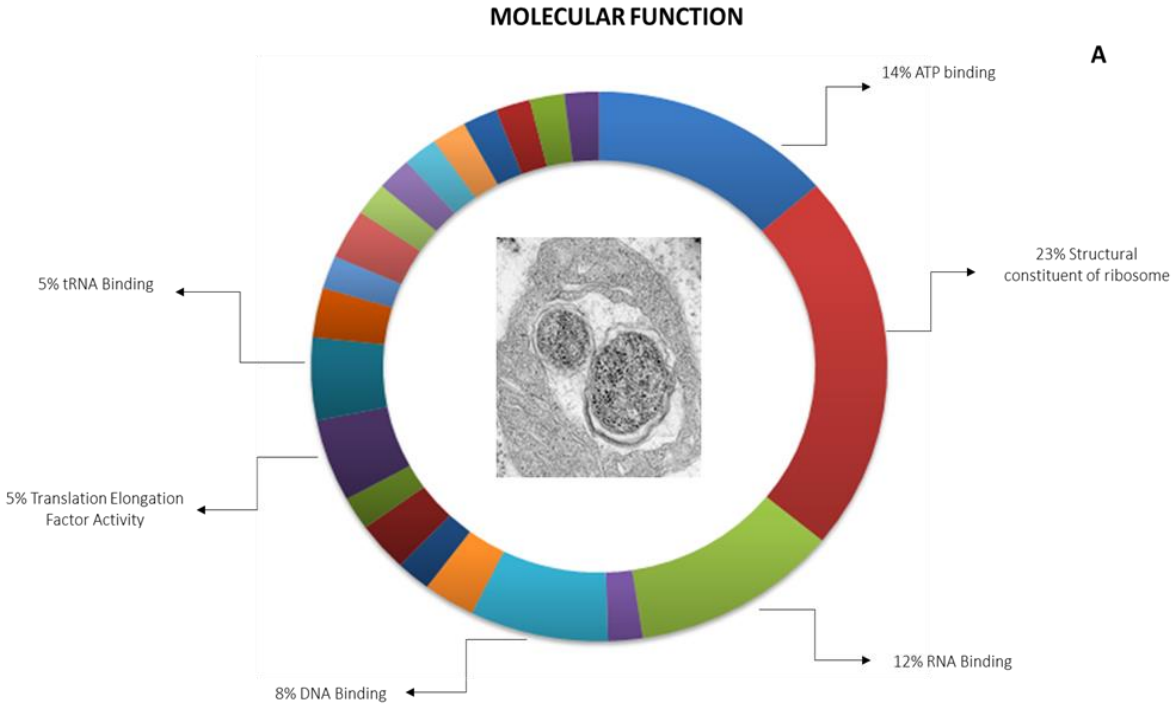
MOLECULAR FUNCTION
A
14% ATP binding
23% Structural constituent of ribosome
12% RNA Binding
8% DNA Binding
5% Translation Elongation Factor Activity
5% tRNA Binding

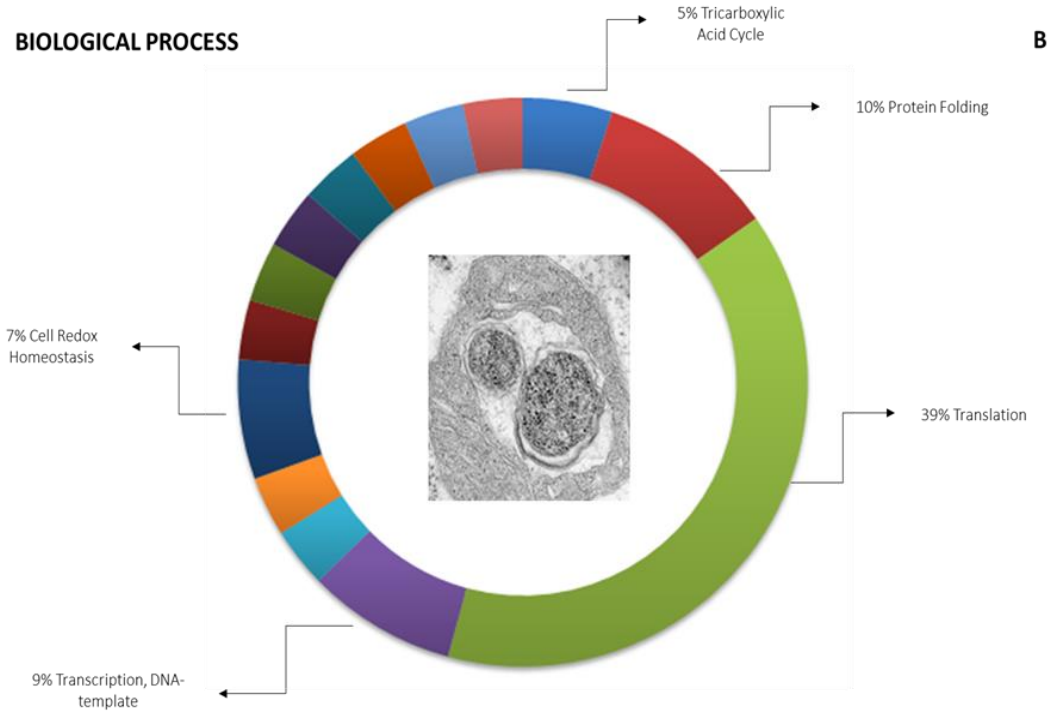
BIOLOGICAL PROCESS
B
5% Tricarboxylic Acid Cycle
10% Protein Folding
39% Translation
9% Transcription, DNA-template
7% Cell Redox Homeostasis

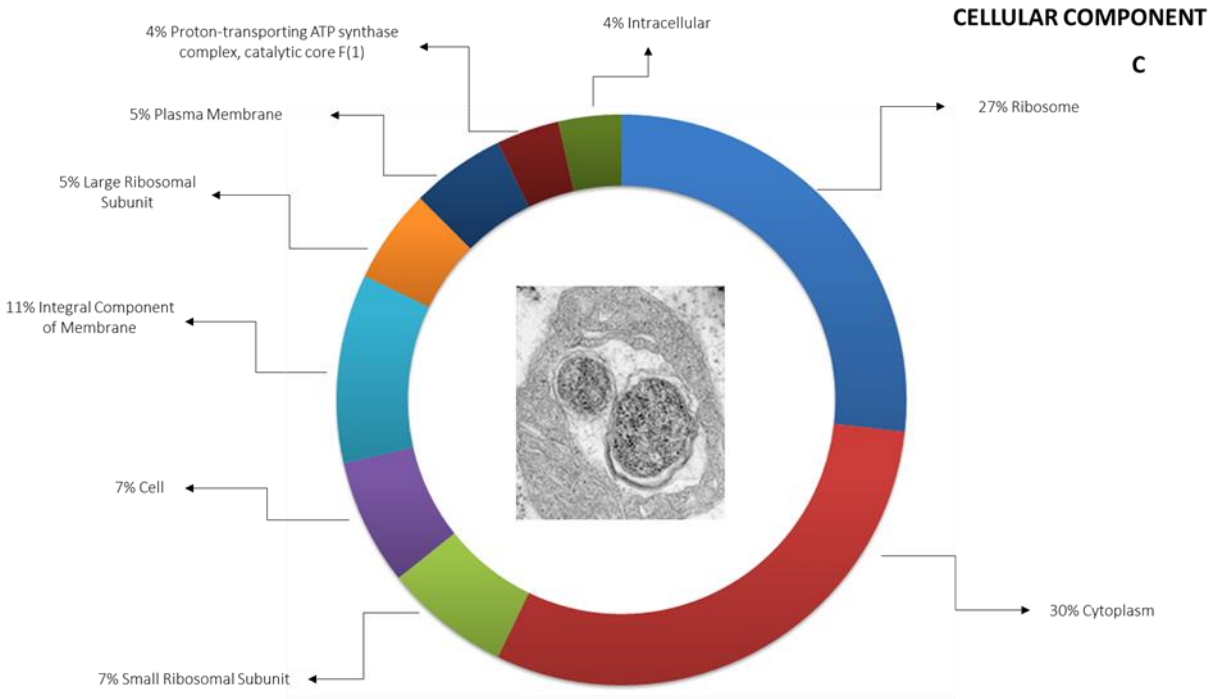

Figure 22. GO annotations of *M. mitochondrii* proteins concerning molecular function (panel A), biological processes (panel B) and cellular components (panel C).

6. Heat map of proteins differentially expressed in endosymbiont

The heat map rows were clustered to highlight proteins with similar or different expression between the different samples (OV and SG) in 5 different stages of engorgement. As shown in figure 23, only the proteins with a p value < 0.05 according to the ANOVA test have been reported.

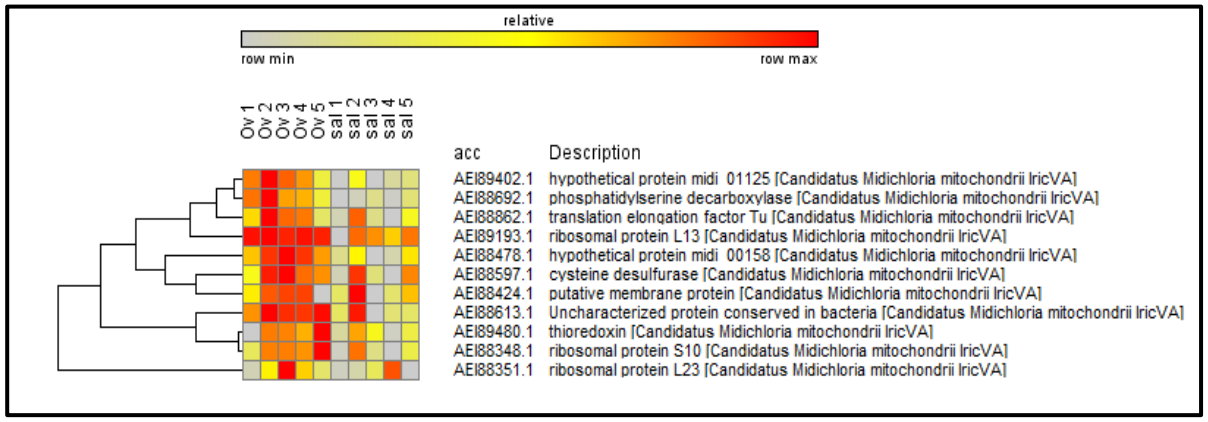

Figure 23. Heat map of differentially expressed proteins of *M. mitochondrii* with a p value<0.05. The bar code represents the relative scale of abundance.

7. KEGG pathway analysis

According to KEGG, the identified proteins were classified into 12 pathways: citrate cycle, oxidative phosphorylation, purine metabolism, pyrimidine metabolism, cysteine and methionine metabolism, glutathione metabolism, pyruvate metabolism, glyoxylate and dicarboxylate metabolism, biotin metabolism, folate biosynthesis, ribosome and RNA polymerase. The general scheme is shown in figure 24.

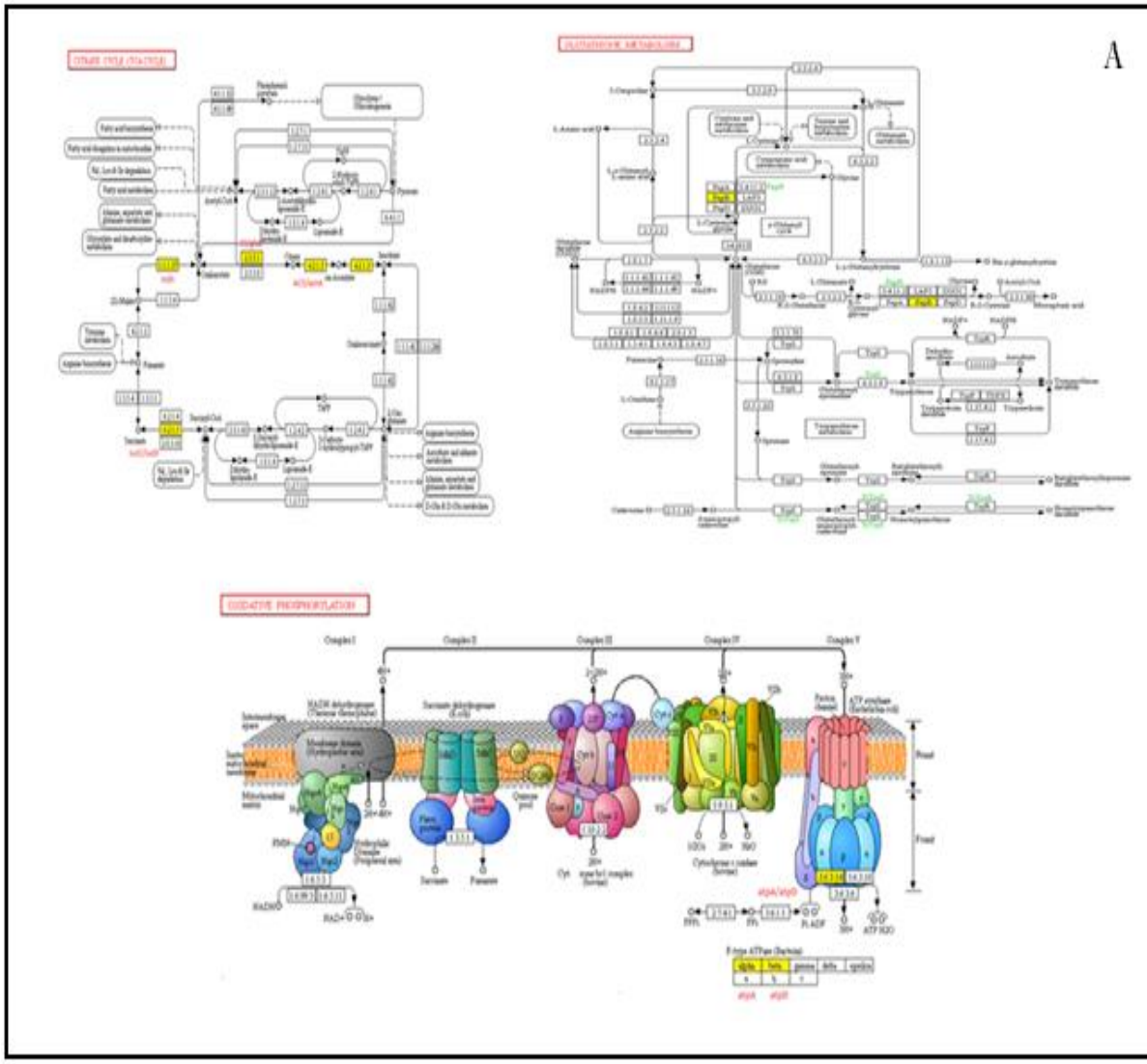
A

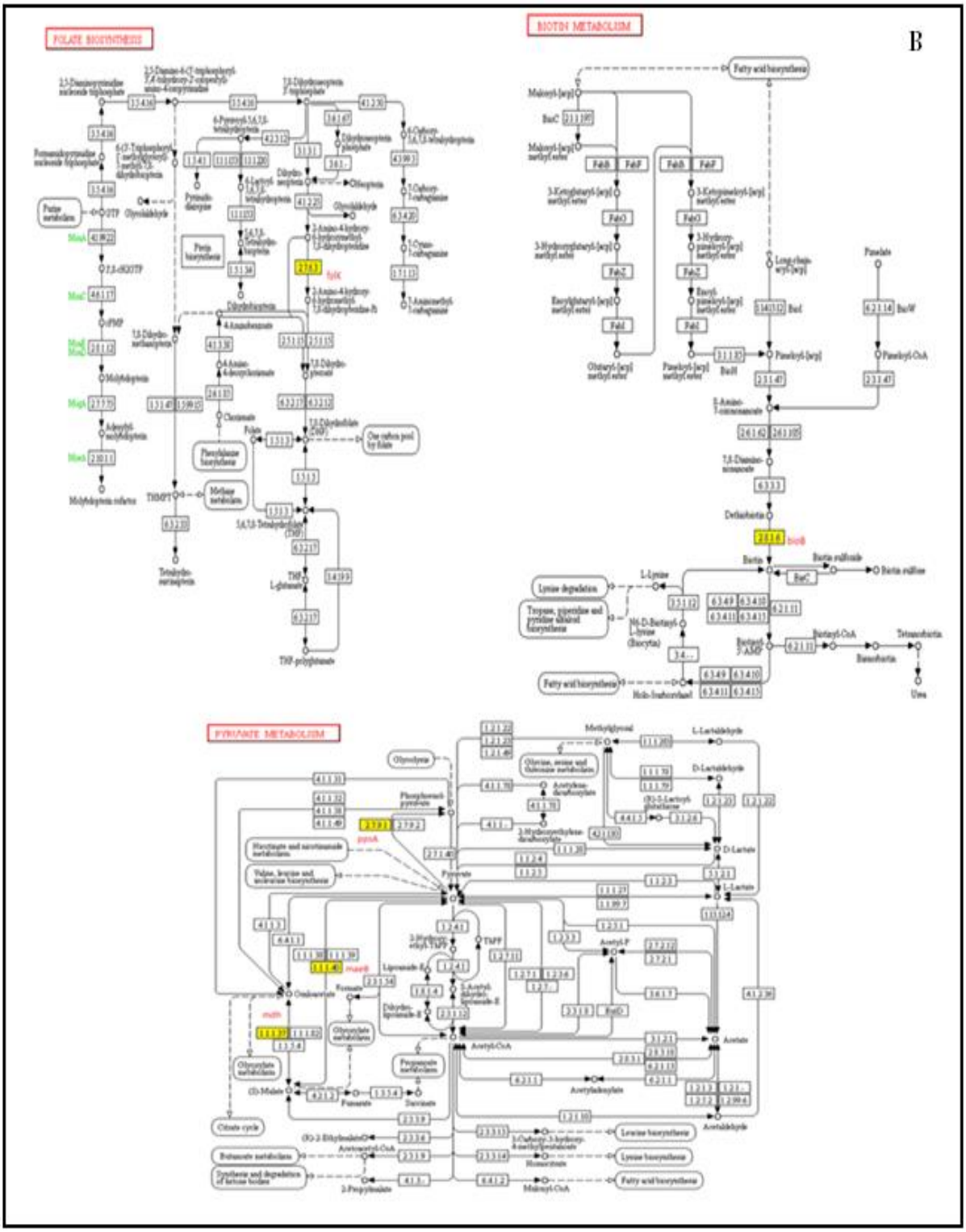
FOLATE BIOSYNTHESIS
BIOTIN METABOLISM
B
PYRUVATE METABOLISM

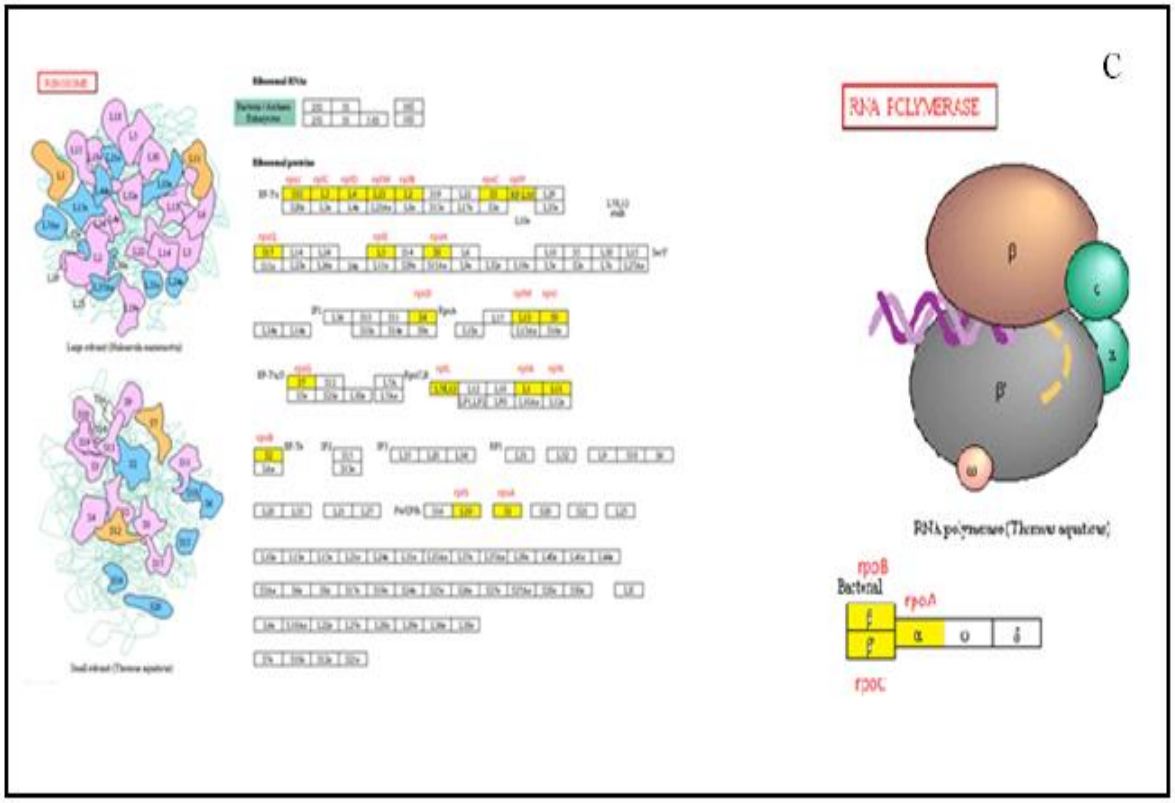

Figure 24. The most representative KEGG pathways. **Panel A** : cytrate cycle, glutathione metabolism and oxidative phosphorilation. **Panel B**: folate metabolism, biotin metabolism and pyruvate metabolism.**Panel C**: ribosome and RNA polymerase. In all panels, the proteins identified in my work have been labelled in yellow.

Discussion

The *I. scapularis* genome is approximately 2.1 Gb in size and contains nearly 70% repetitive DNA (75, 76). The gene counts included 28.486 high confidence protein-coding genes, 316 non-coding genes and 20,771 transcripts (77). While, *I. ricinus* genome size was 2.65 Gb (16) and it was 0.5 Gb or 26% larger than the genome of *I. scapularis*. Among the 25,0000 sequences annotated, hypothetical proteins, zinc finger proteins and metallopeptidases were the largest protein categories. *I. ricinus* scaffolds of high sequencing quality were blast-searched against proteins annotated in *I. scapularis* to match annotations to the *I. ricinus* sequences. More than 50% of *I. ricinus* sequences complied significantly with *I. scapularis* protein sequences, with similar identity distribution in the different protein categories (16). This may demonstrate a high level of protein coding sequences conserved between the two species.

Gut microbiota have an important function in shaping host immunity in a number of organisms, including model arthropods (78). Several studies have established that immune reactivity within the fly gut ensures preservation of beneficial and dietary microorganisms, while mounting robust immune responses to eradicate pathogens (79). There are two models of fly immunity for sensing and preserving beneficial bacterial association while eliminating potentially damaging ones (80). They work together to maintain effective gut microbe homeostasis. The dual oxidase and peroxidase enzymes play a key role in this process (81), while a number of other regulatory molecules (shown in Table 7) may participate in gut homeostasis.

Table 7. List of proteins involved in gut homeostasis and their accession number.

	Name of proteins	**Accession number**
	Putative phospholipid-hydroperoxide glutathione peroxidase, partial [*Ixodes ricinus*]	JAA72909.1
	putative glutathione peroxidase [*Ixodes ricinus*]	JAB71340.1
	thioredoxin peroxidase, putative [*Ixodes scapularis*]	EEC18992.1
	glutathione peroxidase [*Ixodes ricinus*]	ACI49692.1
	Dual oxidase maturation factor, putative [*Ixodes scapularis*]	EEC14047.1

Dual oxidase plays an essential role in gut mucosal immunity and homeostasis (82). It is a member of the nicotinamide adenine dinucleotide phosphate (NADPH) oxidase, NOX family, and is a source of microbicidal reactive oxygen species (ROS) within the fly gut (81). Furthermore, DUOX is able to catalyze the formation of a cellular molecular barrier in the luminal space along the gut epithelial during feeding (83). The barrier decreases the gut

permeability to various immune elicitors protecting the gut microbiota. Further studies on how dual oxidase and peroxidase systems maintain gut microbiota in *I. scapularis* and *I. ricinus* could give novel insights into how pathogens, which are transmitted through ticks, are able to evade the immune system and persist within the vector.

A group of carbohydrate-binding proteins called lectins (84), produced especially in gut, hemocytes or fat bodies, could be key mediators of agglutination, a biological phenomenon by which cells or particles clump together (85). As reported for many arthropod vectors, agglutination has a role: i) in the recognition of receptors for pathogen-associated molecular patterns (86) and ii) in the pathogen-host relationship (87). In *I. ricinus* the hemagglutination was characterized as Ca^{2+} dependent binding, and this activity suggests that lectins may function as recognition molecules of the immune system tick, implying that they could influence the persistence of tick borne, as *B. burgdorferi* (77). Specifically, it was also suggested that the cooperation between lectins and other digestive enzymes facilitates the persistence of Gram-negative bacteria (e.g. *M. mitochondrii*) through the gut lumen. Lectin activities were also documented in salivary glands. According to my data, galectin was over-expressed in SG in the last stage of engorgement. The presence of lectins in SG could influence pathogen transmission; in fact, a tick mannose-binding lectin inhibitor that is produced in the SG has been shown to interfere with the human lectin complement cascade, significantly impacting the transmission and survival of *B. burgdorferi* (88). In conclusion, as shown in table 8, lectins and correlated proteins, could play a role in the immunity of *I. ricinus*.

Table 8. Lectins and correlated proteins with their accession numbers.

Name of protein	Accession number
Putative ferritin [*Ixodes ricinus*]	JAA67728.1
Butative beta-galactosidase [*Ixodes ricinus*]	JAB69297.1
Beta-galactosidase, putative [*Ixodes scapularis]*	EEC01299.1
Galectin, putative [*Ixodes scapularis*]	EEC12826.1
Putative ficolin/ixoderin [*Ixodes ricinus*]	JAA69712.1
Ixoderin B, putative [*Ixodes scapularis*]	EEC11754.1
Hemelipoglycoprotein precursor, putative [*Ixodes scapularis*]	EEC13578.1
Sodium/proton exchanger, putative [*Ixodes scapularis*]	EEC12213.1
Lectin, putative [*Ixodes scapularis*]	EEC17711.1
Mannose-binding endoplasmic reticulum-golgi intermediate compartment lectin [*Ixodes scapularis*]	EEC01036.1

Table 9. Protease inhibitors with their accession numbers.

Name of protein	Accession number
Putative salivary serpin [*Ixodes ricinus*]	JAA66279.1
Putative salivary serpin [*Ixodes ricinus*]	JAA69032.1
Putative salivary serpin, partial [*Ixodes ricinus*]	JAA72940.1
Serpin-4 precursor [*Ixodes ricinus*]	ABI94057.1
Serpin-4 precursor, putative [*Ixodes scapularis*]	EEC19558.1
Putative heparan sulfate proteoglycan 2, partial [*Ixodes ricinus*]	JAB75895.1
Protein disulfide isomerase 1, putative [*Ixodes scapularis*]	EEC04085.1
Putative alkaline phosphatase tissue-nonspecific isozyme [*Ixodes ricinus*]	JAB71539.1
Putative atp-dependent zinc metalloprotease yme1 [*Ixodes ricinus*]	JAB69344.1

In Table 9 different proteins with the activity of specific protease or protease inhibitors have been reported. Proteases, especially serine protease, have a key role in the immune response pathway, including coagulation, antimicrobial peptide synthesis and melanization of pathogens (89). When these proteins are present, clotting factors, that are stored within hemocytes, are readily released into the hemolymph to immobilize the invasive pathogens (90). The group of

serpins contributes to the regulation of inflammation, blood coagulation and complement activation in mammals (91). Mulenga et al. (92) reported the presence of at least 45 serpin genes within the *I. scapularis* genome, most of which are differentially expressed in the gut and salivary glands, and it was speculated that ticks could utilize some of these serpins to manipulate host defense to facilitate tick feeding and subsequent disease transmission. Most recently, a novel serpin, IRS-2, was described in *I. ricinus* (93). IRS-2 was shown to inhibit cathepsin G and chymase, host inflammation and platelet aggregation. Further studies are needed to explore the potentiality of serpins as a targeting antigen for development of a tick vaccine.

Heme and iron homeostasis in most eukaryotic cells is based on a balanced flux between heme biosynthesis and oxygenase-mediated degradation. Unlike most eukaryotes, ticks possess an incomplete heme biosynthetic pathway (94) (Fig. 25). Heme synthesis is a series of eight reactions beginning in the mitochondria by condensation of succinyl coenzyme A with glycine, continuing in cytoplasm, and ending in the mitochondria with the final synthesis of the heme molecule.

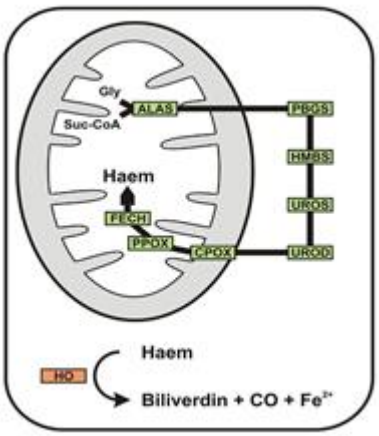

Figure 25. General scheme of heme biosynthetic and degradative pathways in the eukaryotic cell.

The tick genome contains only genes encoding the last three mitochondrial enzymes of heme biosynthesis, namely, coproporphyrinogen-III oxidase, protoporphyrinogen oxidase and ferrochelates. All the three proteins are up-regulated in OV compared to SG and none of other proteins of the pathway was identified in *M. mitochondrii* proteins. One of the future goal will be to understand by which way the tick is able to complete the syntheses and the degradation of heme.

Phagocytosis is a central mechanism in the tissue remodeling, inflammation and defense against infectious agents. A phagosome is formed when the specific receptors on the phagocyte surface recognize ligands on the particle surface. The fusion between phagosomes and lysosomes releases toxic products that destroy most bacteria strategies to escape the bactericidal mechanism associated with phagocytosis and survive within host phagocytes. This process is considered a major evolutionarily conserved cellular immune response in arthropods (95), and is mediated by blood cells, also known as hemocytes, which are primarily present in the hemolymph. Phagocytosis of microbes plays a critical role in the arthropod defense, for example the ability to survive after bacterial infection (96). Table 10 shows some of the proteins involved in the pathway of phagocytosis; further studies would provide insight into whether or how pathogens are phagocytized, as well as how tick-borne pathogens or symbiont, as if *M. mitochondrii*, are able to escape this cellular immune response.

Table 10. Proteins involved in phagocytosis pathway.

Name of protein	Accession number
Putative integrin beta subunit [*Ixodes ricinus*]	JAA73253.1
Putative cadherin egf lag seven pass g-type receptor, partial [*Ixodes ricinus*]	JAB79221.1
Integrin beta subunit, partial [*Ixodes scapularis*]	EEC03623.1
integrin alpha-ps, putative [*Ixodes scapularis*]	EEC04600.1

	Rho GTPase-activating protein RICH2, putative [*Ixodes scapularis*]	EEC03631.1|
	Synaptobrevin 1-2, putative [Ixodes scapularis]	EEC01169.1
	Thrombospondin, putative [*Ixodes scapularis*]	|EEC07256.1

The genome of *M. mitochondrii* consists in a single 1,183,723 bp circular chromosome. Most of the genome content of *M. mitochondrii* is typical of other members of the Rickettsiales (40). Thus, *M. mitochondrii* possesses a relative scarcity of gene encoding amino acid and nucleotide biosynthesis pathways compared with free-living α-proteobacterial relatives. Although *M. mitochondrii* has diminished biosynthetic capabilities, like many others Rickettsiales (97), it does possess genes for the production of several cofactors, including coenzyme A, biotin, lipoic acid, tetrahydrofolate, panthotenate, heme and ubiquinone. *Midichloria mitochondrii* may supply host cells with these essential cofactors. The protein 2-amino-4-hydroxymethyldihydropteridine pyrophosphokinase (folK), is involved in the folic pathway and it was found over-expressed in OV, probably due to the essential functions of folate in cell growth and cell division (98, 99). Folate is required during the period of rapid cell growth and cell division inside hosts, including the engorgement stage after blood meals in arthropod hosts (100). A readily available source of folate synthesized by *M. mitochondrii* may promote rapid cell proliferation not only for the bacterium but also for the tick.

Biotin synthase (bioB) was up-regulated in the last stage of engorgement in SG. BioB is involved in the biotin pathway that synthesizes biotin from 7,8-diaminononanoate. Nikoh et al (101) studied the relationship between the bedbug *Cimex lectularius* and its endosymbiont *Wolbachia*. The lab-strain *C. lectularius* feeded with rabbit blood, supplemented with all B vitamins, showed normal growth and reproduction. When biotin was selectively omitted from the B vitamin supplemented blood meal, the insects exhibited significantly reduced adult emergence rates in comparison with *C. lectularius* reared on the blood meal supplemented with all B vitamins. This confirmed that the biotin synthetic pathway plays an important role in the bedbug fitness. The finding of bioB and enoyl - (acyl-carrier protein)-reductase in *M. mitochondrii* may suggest that the biotin pathway is active and probably the function of the biotin is the same played into *C. lectularius*. This close correlation between the tick and its endosymbiont in terms of fitness, confirms one again the importance of the endosymbiosis.

Midichloria mitochondrii is inferred to have a functional Krebs cycle, gluconeogenesis pathway, and pyruvate dehydrogenase complex, and almost all enzymes required for glycolysis. Aconitate hydratase (acnA), malate/lactate dehydrogenase (mdh), succinyl-CoA synthetase alpha (sucD) and beta subunit (sucC) and citrate synthase I (gltA) were found to be involved in the TCA cycle and Carbon metabolism. These data suggested that the bacterium is able to produce energy for itself and perhaps for the tick, especially during the diapause.

Furthermore, *M. mitochondrii* is able to synthesize ATP. The presence of the protein ATP synthase subunit alpha (atpA) and ATP synthase subunit beta (atpD) that promote ATP/ADP translocase, indicated that it may also be able to import/export ATP from/to host. Like other Rickettsiales, *M. mitochondrii* possesses genes encoding type IV and Sec-independent protein secretion systems, ankyrin repeat proteins, and various putative membrane associated proteins. These genes may be associated with the symbiont's unique ability to invade host mitochondria.

About 30% of identified proteins were ribosomal proteins especially belonging to the large subunit. Moreover, a lot of proteins are involved in the multi-chaperone system, i.e.: ATP-dependent chaperone (clpB), molecular chaperone DnaK (dnaK), molecular chaperone GrpE (grpE) and chaperone protein HtpG (htpG).

Overall, *M. mitochondrii's* genome does not provide a clear answer to the question of whether it is engaged in a mutualistic or parasitic relationship with its tick host.

Chapter III

The presence of the symbiont *M. mitochondrii* in the mammalian host after *I. ricinus* bite and its capacity to induce an antibody response was proven by Bazzocchi *et al* (102). However, whether the inoculation of *M. mitochondrii* could lead to the infection of the host, thus inducing possible pathological alterations, is still unknown. Aim of this chapter is to describe experiments designed at detecting tick and symbiont markers that may produce antigenic molecules. To this purpose, rabbits have been infested with wild *I. ricinus* ticks and with lab strain *I. ricinus* ticks, which did not have *M. Mitochondrii*. This work was performed thanks to a collaboration with the Department of Veterinary of the University of Milan.

Results

1. Experimental infestation

The experiment was carried out on six 10-weeks-old New Zealand White female rabbits that were divided in two groups composed by three individuals each: R1, R2 and R3 parasitized by 20 pathogen-free ticks, and R4, R5 and R6 parasitized with 20 wild ticks each. In both cases, ticks were un-engorged. The ticks were placed on the ear of the rabbit and a cotton ball was stuffed in the inner ear to prevent ticks to fall into it. To study the kinetics of the antibody response against both *M. mitochondrii* and *I. ricinus* SG antigens, nine blood samplings were done, the first indicated as T_0 (7 days before the infestation) and the last as T_8 (16 weeks after infestation), as shown in Table 11.

This study was carried out in strict accordance with good animal care practices recommended by the European guidelines. The protocol was approved by the Ethic Committee for Animal Experiments of the region Pays de la Loire (CEEA PdL 06) (Permit Number: 2015-29).

Table 11. Indication of blood/serum and time of collection**.**

Blood/serum samples	Time of collection
T_0	- 1 week
T_1	+1 week
T_2	+2 weeks
T_3	+3 weeks
T_4	+4 weeks
T_5	+6 weeks
T_6	+8 weeks
T_7	+12 weeks
T_8	+16 weeks

2. PCR and qPCR

The presence of common tick-borne pathogenic bacteria in the DNA samples extracted from SG pools was screened using previously described PCR protocols. Three out of ten wild *I. ricinus* SG pools resulted positive to tick-borne pathogens and were thus excluded from subsequent analysis. The SG pools from the lab strain ticks were all negative for the presence of tested pathogen. qPCR analyses were performed to determine the richest *M. mitochondrii* wild SG pool and to evaluate the *M. mitochondrii* load in the SG pools of lab strain. The pool with the highest *M. mitochondrii* load was chosen for the serological analysis.

3. ELISA assay

The sera sampled from the six rabbits (from T_0 to T_8) were analyzed by ELISA assays. Three different antigens were tested on the sera: i) wild SG protein extract, ii) lab strain SG protein extract and iii) *M. mitochondrii FliD* protein.

ELISA assay using wild SG protein extract on serum indicated that the rabbits infested with lab strain ticks (R1 to R3) presented lower OD values compared to the ones infested with wild *I. ricinus* (R4 to R6). These results are shown in Figure 26.

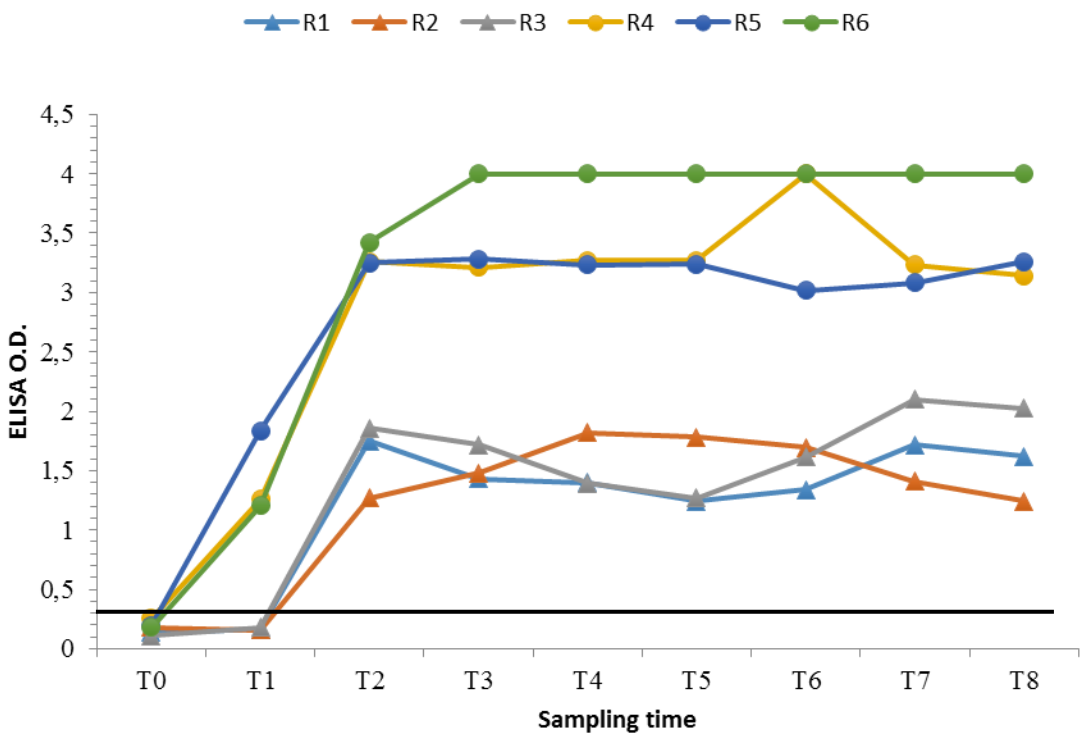

Figure 26. Antibody response, detected by ELISA, against wild *I. ricinus* salivary glands antigens

The second ELISA assay was carried out using the lab strain SG protein extract. The data evidenced no difference between the kinetics of antibody response in the two groups of infested rabbits (Fig. 27).

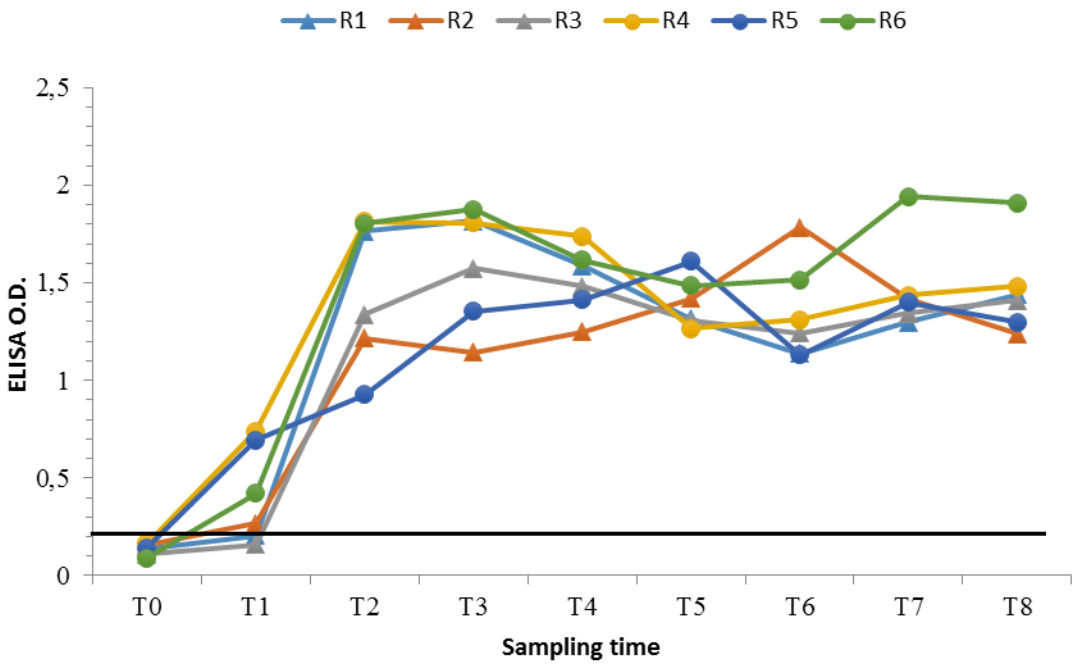

Figure 27. Antibody response, detected by ELISA, against lab strain *I. ricinus* salivary glands antigens

The third ELISA test was performed on sera from rabbits R1-R6 using *M. mitochondrii* FliD protein as antigen. Serum-conversion against FliD could be observed at one week after the infestation with wild *I. ricinus* (Fig. 28).

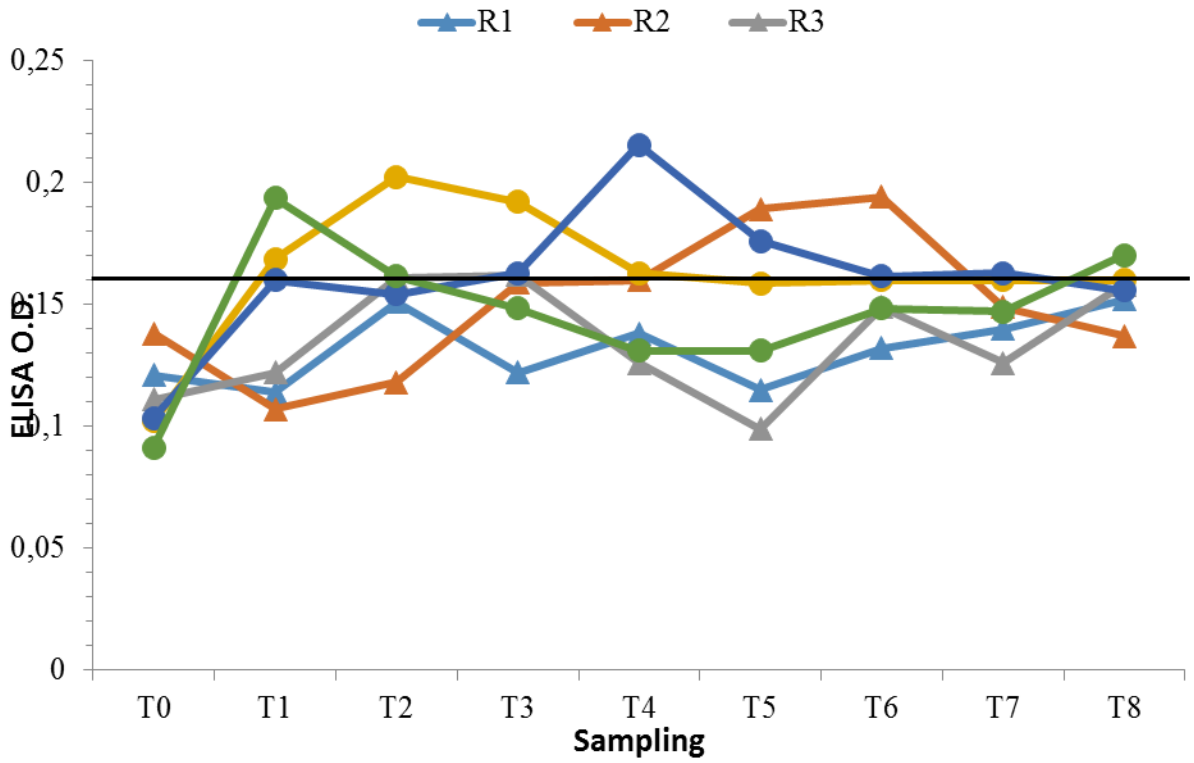

Figure 28. Antibody response, detected by ELISA, against FliD protein.

The antibody response against the flagellar protein seemed to be higher between the first and the fifth week after tick infestation, with a decrease around the end of the screening.

4. 2-DE and Western Blotting analysis

To detect *I. ricinus* proteins immuno-reactive to the sera of rabbits, 2DE followed by Western Blotting analysis was performed. About 100 µg of SG proteins were loaded on 7cm strips, with NL 3-10 pH gradient. Proteins were then transferred onto a PVDF membrane, and incubated with R3 serum at two different times of collection T_0 (- 1 week) and T_5 (+6 weeks) (Fig. 29). The serum choice relapsed on R3, because this was the one showing an optimal kinetics of serum-conversion.

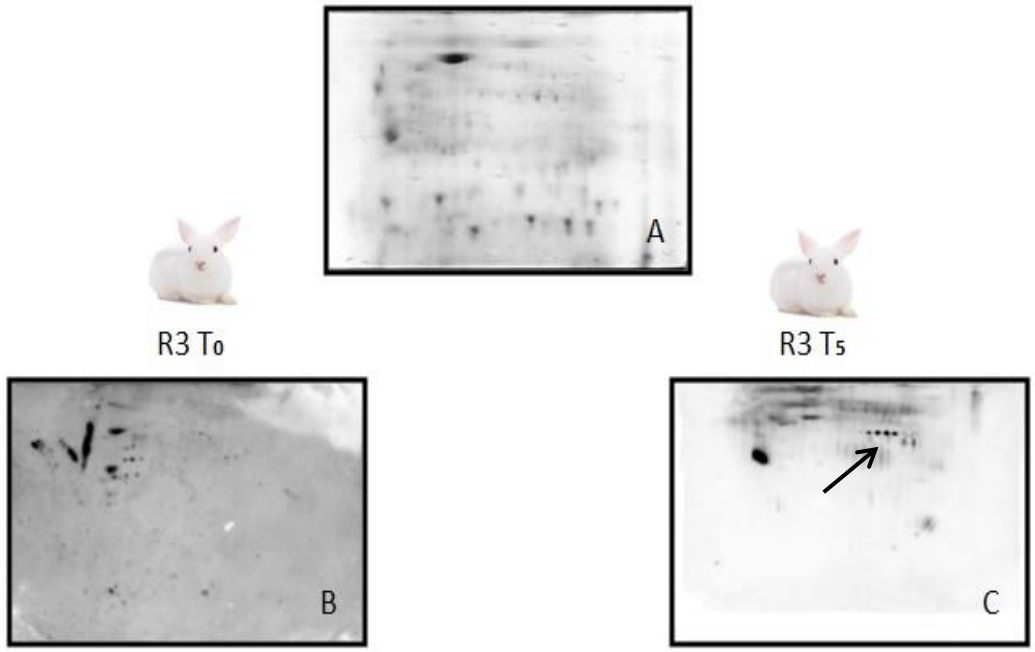

Figure 29. A) 2-DE map of SG obtained by performing IEF on a 3-10 NL pH range and SDS-PAGE on a constant 12,5% T in the second dimension. **B** and **C)** PVDF membrane incubated with serum R3 at T_0 and T_5 respectively. The spots indicated by an arrow in panel C were the immuno-reactive spot after 6 weeks from the bite of wild *I. ricinus*.

5. Identification of immunoreactive spots

To achieve identification of the proteins immuno-reactive to serum after 6 weeks from the bite of wild *I. ricinus*, the positive spots were excised, digested with trypsin and submitted to LC-MS/MS. The results, shown in Table 12, confirmed the presence of a single protein under each spot.

Table 12. List of proteins identified under the immunoreactive spots.

Accession	Description	Score %	pI
gi|556064409|gb|JAB75240.1|	putative cytosol aminopeptidase, partial [*Ixodes ricinus*]	28,39	7,6
gi|442757299|gb|JAA70808.1|	Putative catalase pediculus us corporis catalase [*Ixodes ricinus*]	14,04	8,1
gi|442746363|gb|JAA65341.1|	Putative mitochondrial/plastidial beta-ketoacyl-acp reductase [*Ixodes ricinus*]	11,49	7,4
gi|442749025|gb|JAA66672.1|	Putative metalloprotease [*Ixodes ricinus*]	7,07	6,2

To validate the identified proteins, the antigenic peptide was synthesized. To recognize the antigenic epitopes, three different bioinformatic tools were applied: SVMtrip, Imed and Emboss Antigenic. The results obtained were interesting, and the antigenic peptides, positive in two cases out of three (Table 13), were considered suitable for the synthesis.

Table 13. List of peptides synthesized.

Name of protein	Antigenic Epitope
Putative cytosol aminopeptidase [*I. ricinus*]	AAFLKEFVKAEHWAH VGAFSAVASLGIPIK VAENVRVAISAGVRG
Putative catalase pediculus us corporis catalase [*I. ricinus*]	QDVVFLDEMAHFDRE ITKYCKAAIFNQVGK
Putative mitochondrial/plastidial beta-ketoacyl-acp reductase [*I. ricinus*]	IAFTKSVALELATSG HKLVCYLVFGCLVTG ILHHITPLVKLSEDI
Putative metalloprotease [*I. ricinus*]	CAKKYGYLTSLLDDT

6. Discussion

To determine the time of serum-conversion and to identify immuno-reactive spots, an immuno-proteomic approach was carried out on a vertebrate model parasitized by wild and lab-free *I. ricinus*. ELISA tests performed on SG protein extracts from wild *I. ricinus* showed an interesting trend of serum-conversion in contrast with the data obtained with lab strain ticks. For this reason, the further experiments were done on SG extracts from wild ticks exclusively. The experimental infestation showed the first serum-conversion of a vertebrate model against *I. ricinus* bite. In addition, the western blotting data confirmed that the serum-conversion occurred around the first and the second week with a peak after 6 weeks from tick infections. Although the immuno-reactive spots have been identified, additional studies are needed to develop a possible marker for *I. ricinus* bite detection. To obtain preliminary data the antigenic portions of identified proteins were synthesized. This work is still in progress.

Most likely, the antigenic epitopes could help in the future to design vaccine components and immuno-diagnostic reagents.

Conclusions

This proteomic study aimed to widen the characterization of the proteome of *I. ricinus* and its endosymbiont *M. mitochondrii*. In particular, I carried out two complementary "in gel" and "of gel" approaches on the principal tissues containing *M. mitochondrii*.

Upon the application of 2DE followed by LC-MS/MS a total of 47 proteins, 27 from OV and 20 from SG have been identified. Among the common proteins, 21 were found differentially expressed with a pvalue < 0.01. In addition, an immunoproteomic approach confirmed the presence of the symbiont inside SG and OV (103).

In an effort to integrate the "in gel" results and to explore more in depth the relation between *I. ricinus* and *M. mitochondrii*, a high-resolution shotgun proteomic approach was also performed. A whole of 3998 proteins were identified, of which 3906 belonging to *I. ricinus* and 92 to the symbiont. To understand the role of these proteins, different bioinformatics tools (e.g. GO, PANTHER, KEGG) were applied. Sixteen proteins, among those detected for *I. ricinus*, which belonged to a variety of pathways, were identified for the first time. A huge number of tick proteins were involved in the gut homeostasis, agglutination, protease inhibition, iron homeostasis, phagocytosis and energetic pathway. The *M. mitochondrii* proteins were implicated in the folic pathway, biotin synthesis, TCA cycle, ATP synthesis and carbon metabolism.

These data suggested that the bacterium was able to produce energy for itself and for the host especially during diapause, but none of these data provided a complete answer about the endosymbiotic relationship between *M. mitochondrii* and tick.

Lastly, to develop a serological test to detect whether a human or animal subject was parasitized by *I. ricinus*, I designed an immunoproteomic experiment with infested rabbits. The experimental infestation showed the first seroconversion of a vertebrate model against *I. ricinus* but, although the immunoreactive spots have been identified, additional studies are needed to develop a possible marker for *I. ricinus* bite detection.

In conclusion, my thesis work introduces a methodological framework that will pave the way for the future studies on the proteomics of *I. ricinus*, with the goal of better understanding the biology of this vector and its endosymbiont *M. Mitochondrii*. It also intends to become the

basis of immunoproteomic approaches that could prove useful for detecting novel antigenic proteins for innovative diagnostic and vaccination approaches.

References

1. Sonenshine DE. Biology of ticks. Vol 1. New York: Oxford University Press, 1991.
2. Gubler DJ. The global pandemic of dengue/dengue haemorrhagic fever: current status and prospects for the future. Ann Acad Med Singapore. 1998, 27:22-34.
3. Parola P, Raoult D. Tick and tickborne bacterial diseases in humans: an emerging infectious threat. Clin Infect Dis. 2001, 32: 897-928.
4. Mohamed A. Roshdy; Harry Hoogstraal; Abdulelah A. Banaja; Samir M. El Shoura (1983). "Nuttalliella namaqua (Ixodoidea: Nuttalliellidae): spiracle structure and surface morphology". Parasitology Research. 69(6): 817–821. doi:10.1007/BF00927431.
5. Hoogstral H, Aeschlimann A. Tick-host specificity. Bull Soc Entomol Suisse 1982; 55:5–32
6. Johnson RC, Schmid GP, Hyde FW, Steigerwalt AG, Brenner DJ. Borrelia burgdorferi sp. nov.: etiological agent of Lyme disease. Int J Syst Bacteriol 1984; 34:496–7.
7. Guglielmone, A.A., Robbins, R.G., Apanaskevich, D.A., Petney, T.N., Estrada-Pena, A, Horak, I.G., Shao, R.F., Barker, S.C., 2010. The Argasidae, Ixodidae and Nutalliellidae (Acari: Ixodida) of the world: a list of valid species names. Zootaxa 2528, 1–28.
8. Jongejan, F., Uilenberg, G., 2004. The global importance of ticks. Parasitology 129, S3–14.
9. Kiszewski, A.E., Matuschka, F.R., and Spielman, A., Mating strategies and spermiogenesis in ixodid tick. Annu Rev Entomol 46: 167-182 2001.
10. Socolovschi C, Mediannikov O, Raoult D, Parola P. The relationship between spotted fever group Rickettsiae and ixodid ticks. Vet Res, 2009; 40, 34.
11. Perronne C. Lyme and associated tick-borne disease: global challenges in the context of a public health threat. Front Cell Infect Microbiol. 2014; 3: 74.
12. Gray js, Dautel H, Estrada- Peña A, Kahl O, Lindgren E. Effects of climate change on ticks and tick-borne diseases in Europe. Interdiscip Perspect Infect Dis. 2009; 2009:593232. doi: 10.1155/2009/593232. Epub 2009 Jan 4.
13. Estrada-Pena A, de la Fuente. The ecology of ticks and epidemiology of tick-borne viral disease. Antiviral Res. 2014, 108: 104-28
14. Jaenson TG, Jaenson DG, Eisen L, Petersson E, Lindgren E. Changes in the geographical distribution and abundance of the tick Ixodes ricinus during the past 30 years in Sweden. Parasit. Vectros 2012, 5:8.
15. Zakovska A, Nejezchlebova H, Bartonkova N, Rosovka T, Kucerova H, Norek A, Ovesna P. Activity of the tick Ixodes ricinus monitored in a suburban park in Brno, Czech

Republic, in association with the evaluation of selected repellents. J Vector Ecol. 2013; 38: 295-300. doi: 10.1111/j.1948-7134.2013.12043.
16. Cramaro WJ, Hunewald OE, Bell-Sakyi L, Muller CP. Genome scaffolding and annotation for the pathogen vector Ixodes ricinus by ultra-long single molecule sequencing. Parasit Vectors. 2017 Feb 8; 10(1):71. doi: 10.1186/s13071-017-2008-9.
17. Rizzoli A, Silaghi C, Obiegala A, Rudolf I, Hubàlek Z, Földvàri G, et al. Ixodes ricinus and its transmitted Pathogens in Urban ann Peri-urban Areas in Europe: New Hazards and Relevance for Public Health Front Public Health. 2014, 2:251.
18. Sassera D, Beninati T, Bandi C, Bouman EA, Sacchi L, Fabbi M, Lo N. "Candidatus Midichloria mitochondrii", an endosymbiont of the tick Ixodes ricinus with a unique intramitochondrial lifestyle. Int J Syst Envol Microbiol 2006; 56, 2535-2540.
19. Hillyard PD. In: Barns RSK, Crothers JH, eds. Ticks of north-west Europe. Shrewsbury, UK: Field Studies Council, 1996.
20. Mejlon HA, Jaenson TG (1997) Questing behaviour of Ixodes ricinus ticks (Acari: Ixodidae). Exp Appl Acarol 21(12):747–754. doi:10.1023/A:1018421105231.
21. Talleklint L, Jaenson TG (1994) Transmission of Borrelia burgdorferi sl from mammal reservoirs to the primary vector of Lyme borreliosis, Ixodes ricinus (Acari: Ixodidae), Sweden. J Med Entomol 31(6):880–886. doi:10.1093/jmedent/31.6.880.
22. Gern L, Estrada-Pena A, Frandsen F, Gray JS, Jaenson TGT, Jongejan F, Kahl O, Korenberg E, Mehl R, Nuttall PA (1998) European reservoir hosts of Borrelia burgdorferi sensu lato. Zentralblat Bakteriol 287(3):196–204. doi:10.1016/S0934-8840(98)80121-7.
23. Cadenas FM, Rais O, Humair PF, Douet V, Moret J, Gern L (2007) Identification of host bloodmeal source and Borrelia burgdorferi sensu lato in field-collected Ixodes ricinus ticks in Chaumont (Switzerland). J Med Entomol 44(6):1109–1117. doi:10.1093/jmedent/44.6.1109.
24. Sonenshine DE. Biology of ticks. Vol 2. New York: Oxford University Press, 1993.
25. Harvey WT, Martz D. Motor neuron disease recovery associated with IV ceftriaxone and anti-Babesia therapy. Acta Neurol Scand. 2007, 115: 129-131.
26. Steere AC. Borrelia burgdorferi (Lyme disease, Lyme borreliosis). In: Mandel GL, Bennett JE, Dolin R, eds. Mandell, Douglas, and Bennett's principles and practice of infectious diseases. New York: Churchill Livingstone, 2000:2504–18.
27. Nadelman BN, Wormser GP. Lyme borreliosis. Lancet 1998; 352: 557–65.
28. Brown SL, Hansen SL, Langon JJ. Role of serology in the diagnosis of Lyme disease. JAMA 1999; 282:62–6.
29. Pahl A, Ku¨hlbrandt U, Brune K, Ro¨llinghoff, Gessner A. Quantitative detection of Borrelia burgdorferi by real-time PCR. J Clin Microbiol 1999; 37:1958–63.

30. Thanassi WT, Schoen RT. The Lyme disease vaccine: conception, development, and implementation. Ann Intern Med 2000; 132:661–8.
31. Evans ME, Gregory DW, Schaffner W, McGee ZA. Tularemia: a 30- year experience with 88 cases. Medicine (Baltimore) 1985; 64:251–69.
32. Dumler JS, Bakken JS. Human ehrlichiosis: newly recognized infections transmitted by ticks. Annu Rev Med 1998; 49:201–13.
33. Comer JA, Nicholson WL, Sumner JW, Olson JG, Childs JE. Diagnosis of human ehrlichiosis by PCR assay of acute phase serum. J Clin Microbiol 1999; 37:31–4.
34. Cheng TC. Is parasitism symbiosis? A definition of terms and the evolution of concepts. In: Toft CA, Aeschlimann A, Bolis L, eds. Parasite-host associations: coexistence or conflict? New York: Oxford University Press, 1993:15–36.
35. Lewis, D. The detection of rickettsia-like microorganism within the ovaries of female Ixodes ricinus ticks. Z Parasitenkd. 1979, 59: 295-298.
36. Sacchi L, Bigliardi E, Corona S, Beninati T, Lo N, and Franceschi A. A symbiont of the tick Ixodes ricinus invades and consumes mitochondria in a mode similar to that the parasitic Bdellovibrio bacteriovorus. Tissue Cell. 2004, 36: 43-53.
37. Lo N, Beninati T, Sassera D, Bouman E.A.P., Santagati S., Gern L., Sambri V., Masuzawa T, Gray J.S. Jaenson T.G.T., Bouattour A., Kenny M.J., Guner E.S., Kharitonenkov I.G., I. Bitam, Bandi C. Widespread distribution and high prevalence of an alpha-proteobacterial symbiont in the tick Ixodes ricinus. Environ Microbiol. 2006, 8, 1280-1287.
38. Mariconti M, Epis S, Gaibani P, Della Valle C, Sassera D, Tomao P, Fabbi M, Castelli F, Marone P, Sambri V, Bazzocchi C, Bandi C. Humans parasitized by the hard ticks Ixodes ricinus are seropositive to Midichloria mitochondrii: is Midichloria a novel pathogen, or just a marker of tick bite? Pathog Glob Health. 2012 Nov;106(7):391-6. doi: 10.1179/2047773212Y.0000000050.
39. Sassera D, Lo N, Bouman E.A.P., Epis S, Mortarino M, Bandi C. Appl Environ Microbiol. 2008 Oct;74(19):6138-40. doi: 10.1128/AEM.00248-08. Epub 2008 Aug 8
40. Sassera D, Lo N, Epis S, D'Auria G, Montagna M, Comandatore F, Horner D, Peretó J, Luciano AM, Franciosi F, Ferri E, Crotti E, Bazzocchi C,Daffonchio D, Sacchi L, Moya A, Latorre A, Bandi C. Phylogenomic evidence for the presence of a flagellum and cbb (3) oxidase in the free-living mitochondrial ancestor. Mol Biol Evol. 2011 Dec;28(12):3285-96. doi: 10.1093/molbev/msr159. Epub 2011 Jun 20.
41. Michelet L, Delannoy S, Devillers E, Umhang G, Aspan A Et al. High-throughput screening of tick-borne pathogens in Europe. Front Cell Infect Microbiol. 2014, 29:4-103. Doi: 10.3389/fcimb.2014.00103

42. Pistone D, Pajoro M, Fabbi M, Vicari N, Marone P, Genchi C et al. Lyme borreliosis, Po river Valley, Italy. Emerg Infect Dis. 2010; 16: 1289-1291. doi: 10.3201/eid1608.100152PMID:20678327
43. Pesquera C, Portillo A, Palomar AM, Oteo JA. Investigation of tick-borne bacteria (Rickettsia spp., Anaplasma spp., Ehrlichia spp., and Borrelia spp.) in ticks collected from Andean tapirs, cattle and vegetation from a protected area in Ecuador. Parasit Vectros. 2015, 24:26.
44. Smith PK, Krohn RI; Hermanson GT, Mallia AK, Gartner FH, Provenzano MD, et al Measurement of protein using bicinchoninic acid. Anal.Biochem. 1985; 150: 76-85 PMID: 3843705.
45. Candiano G, Bruschi M, Musante L, Santucci, Ghiggeri GM, Carnemolla B, et al. Blue silver: a very sensitive colloidal Coomassie G-250 staining for proteome analysis. Electrophoresis. 2004; 25: 1327-1333. PMID:15174055.
46. Von Mering C, Huynen M, Jaeggi D, Schmidt S, Bork P, Snel B. STRING: a database of predicted functional associations between proteins. Nucleic Acids Res. 2003; 31: 258-261.
47. Szkarczyk D, Franceschini A, Kuhn M, Simonovic M, Roth A, Minguez P, Doerks T, Stark M, Muller J, Bork P. Jensen L.J. and von Mering C. The String Database in 2011: functional interaction networks of protiens, globally integrated and scored. Nucleic Acids Res. 2011; 39: D561-D568.
48. Mi H, Poudel S, Muruganujan A, Casagrande JT, Thomas PD. PANTHER version 10: expanded protein families and functions, and analysis tools. Nucleic Acids Research. 2016;44(Database issue): D336-D342. doi:10.1093/nar/gkv1194.
49. Kanehisa M. The KEGG database. Novartis found Symp. 2002; 247:91-101; Discussion 101-3, 119-28, 244-52.
50. Kanehisa M, Goto S, Sato Y, Furumichi M, Tanabe M. KEGG for integration and interpretation of large scale molecular data sets. Nucleic Acids Res. 2012; 40: 109-114.
51. Atlman T, Travers M, Kothari A, Caspi R, Karp PD. A systemic comparison of the MetaCyc and KEGG pathway databases. BMC Bioinformatics. 2013; 14: 112.
52. Vu Hau V, Pages F, Boulanger N, Audebert S, Parola P, Almeras L. Immunoproteomic identification of antigenic salivary biomarkers detected by Ixodes ricinus exposed rabbit sera. Ticks Tick Borne Dis. 2013; 4:459-468.
53. Schwartz, I, Fish D, Daniels TJ. Prevalence of the rickettsial agent of human granulocytic ehrlichiosis in ticks from a hyperendemic focus of Lyme disease. N Engl J Med 1997; 337:49–50.
54. Cotté V, Sabatier L, Schnell G, Carmi-Leroy A, Rousselle JC, Arsène-Ploetze F, Malandrin L, Sertour N, Namane A, Ferquel E, Choumet V. Differential expression of

Ixodes ricinus salivary gland proteins in the presence of the Borrelia burgdorferi sensu lato complex. J Proteomics. 2014 Jan 16;96:29-43. doi: 10.1016/j.jprot.2013.10.033. Epub 2013 Nov 2.

55. Mayer MP, Bukau B. Hsp70 chaperones: cellular functions and molecular mechanism. Cell Mol Life Sci. 2005, pp.670-684
56. Rinehart JP, Li A, Yocum GD, Robich RM, Hayward SAL, Denlinger DL. Up-regulation of heat shock proteins is essential for cold survival during insect diapause. Proceedings of the National Academy of Sciences of the United States of America. 2007;104(27):11130-11137. doi:10.1073/pnas.0703538104.
57. Busby, A. T., Ayllón, N., Kocan, K. M., Blouin, E. F., De La Fuente, G., Galindo, R. C., Villar, M. And De La Fuente, J. (2012), Expression of Heat Shock Proteins and Subolesin Affects Stress Responses, Anaplasma Phagocytophilum Infection and Questing Behaviour in The Tick, Ixodes Scapularis. Medical and Veterinary Entomology, 26: 92–102. Doi:10.1111/J.1365-2915.2011. 00973.X
58. Sonenshine DE, Hynes WL. Molecular characterization and related aspects of the innate immune response in ticks. Front Biosci. 2008 May 1; 13:7046-63.
59. Narasimhan S, Montgomery RR, DePonte K, et al. Disruption of Ixodes scapularis anticoagulation by using RNA interference. Proceedings of the National Academy of Sciences of the United States of America. 2004;101(5):1141-1146. doi:10.1073/pnas.0307669100.
60. Cameron LA, Giardini PA, Soo FS, Theriot JA. Secrets of actin-based motility revealed by a bacterial pathogen. Nat Rev Mol Cell Biol. 2000 Nov;1(2):110-9.
61. Gouin E, Welch MD, Cossart P Actin-based motility of intracellular pathogens. Curr Opin Microbiol. 2005 Feb;8(1):35-45.
62. Stevens JM, Galyov EE, Cossart P. Actin-dependent movement of bacterial pathogens. Nat Rev Microbiol. 2006; 8: 35-49. PMID: 16415925.
63. Horigane M, Ogihara K, Nakajima Y, Honda H, Taylor D. Identification and expression analysis of an actin gene from the soft ticks, Ornithodoros moubata (Acari: Argasidae). Arch Insect Biochem Physiol, 2007; 64: 188-199. PMID:8805079.
64. Schwan TG. Ticks and Borrelia: model systems for investigating pathogen-arthropod interactions. Infect Agents Dis. 1996 Jun;5(3):167-81.
65. Dumler JS, Bakken JS. Human ehrlichiosis: newly recognized infections transmitted by ticks. Annu Rev Med 1998; 49:201–13.
66. Amit P. Bhavsar, Julian A. Guttman1,2 & B. Brett Finlay1 Manipulation of host-cell pathways by bacterial pathogens. Nature 449, 827-834 (18 October 2007) | doi:10.1038/nature06247; Published online 17 October 2007

67. Pancholi V.Multifunctional alpha-enolase: its role in diseases. Cell Mol Life Sci. 2001 Jun;58(7):902-20
68. Xu, XL., Cheng, TY. & Yang, H. Parasitol Res (2016) 115: 1955. doi:10.1007/s00436-016-4938-0
69. Maritz-Olivier C, Stutzer C, Jongejan F, Neitz AW, Gaspar AR. Tick anti-hemostatics: targets for future vaccines and therapeutics. Trends Parasitol. 2007 Sep;23(9):397-407. Epub 2007 Jul 26.
70. Moraes J, Galina A, Alvarenga PH, Rezende GL, Masuda A, da Silva Vaz I Jr, Logullo C. Glucose metabolism during embryogenesis of the hard tick Boophilus microplus. Comp Biochem Physiol a Mol Integr Physiol. 2007 Apr;146(4):528-33. Epub 2006 May 23.
71. Da Silva RM, Della Noce B, Waltero CF, et al. Non-Classical Gluconeogenesis-Dependent Glucose Metabolism in Rhipicephalus microplus Embryonic Cell Line BME26. Iriti M, ed. International Journal of Molecular Sciences. 2015;16(1):1821-1839. doi:10.3390/ijms16011821.
72. Liao M, Boldbaatar D, Gong H, Huang P, Umemiya R, Harnnoi T, Zhou J, Tanaka T, Suzuki H, Xuan X, Fujisaki K. Functional analysis of protein disulfide isomerases in blood feeding, viability and oocyte development in Haemaphysalis longicornis ticks. Insect Biochem Mol Biol. 2008 Mar;38(3):285-95. doi: 10.1016/j.ibmb.2007.11.006. Epub 2007 Nov 24.
73. Radulović ŽM, Kim TK, Porter LM, Sze S-H, Lewis L, Mulenga A. A 24-48 h fedAmblyomma americanum tick saliva immuno-proteome. BMC Genomics. 2014; 15:518. doi:10.1186/1471-2164-15-518.
74. Cramaro WJ, Revets D, Hunewald OE, Sinner R, Reye AL, Muller CP. Integration of Ixodes ricinus genome sequencing with transcriptome and proteome annotation of the naive midgut. BCM Genomics. 2015; 16: 871
75. Ullmann A. J., Lima C. M., Guerrero F. D., Piesman J., Black W. C. T. (2005). Genome size and organization in the blacklegged tick, *Ixodes scapularis* and the Southern cattle tick, *Boophilus microplus*. Insect Mol. Biol. 14, 217–222 10.1111/j.1365-2583.2005.00551.
76. Pagel Van Zee J., Geraci N. S., Guerrero F. D., Wikel S. K., Stuart J. J., Nene V. M., et al. (2007). Tick genomics: the *Ixodes* genome project and beyond. Int. J. Parasitol. 37, 1297–1305 10.1016/j.ijpara.2007.05.011
77. Smith AA, Pal U. Immunity-related genes in Ixodes scapularis-perspectives from genome information. Frontiers in Cellular and Infection Microbiology. 2014; 4: 116. doi:10.3389/fcimb.2014.00116.
78. Schuijt, T. J., van der Poll, T., de Vos, W. M., and Wiersinga, W. J. (2013). The intestinal microbiota and host immune interactions in the critically ill. Trends Microbiol. 21, 221–229. doi: 10.1016/j.tim.2013.02.001

79. Buchon, N., Broderick, N. A., and Lemaitre, B. (2013). Gut homeostasis in a microbial world: insights from Drosophila melanogaster. Nat. Rev. Microbiol. 11, 615–626. doi: 10.1038/nrmicro3074
80. Lazzaro, B. P., and Rolff, J. (2011). Immunology. Danger, microbes, and homeostasis. Science 332, 43–44. doi: 10.1126/science.1200486
81. Kim, S. H., and Lee, W. J. (2014). Role of DUOX in gut inflammation: lessons from model of gut-microbiota interactions. Front. Cell. Infect. Microbiol. 3:116. doi: 10.3389/fcimb.2013.00116
82. Deken, X. D., Corvilain, B., Dumont, J. E., and Miot, F. (2013). Roles of DUOXmediated hydrogen peroxide in metabolism, host defense, and signaling. Antioxid. Redox Signal. 20, 2776–2793. doi: 10.1089/ars.2013.5602
83. Kumar, S., Molina-Cruz, A., Gupta, L., Rodrigues, J., and Barillas-Mury, C. (2010). A peroxidase/dual oxidase system modulates midgut epithelial immunity in Anopheles gambiae. Science 327, 1644–1648. doi: 10.1126/science. 1184008
84. Grubhoffer, L., and Jindrak, L. (1998). Lectins and tick-pathogen interactions: a minireview. Folia Parasitol. (Praha) 45, 9–13.
85. Grubhoffer, L., Kovar, V., and Rudenko, N. (2004). Tick lectins: structural and functional properties. Parasitology 129(Suppl.), S113–S125. doi: 10.1017/S0031182004004858
86. Dam, T. K., and Brewer, C. F. (2010). Lectins as pattern recognition molecules: the effects of epitope density in innate immunity. Glycobiology 20, 270–279. doi: 10.1093/glycob/cwp186
87. James, A. A. (2003). Blocking malaria parasite invasion of mosquito salivary glands. J. Exp. Biol. 206, 3817–3821. doi: 10.1242/jeb.00616
88. Schuijt, T. J., Coumou, J., Narasimhan, S., Dai, J., Deponte, K., Wouters, D., et al. (2011). A tick mannose-binding lectin inhibitor interferes with the vertebrate complement cascade to enhance transmission of the lyme disease agent. Cell Host Microbe 10, 136–146. doi: 10.1016/j.chom.2011. 06.010
89. Jiravanichpaisal, P., Lee, B. L., and Soderhall, K. (2006). Cell-mediated immunity in arthropods: haematopoiesis, coagulation, melanisation and opsonization. Immunobiology 211, 213–236. doi: 10.1016/j.imbio.2005.10.015
90. Smith AA, Pal U. Immunity-related genes in Ixodes scapularis—perspectives from genome information. Frontiers in Cellular and Infection Microbiology. 2014; 4: 116. doi:10.3389/fcimb.2014.00116.
91. Kanost, M. R. (1999). Serine proteinase inhibitors in arthropod immunity. Dev. Comp. Immunol. 23, 291–301. doi: 10.1016/S0145-305X (99) 00012-9.

92. Mulenga, A., Khumthong, R., and Chalaire, K. C. (2009). Ixodes scapularis tick serine proteinase inhibitor (serpin) gene family; annotation and transcriptional analysis. BMC Genomics 10:217. doi: 10.1186/1471-2164-10-217
93. Chmelar, J., Oliveira, C. J., Rezacova, P., Francischetti, I. M., Kovarova, Z., Pejler, G., et al. (2011). A tick salivary protein targets cathepsin G and chymase and inhibits host inflammation and platelet aggregation. Blood 117, 736–744. doi: 10.1182/blood-2010-06-293241
94. Perner J, Sobotka R, Sima R, et al. Acquisition of exogenous haem is essential for tick reproduction. Pal U, ed. eLife. 2016;5: e12318. doi:10.7554/eLife.12318.
95. Sideri, M., Tsakas, S., Markoutsa, E., Lampropoulou, M., and Marmaras, V. J. (2008). Innate immunity in insects: surface-associated dopa decarboxylasedependent pathways regulate phagocytosis, nodulation and melanization in medfly haemocytes. Immunology 123, 528–537. doi: 10.1111/j.13652567.2007.02722.
96. Elrod-Erickson, M., Mishra, S., and Schneider, D. (2000). Interactions between the cellular and humoral immune responses in Drosophila. Curr. Biol. 10, 781–784. doi: 10.1016/S0960-9822(00)00569-8
97. Dunning Hotopp JC, Lin M, Madupu R, et al. Comparative Genomics of Emerging Human Ehrlichiosis Agents. Richardson PM, ed. PLoS Genetics. 2006;2(2): e21. doi: 10.1371/journal.pgen.0020021.
98. Sybesma W, Burgess C, Starrenburg M, van Sinderen D, Hugenholtz J. Multivitamin production in *Lactococcus lactis* using metabolic engineering. Metab Eng. 2004;6: 109–115. pmid:15113564
99. Fenech M. Folate (vitamin B9) and vitamin B12 and their function in the maintenance of nuclear and mitochondrial genome integrity. Mutat Res. 2012;733: 21–33. pmid:22093367
100. Hunter DJ, Torkelson JL, Bodnar J, Mortazavi B, Laurent T, Deason J, et al. (2015) The *Rickettsia* Endosymbiont of *Ixodes pacificus* Contains All the Genes of De Novo Folate Biosynthesis. PLoS ON
101. Nikoh N, Hosokawa T, Moriyama M, Oshima K, Hattori M, Fukatsu T. Evolutionary origin of insect–Wolbachia nutritional mutualism. Proceedings of the National Academy of Sciences of the United States of America. 2014;111(28):10257-10262. doi:10.1073/pnas.1409284111.
102. Bazzocchi C, Mariconti M, Sassera D, et al. Molecular and serological evidence for the circulation of the tick symbiont Midichloria (Rickettsiales: Midichloriaceae) in different mammalian species. Parasites & Vectors. 2013; 6:350. doi:10.1186/1756-3305-6-350.
103. Di Venere M, Fumagalli M, Cafiso A, De Marco L, Epis S, Plantard O, et al. *Ixodes ricinus* and Its Endosymbiont *Midichloria mitochondrii*: A Comparative Proteomic Analysis

of Salivary Glands and Ovaries. PLoS ONE, 2015: e0138842. https://doi.org/10.1371/journal.pone.0138842

SUPPLEMENTARY MATERIAL

Table S1. Complete list of 47 identified proteins, 27 from ovaries (S1A) and 20 from salivary glands (S1B).

Table S1A

ACCESSION	PM	SCORE %	Description
gi|215494047|gb|EEC03688.1|	71,16	99	Heat shock protein, putative [*I. scapularis*]
gi|597718071|gb|AHN19768.1|	66,15	99	Serum albumin, partial [*Cervus nippon*]
gi|215491972|gb|EEC01613.1|	54,92	98	Protein disulfide isomerase, putative [*I. scapularis*]
gi|215497327|gb|EEC06821.1|	21,49	90	Enolase, putative [*I. scapularis*]
gi|442760941|gb|JAA72629.1|	34,89	99	Putative carbonic anhydrase, partial [*I. ricinus*]
gi|442753241|gb|JAA68780.1|	47,14	99	Putative enolase [*I. ricinus*]
gi|442747467|gb|JAA65893.1|	52,11	99	Putative erp60 [*I. ricinus*]
gi|442747295|gb|JAA65807.1|	54,70	99	Putative erp60 [*I. ricinus*]
gi|122555|sp|P02073.1|HBB_ALCAA	16,22	99	RecName: Full=Hemoglobin subunit beta
gi|122678|sp|P21380.1|HBB_RANTA	16,16	99	RecName: Full=Hemoglobin subunit beta
gi|556054634|gb|JAB70362.1|	161,4	99	Putative vitellogenin-2 [*I. ricinus*]
gi|556054820|gb|JAB70455.1|	175,6	99	Putative vitellogenin-2 [*I. ricinus*]
gi|215508461|gb|EEC17915.1|	151,6	95	Hemelipoglycoprotein precursor, putative [*I. scapularis*]
gi|215504084|gb|EEC13578.1|	177,6	92	Hemelipoglycoprotein precursor, putative [*I. scapularis*]
gi|215505979|gb|EEC15473.1|	56,91	99	Protein disulfide isomerase, putative [*I. scapularis*]
gi|215495481|gb|EEC05122.1|	60,48	99	Chaperonin subunit, putative [*I. scapularis*]
gi|215495481|gb|EEC05122.1|	60,48	99	Chaperonin subunit, putative [*I. scapularis*]

gi|442757975|gb|JAA71146.1|	47,87	99	Putative protein disulfide-isomerase [*I. ricinus*]
gi|556054818|gb|JAB70454.1|	15,29	90	Putative ml domain-containing protein [*I. ricinus*]
gi|442746893|gb|JAA65606.1|	17,19	99	Putative nucleoside diphosphate kinase [*I. ricinus*]
gi|442756551|gb|JAA70434.1|	72,59	99	Putative heat shock 70 kda protein 5 [*I. ricinus*]
gi|442756551|gb|JAA70434.1|	72,59	99	Putative heat shock 70 kda protein 5 [*I. ricinus*]
gi|215510729|gb|EEC20182.1|	14,85	99	Fatty acid-binding protein FABP, putative [*I. scapularis*]
gi|215491972|gb|EEC01613.1|	54,92	99	Protein disulfide isomerase, putative [*I. scapularis*]
gi|442747295|gb|JAA65807.1|	54,70	99	Putative erp60 [*I. ricinus*]
gi|442758229|gb|JAA71273.1|	39,17	99	Putative fructose-biphosphate aldolase [*I. ricinus*]
gi|215504607|gb|EEC14101.1|	39,44	99	Fructose 1,6-bisphosphate aldolase, putative [*I. scapularis*]
gi|215510720|gb|EEC20173.1|	79,11	90	Elongation factor, putative [*I. scapularis*]

Table S1B

ACCESSION	PM	SCORE %	Description
gi|556054634|gb|JAB70362.1|	161,482	99	Putative vitellogenin-2 [*I. ricinus*]
gi|556054820|gb|JAB70455.1|	175,61	99	Putative vitellogenin-2 [*I. ricinus*]
gi|215504084|gb|EEC13578.1|	177,654	99	Hemelipoglycoprotein precursor, putative [*I. scapularis*]
gi|442753241|gb|JAA68780.1|	47,145	99	Putative enolase [*I. ricinus*]
gi|442752113|gb|JAA68216.1|	55,243	99	Putative imp dehydrogenase/gmp reductase [*I. ricinus*]
gi|215491939|gb|EEC01580.1|	47,043	99	IMP dehydrogenase, putative [*I. scapularis*]
gi|556066176|gb|JAB76114.1|	42,73	99	Putative imp dehydrogenase/gmp reductase, partial [*I. ricinus*]
gi|442757299|gb|JAA70808.1|	57,181	99	Putative catalase pediculus us corporis catalase [*I. ricinus*]
gi|215491559|gb|EEC01200.1|	49,612	90	D-3-phosphoglycerate dehydrogenase, putative [*I. scapularis*]
gi|215507080|gb|EEC16574.1|	59,844	90	F0F1-type ATP synthase, alpha subunit, putative [*I. scapularis]*
gi|322422107|gb|ADX01224.1	16,038	90	Beta actin [*I. ricinus*]
gi|215494293|gb|EEC03934.1|	37,593	99	Actin, putative [*I. scapularis*]
gi|442760565|gb|JAA72441.1|	22,911	99	Putative thioredoxin peroxidase, partial [*I. ricinus*]
gi|556084942|gb|JAB82892.1|	20,241	99	Putative alpha crystallins [*I. ricinus*]
gi|122678|sp|P21380.1|HBB_RANTA	16,167	73	RecName: Full=Hemoglobin subunit beta
gi|215510489|gb|EEC19942.1|	17,424	68	Small heat shock protein, putative [*I. scapularis*]
gi|215495480|gb|EEC05121.1|	10,868	95	Heat shock protein [*I. scapularis]*
gi|442752151|gb|JAA68235.1|	14,78	90	Putative pterin carbinolamine dehydratase pcbd [*I. ricinus*]
gi|215510489|gb|EEC19942.1|	17,424	74	Small heat shock protein, putative [*I. scapularis*]
gi|215510489|gb|EEC19942.1|	17,424	63	Small heat shock protein, putative [*I. scapularis*]
gi|39725997|gb|AAR29950.1|	47,377	98	Calreticulin [*I. minor*]

gi|215505979|gb|EEC15473.1|	56,912	99	Protein disulfide isomerase, putative [*I.scapularis*]
gi|604824672|gb|JAC34673.1|	61,067	99	Putative chaperonin subunit [Amblyomma triste]
gi|556053694|gb|JAB69892.1|	37,871	90	Putative calreticulin [*I. ricinus*]
gi|442757321|gb|JAA70819.1|	56,896	99	Putative protein disulfide-isomerase [*I. ricinus*]
gi|215495481|gb|EEC05122.1|	60,484	99	Chaperonin subunit, putative [*I. scapularis*]
gi|556063403|gb|JAB74737.1|	44,872	92	Putative glutamine synthetase [*I. ricinus*]
gi|215498464|gb|EEC07958.1|	16,858	90	Actin depolymerizing factor, putative [*I.scapularis*]
gi|556054818|gb|JAB70454.1|	15,293	90	Putative ml domain-containing protein [*I.ricinus*]
gi|442746893|gb|JAA65606.1|	17,198	99	Putative nucleoside diphosphate kinase [*I. ricinus*]
gi|122555|sp|P02073.1|HBB_ALCAA	16,223	99	RecName: Full=Hemoglobin subunit beta
gi|376324229|gb|AFB21470.1|	99,128	22	DNA polymerase I [Rickettsia canadensis str. CA410]

Table S2. List of 92 proteins of *M. mitochondrii*.

Description	Accession	GENE names
malate/lactate dehydrogenase [Candidatus Midichloria mitochondrii IricVA]	AEI89207.1	**mdh** midi_00923
molecular chaperone DnaK [Candidatus Midichloria mitochondrii IricVA]	AEI89491.1	**dnaK**midi_01215
ribosomal protein L3 [Candidatus Midichloria mitochondrii IricVA]	AEI88349.1	**rplC** midi_00023
chaperonin GroEL [Candidatus Midichloria mitochondrii IricVA]	AEI89468.1	**groL** midi_01192
superoxide dismutase [Candidatus Midichloria mitochondrii IricVA]	AEI88755.1	**sodA**midi_00448
ribosomal protein S4 [Candidatus Midichloria mitochondrii IricVA]	AEI88541.1	**rpsD** midi_00223
DNA-directed RNA polymerase, beta' subunit [Candidatus Midichloria mitochondrii IricVA]	AEI88813.1	**rpoC** midi_00506
hypothetical protein midi_00158 [Candidatus Midichloria mitochondrii IricVA]	AEI88478.1	midi_00158
cysteine desulfurase [Candidatus Midichloria mitochondrii IricVA]	AEI88597.1	**nifS** iscS, midi_00282
transcription termination factor Rho [Candidatus Midichloria mitochondrii IricVA]	AEI88510.1	**rho** midi_00191
thioredoxin [Candidatus Midichloria mitochondrii IricVA]	AEI89480.1	midi_01204
amino-acid ABC transporter binding protein [Candidatus Midichloria mitochondrii IricVA]	AEI89282.1	**hisJ** midi_01002
2-amino-4-hydroxy-6-hydroxymethyldihydropteridine pyrophosphokinase [Candidatus Midichloria mitochondrii IricVA]	AEI89217.1	**folK** midi_00936
transcription elongation factor GreA [Candidatus Midichloria mitochondrii IricVA]	AEI88514.1	**greA** midi_00195
peptidoglycan-associated lipoprotein [Candidatus Midichloria mitochondrii IricVA]	AEI88792.1	midi_00485
ribosomal protein L30 [Candidatus Midichloria mitochondrii IricVA]	AEI88367.1	**rpmD**midi_00041
rod shape-determining protein MreB [Candidatus Midichloria mitochondrii IricVA]	AEI88505.1	**mreB**midi_00185
ribosomal protein L27 [Candidatus Midichloria mitochondrii IricVA]	AEI88584.1	**rpmA**midi_00269
outer membrane protein [Candidatus Midichloria mitochondrii IricVA]	AEI88721.1	midi_00412
ribosomal protein S10 [Candidatus Midichloria mitochondrii IricVA]	AEI88348.1	**rpsJ** midi_00022
elongation factor Ts [Candidatus Midichloria mitochondrii IricVA]	AEI88954.1	**tsf** midi_00657
succinyl-CoA synthetase, beta subunit [Candidatus Midichloria mitochondrii IricVA]	AEI89160.1	**sucC** midi_00874
ribosomal protein L23 [Candidatus Midichloria mitochondrii IricVA]	AEI88351.1	**rplW** midi_00025
ribosomal protein L2 [Candidatus Midichloria mitochondrii IricVA]	AEI88352.1	**rplB** midi_00026
replicative DNA helicase [Candidatus Midichloria mitochondrii IricVA]	AEI88564.1	**dnaB**midi_00248
elongation factor G [Candidatus Midichloria mitochondrii IricVA]	AEI89114.1	**fusA** midi_00824

trigger factor Tig [Candidatus Midichloria mitochondrii IricVA]	AEI89067.1	**tig** midi_00777
peptidase S1C, Do [Candidatus Midichloria mitochondrii IricVA]	AEI89257.1	midi_00976
hypothetical protein midi_00335 [Candidatus Midichloria mitochondrii IricVA]	AEI88645.1	midi_00335
alkyl hydroperoxide reductase/ Thiol specific antioxidant/ Mal allergen [Candidatus Midichloria mitochondrii IricVA]	AEI89212.1	midi_00929
ribosomal protein L1 [Candidatus Midichloria mitochondrii IricVA]	AEI88808.1	**rplA** midi_00501
ompH family outer membrane protein [Candidatus Midichloria mitochondrii IricVA]	AEI88498.1	**hlpA** midi_00178
DNA-binding protein HU [Candidatus Midichloria mitochondrii IricVA]	AEI88824.1	midi_00519
30S ribosomal protein S2 [Candidatus Midichloria mitochondrii]	CBJ36197.1	**rpsB**
1-deoxy-D-xylulose-5-phosphate synthase [Candidatus Midichloria mitochondrii IricVA]	AEI89013.1	**dxs** midi_00719
probable integral membrane proteinase [Candidatus Midichloria mitochondrii IricVA]	AEI89064.1	midi_00774
protein-export protein SecB [Candidatus Midichloria mitochondrii IricVA]	AEI88677.1	**secB** midi_00367
ribosomal protein S7 [Candidatus Midichloria mitochondrii IricVA]	AEI89113.1	**rpsG** midi_00823
polyribonucleotide nucleotidyltransferase [Candidatus Midichloria mitochondrii IricVA]	AEI88762.1	**pnp** midi_00455
Uncharacterized protein conserved in bacteria [Candidatus Midichloria mitochondrii IricVA]	AEI88613.1	midi_00303
citrate synthase I [Candidatus Midichloria mitochondrii IricVA]	AEI89177.1	**gltA** midi_00893
ATP synthase subunit beta [Candidatus Midichloria mitochondrii IricVA]	AEI89394.1	**atpD** midi_01117
recombinase A [Candidatus Midichloria mitochondrii IricVA]	AEI88565.1	**recA** midi_00249
enoyl-(acyl-carrier-protein) reductase [Candidatus Midichloria mitochondrii IricVA]	AEI88694.1	**fabI** midi_00384
putative membrane protein [Candidatus Midichloria mitochondrii IricVA]	AEI88424.1	midi_00102
transcriptional regulator XRE family [Candidatus Midichloria mitochondrii IricVA]	AEI89325.1	midi_01048
phosphate regulon transcriptional regulatory protein PhoB [Candidatus Midichloria mitochondrii IricVA]	AEI89122.1	**phoB**midi_00834
translation elongation factor Tu [Candidatus Midichloria mitochondrii IricVA]	AEI88862.1	**tufB** tuf, midi_00560
toluene tolerance transporter, putative [Candidatus Midichloria mitochondrii IricVA]	AEI88724.1	midi_00416
30S ribosomal protein S1 [Candidatus Midichloria mitochondrii IricVA]	AEI88883.1	**rpsA** midi_00583
DNA-directed RNA polymerase, beta subunit [Candidatus Midichloria mitochondrii IricVA]	AEI88812.1	**rpoB** midi_00505
ribosomal protein S8 [Candidatus Midichloria mitochondrii IricVA]	AEI88363.1	**rpsH** midi_00037
Hflc protein [Candidatus Midichloria mitochondrii IricVA]	AEI89063.1	**hflC** midi_00773
ribosomal protein L11 [Candidatus Midichloria mitochondrii IricVA]	AEI88807.1	**rplK** midi_00500
excinuclease ABC subunit A [Candidatus Midichloria mitochondrii IricVA]	AEI88992.1	**uvrA** midi_00695

peroxiredoxin reductase [Candidatus Midichloria mitochondrii IricVA]	AEI88711.1	**ahpD**midi_00401
phosphatidylserine decarboxylase [Candidatus Midichloria mitochondrii IricVA]	AEI88692.1	**psd** midi_00382
hypothetical protein midi_01125 [Candidatus Midichloria mitochondrii IricVA]	AEI89402.1	midi_01125
uncharacterized protein conserved in bacteria [Candidatus Midichloria mitochondrii IricVA]	AEI88591.1	midi_00276
chaperonin GroS [Candidatus Midichloria mitochondrii IricVA]	AEI89467.1	**groS groES**, midi_01191
TrpR like protein, YerC/YecD [Candidatus Midichloria mitochondrii IricVA]	AEI88520.1	midi_00202
succinyl-CoA synthetase, alpha subunit [Candidatus Midichloria mitochondrii IricVA]	AEI89159.1	**sucD** midi_00873
DNA-directed RNA polymerase, alpha subunit [Candidatus Midichloria mitochondrii IricVA]	AEI88372.1	**rpoA** midi_00046
ribosomal protein L4 [Candidatus Midichloria mitochondrii IricVA]	AEI88350.1	**rplD** midi_00024
uncharacterized protein conserved in bacteria [Candidatus Midichloria mitochondrii IricVA]	AEI88981.1	midi_00684
type I secretion outer membrane protein [Candidatus Midichloria mitochondrii IricVA]	AEI88376.1	**tolC** midi_00050
ribosomal protein S17 [Candidatus Midichloria mitochondrii IricVA]	AEI88358.1	**rpsQ** midi_00032
chaperone protein htpG [Candidatus Midichloria mitochondrii IricVA]	AEI89378.1	**htpG** midi_01101
peroxiredoxin [Candidatus Midichloria mitochondrii IricVA]	AEI89139.1	**ahpC**midi_00851
ribosomal protein L16 [Candidatus Midichloria mitochondrii IricVA]	AEI88355.1	**rpsC** midi_00029
hypothetical protein midi_01103 [Candidatus Midichloria mitochondrii IricVA]	AEI89380.1	midi_01103
ribosomal protein L9 [Candidatus Midichloria mitochondrii IricVA]	AEI88335.1	**rplI** midi_00009
ribosomal protein L19 [Candidatus Midichloria mitochondrii IricVA]	AEI88849.1	**rplS** midi_00544
ribosomal protein L7/L12 [Candidatus Midichloria mitochondrii IricVA]	AEI88811.1	**rplL** midi_00504
putative Extracellular ligand-binding receptor [Candidatus Midichloria mitochondrii IricVA]	AEI89090.1	midi_00800
TPR domain protein [Candidatus Midichloria mitochondrii IricVA]	AEI88722.1	midi_00414
ribosomal protein S9 [Candidatus Midichloria mitochondrii IricVA]	AEI89192.1	**rpsI** midi_00908
Translation elongation factor P [Candidatus Midichloria mitochondrii IricVA]	AEI88449.1	**efp** midi_00128
NADP-dependent malic enzyme [Candidatus Midichloria mitochondrii IricVA]	AEI89239.1	**maeB**midi_00958
leucyl aminopeptidase [Candidatus Midichloria mitochondrii IricVA]	AEI88516.1	**pepB** pepA, midi_00198
single-strand DNA-binding protein [Candidatus Midichloria mitochondrii IricVA]	AEI88840.1	midi_00535
Biotin synthase [Candidatus Midichloria mitochondrii IricVA]	AEI88447.1	**bioB** midi_00126
aconitate hydratase [Candidatus Midichloria mitochondrii IricVA]	AEI88620.1	**acnA**midi_00310
transcription antitermination protein [Candidatus Midichloria mitochondrii IricVA]	AEI88806.1	**nusG**midi_00499

pyruvate phosphate dikinase [Candidatus Midichloria mitochondrii IricVA]	AEI88566.1	**ppsA**midi_00250
2-dehydro-3-deoxyphosphooctonate aldolase [Candidatus Midichloria mitochondrii IricVA]	AEI88970.1	**kdsA** midi_00673
ribosomal protein L13 [Candidatus Midichloria mitochondrii IricVA]	AEI89193.1	**rplM** midi_00909
ribosomal protein L5 [Candidatus Midichloria mitochondrii IricVA]	AEI88361.1	**rplE** midi_00035
F0F1 ATP synthase subunit alpha [Candidatus Midichloria mitochondrii]	CBJ36209.1	**atpA**
ribosomal protein S10 [Candidatus Midichloria mitochondrii IricVA]	AEI88356.1	**rplP** midi_00030
molecular chaperone GrpE (heat shock protein) [Candidatus Midichloria mitochondrii IricVA]	AEI89206.1	**grpE** midi_00922
ATP-dependent chaperone ClpB [Candidatus Midichloria mitochondrii IricVA]	AEI89231.1	**clpB** midi_00950

Table S3. List of *I. ricinus* pathway

Pathway	KEGG code
Glycolysis and Gluconeogenesis	ISC00010
TCA cycle	ISC00020
Pentose phosphate pathway	ISC00030
Galactose metabolism	ISC00052
Fatty acid degradation	ISC00071
Synthesis and degradation of ketone bodies	ISC00072
Arginine biosynthesis	ISC00220
Purine metabolism	ISC00230
Pyrimidine metabolism	ISC00240
Lysine biosynthesis and degradation	ISC00300; ISC00310
Tryptophan metabolism	ISC00380
Beta-alanine metabolism	ISC00410
Selenocompound metabolism	ISC00450
Glutathione metabolism	ISC00480
N-Glycan biosynthesis	ISC00510
Amino sugar and nucleotide metabolism	ISC00520
Arachidonic acid metabolism	ISC00590
Sphingolipid metabolism	ISC00600
Pyruvate metabolism	ISC00620

Glycosylate and dicarboxylate metabolism	ISC00630
One carbon pool by folate	ISC00670
Vitamin B6 metabolism	ISC00750
Retinol metabolism in animals	ISC00830
Ammino-tRNA biosynthesis	ISC00970
Metabolism of xenobiotics by cytochrome P450	ISC00980
Insect hormone biosynthesis	ISC00981
Ribosome	ISC03010
RNA transport	ISC03013
mRNA surveillance pathway	ISC03015
Ubiquitine mediated proteolysis	ISCO04120
Snare interactions in vesicular transport	ISC04130
Protein processing in endoplasmic reticulum	ISC04141
Lysosome	ISC04142
WNT signaling pathway and ECM-receptor	ISC04310-ISCO04512

PLOS | ONE

RESEARCH ARTICLE

Ixodes ricinus and Its Endosymbiont *Midichloria mitochondrii*: A Comparative Proteomic Analysis of Salivary Glands and Ovaries

Monica Di Venere[1], Marco Fumagalli[2], Alessandra Cafiso[3], Leone De Marco[3,4], Sara Epis[3], Olivier Plantard[5,6], Anna Bardoni[1], Roberta Salvini[1], Simona Viglio[1], Chiara Bazzocchi[3], Paolo Iadarola[1], Davide Sassera[2]*

1 Department of Molecular Medicine, University of Pavia, Pavia, Italy, 2 Department of Biology and Biotechnology, University of Pavia, Pavia, Italy, 3 Department of Veterinary Science and Public Health, University of Milan, Milan, Italy, 4 School of Biosciences and Veterinary Medicine, University of Camerino, Camerino, Italy, 5 INRA, UMR1300 Biologie, Epidémiologie et Analyse de Risque en santé animale, CS 40706, Nantes, France, 6 LUNAM Université, Oniris, Ecole nationale vétérinaire, agroalimentaire et de l'alimentation Nantes-Atlantique, UMR BioEpAR, Nantes, France

* davide.sassera@unipv.it

Citation: Di Venere M, Fumagalli M, Cafiso A, De Marco L, Epis S, Plantard O, et al. (2015) *Ixodes ricinus* and Its Endosymbiont *Midichloria mitochondrii*: A Comparative Proteomic Analysis of Salivary Glands and Ovaries. PLoS ONE 10(9): e0138942. doi: 10.1371/journal.pone.0138942

Editor: Ulrike Gertrud Munderloh, University of Minnesota, UNITED STATES

Received: June 25, 2015

Accepted: September 3, 2015

Published: September 23, 2015

Data Availability Statement: All relevant data are within the paper and its Supporting Information files.

Funding: Funding for this work was provided by the Ministero dell'Istruzione, dell'Università e della Ricerca through FIR 2013—RBFR13BWBC_001 to Davide Sassera and PRIN 2012-2012A4FB28 to Chiara Bazzocchi.

Competing Interests: The authors have declared that no competing interests exist.

Abstract

Hard ticks are hematophagous arthropods that act as vectors of numerous pathogenic microorganisms of high relevance in human and veterinary medicine. *Ixodes ricinus* is one of the most important tick species in Europe, due to its role of vector of pathogenic bacteria such as *Borrelia burgdorferi* and *Anaplasma phagocytophilum*, of viruses such as tick borne encephalitis virus and of protozoans as *Babesia* spp. In addition to these pathogens, *I. ricinus* harbors a symbiotic bacterium, *Midichloria mitochondrii*. This is the dominant bacteria associated to *I. ricinus*, but its biological role is not yet understood. Most *M. mitochondrii* symbionts are localized in the tick ovaries, and they are transmitted to the progeny. *M. mitochondrii* bacteria have however also been detected in the salivary glands and saliva of *I. ricinus*, as well as in the blood of vertebrate hosts of the tick, prompting the hypothesis of an infectious role of this bacterium. To investigate, from a proteomic point of view, the tick *I. ricinus* and its symbiont, we generated the protein profile of the ovary tissue (OT) and of salivary glands (SG) of adult females of this tick species. To compare the OT and SG profiles, 2-DE profiling followed by LC-MS/MS protein identification were performed. We detected 21 spots showing significant differences in the relative abundance between the OT and SG, ten of which showed 4- to 18-fold increase/decrease in density. This work allowed to establish a method to characterize the proteome of *I. ricinus*, and to detect multiple proteins that exhibit a differential expression profile in OT and SG. Additionally, we were able to use an immunoproteomic approach to detect a protein from the symbiont. Finally, the method here developed will pave the way for future studies on the proteomics of *I. ricinus*, with the goals of better understanding the biology of this vector and of its symbiont *M. mitochondrii*.

Introduction

Vector-borne diseases are among the leading causes of sanitary concern worldwide, being responsible for millions of deaths every year [1]. Although most vectors (such as mosquitoes) mainly exert their toll on developing countries, ticks are also widespread in the Northern hemisphere and are indeed considered the most important disease vectors in Europe and North America [2]. Many species of this order of obligate hematophagous parasites, the Ixodida, are capable of transmitting numerous viral, bacterial, and protozoan pathogens through the blood meal. Hard ticks in particular are dangerous vectors and, among them, the sheep tick *Ixodes ricinus* is one of the most relevant species. The importance of *I. ricinus* is due to its wide area of distribution (i.e. Europe and Northern Africa), to its low host specificity and capacity to parasitize humans, and to its central role in the transmission of multiple infectious agents [3]. *Borrelia* spp, the causative agent of Lyme disease, is possibly the most important microorganism vectored by *I. ricinus*. This bacterium is responsible for hundreds of thousands of novel infections each year and its role in multiple chronic pathologies is currently being investigated [4]. Additionally, *I. ricinus* is capable of transmitting numerous other bacteria, such as *Rickettsia* spp. and *Ehrlichia* spp., but also the flavivirus responsible for Tick Borne Encephalitis and the etiological protozoan agents of babesiosis [5].

In addition to the aforementioned pathogens, *I. ricinus* harbors a recently described bacterium named *Midichloria mitochondrii* [6]. The importance of this bacterial presence is testified by its prevalence in the field, as 100% of females, eggs and immatures of *I. ricinus* harbor *M. mitochondrii* bacteria [7]. Additionally, the bacterial load has been found to be important, with up to 15 million bacteria counted in one single tick, localized mainly in the ovaries or ovarian primordia [8, 9]. As all member of the bacterial order Rickettsiales, *M. mitochondrii* is intracellular, however its uniqueness lays in that it was observed inside the mitochondria of the host ovarian cells [9]. Finally, *M. mitochondrii* has also been detected in the salivary glands of adult females of *I. ricinus*, as well as in the blood of mammalian tick hosts [10, 11]. However, investigations on its potential role as infectious agent have never provided adequate answers concerning the possible link to pathological effects. As a consequence, new tools are required for answering this question.

With the advent of proteomics, the screening of proteins as potential biomarkers has achieved important progresses. Detection and identification of proteins in different organs/tissues, with the aim of understanding whether they represent an attractive tool for monitoring alterations in these districts, is currently an area of increasing interest. Recently, studies have been focused on the characterization of *I. ricinus* salivary glands and midgut proteomes, in a much-needed effort to better understand the role of these organs, fundamental in the tick bite and metabolism [12, 13].

Our plan was then to expand the knowledge of *I. ricinus* protein profiles by applying two-dimensional electrophoresis (2-DE) as a tool for comparing the protein pattern of the ovary with that of salivary glands (i.e. the sialome). The first goal of this study is to give insight into the process of oogenesis, central to the tick life cycle. Additionally we planned to provide clues on the symbiotic relationship between *I. ricinus* and its symbiont *M. mitochondrii*, which is highly prevalent in the ovaries. Moreover, to seek the best possible protocol for future studies on *I. ricinus* proteomics, we focused on a careful optimization of the proteomic analysis pipeline.

Materials and Methods

Ethics Statement

I. ricinus ticks were collected from roe-deer (*Capreolus capreolus*) in the Chize forest (Northern France) in February 2014, in strict accordance with the recommendations in the french

National charter on the ethics of animal experimentation and the DIRECTIVE 2010/63/EU OF THE EUROPEAN PARLIAMENT AND OF THE COUNCIL of 22 September 2010 on the protection of animals used for scientific purposes. The protocol was approved by the "Comité d'Ethique en Expérimentation Animale de l'Université Claude Bernard Lyon 1" (CEEA-55; DR2014-09). The capture of roe deers was carried out only by competent persons using methods which do not cause the animals avoidable pain, suffering, distress or lasting harm.

Ticks collection, protein and DNA extraction

One hundred and twenty semi-engorged *I. ricinus* ticks were collected from roe-deer (*Capreolus capreolus*) in the Chize forest (Northern France) in February 2014. semi-engorged ticks were selected as this stage presents the highest combined development of the two investigated organs, ovaries and salivary glands, and also presents a high concentration of *M. mitochondrii* symbionts [8]. Ticks were manually dissected under a stereomicroscope Leica (Wetzlar, Germany), to collect salivary glands and ovaries. Salivary glands and ovaries from twenty ticks were pooled in 100 μL PBS with 1.5 μL of 1x protease inhibitor (Sigma). After mechanical disruption of tissues, 20 μL of lysate were recovered for subsequent DNA extraction. The remaining volume was subjected to sonication with Digital Sonifier 450 (Branson Ultrasonic Corporation, Danbury, CT, USA), with three five-second treatments. Each sample was then centrifuged at maximum speed for 10 min and supernatants were recovered and stored at -80°C until use. DNA from each sample was extracted using the Qiagen DNeasy Blood and Tissue Kit (Hilden, Germany) following manufacturer instructions. DNAs were eluted in 50 μL of sterile water and stored at -20°C until molecular analysis.

PCR

The presence of common tick-borne pathogenic bacteria [14] in the extracted DNA was screened using previously described PCR protocols for *Borrelia burgdorferi* [15], *Anaplasma* spp., *Ehrlichia* spp. and *Rickettsia* spp. [16]. Samples negative for the presence of pathogens were subsequently analyzed for absolute quantification of *M. mitochondrii* content using a previously described Sybr green real-time PCR approach [8] based on the amplifications of a fragment of the *M. mitochondrii gyrB* gene (coding for the protein gyrase B) and a fragment of the *I. ricinus* nuclear gene *cal* (coding for the protein calreticulin). Results were expressed as ratio of *gyrB*/*cal* copy numbers.

Quantification of proteins

The Bicinchoninic Acid (BCA) assay [17] was applied to obtain the exact quantification of each pool of proteins extracted from salivary glands and ovaries. Bovine serum albumin was the standard protein used for the production of calibration curves, in the range of concentrations between 5 and 25 μg/mL.

Two-Dimensional Electrophoresis (2-DE)

About 250 μg of extracted proteins were dissolved in 125 μL of rehydration buffer (8 M urea, 4% CHAPS (w/v), 65 mM DTE, 0.8% carrier ampholytes (v/v), 0.5% bromophenol blue) and loaded onto 7 cm IPG strips, with nonlinear (NL) pH 3–10 or linear pH 4–7 gradient range, Amersham Biosciences (Amersham, UK). Strips were rehydrated without applying voltage for 1 h at 20°C. The first-dimensional IEF was carried out at 15°C using an Ettan IPGphor system (Amersham Biosciences), programmed with the following voltage gradient: 30 V for 8 h, 120 V for 1 h, 500 V for 0.5 h, 1000 V for 0.5 h and 5000 V until a total of 25–27 kV/h was reached.

Reduction/alkylation steps were applied between the first and the second dimension. The focused IPG strips were incubated for 15 min at room temperature in 6 M urea, 2% (w/v) SDS, 50 mM Tris pH 6.8, glycerol 30%, containing 2% (w/v) DTE, followed by a second incubation of 15 min in the same buffer containing 2.5% (w/v) iodoacetamide and 0.5% bromophenol blue. At the end of the IEF step, strips were hold in place with 0.4% low melting temperature agarose and loaded onto 8x6 cm slabs, 12.5% SDS polyacrylamide gels. Electrophoresis was carried out at a constant current of 10 mA per gel in a PROTEAN II xi 2-D Cell equipment Bio-Rad (Berkeley, California), until the buffer front line was 1 mm from the bottom of the gels. The 2-DE gels were stained with "Blue silver" (colloidal Coomassie G-250 staining), according to Candiano et al [18]. Digital images of stained gels were acquired using VersaDoc Imaging Model 3000 (BioRad) and then subjected to quali/quantitative analysis using the PD Quest (BioRad) version 8.0.1 software. Scanned images were filtered and smoothed to remove background noise, vertical/horizontal streaking and gel artifacts and then normalized to eliminate the variability of each sample. The software then determined the amount of spots present and calculated their intensity by applying the following algorithm: peak value (ODs/image units) $*\sigma_x*\sigma_y$ (standard deviations in x and y).

Reproducibility of the study

To verify the reproducibility of the study, 2-DE maps were obtained in triplicate for each of the analyzed salivary glands (SG) and ovary tissues (OT) pools. Those presented in this report are the best representative gels among all generated that showed spots consistently present. Experimental steps concerning sample preparation, electrophoretic run and gel staining were performed "in parallel" on all samples.

In situ enzymatic digestion

Enzymatic digestion was performed as previously described [19]. Briefly, the selected spots were carefully excised from the gel, placed into Eppendorf tubes and broken in to small pieces. This material was then washed twice with aliquots (200 μL) of 100 mM ammonium bicarbonate buffer pH 7.8, 50% acetonitrile (ACN) and kept under stirring overnight, until complete destaining. Gels were dehydrated by addition of ACN (100 μL). After removal of the organic solvent, reduction was performed by addition of 50 μL of 10 mM Dithiothreitol (DTT) solution (40 min at 37°C). DTT was replaced with 50 μL of 55 mM iodoacetamide for 45 min at 56°C. This solution was removed and the gel pieces were washed twice with 200 μL of 100 mM ammonium bicarbonate for 10 min, while vortexing. The wash solution was removed and gel dehydrated by addition of 200 μL of ACN until the gel pieces became an opaque-white color. ACN was finally removed and gel pieces were dried under vacuum. Gels were rehydrated by addition of 75 μL of 100 mM ammonium bicarbonate buffer pH 7.8, containing 20 ng/μL sequencing grade trypsin (Promega, Madison, WI, USA) and digestion was performed incubating overnight at 37°C. Following enzymatic digestion, the resultant peptides were extracted sequentially from gel matrix by a three-step treatment (each step at 37°C for 15 min) with 50 μL of 50% ACN in water, 5% trifluoroacetic acid (TFA) and finally with 50 μL of 100% ACN. Each extraction involved 10 min of stirring followed by centrifugation and removal of the supernatant. The original supernatant and those obtained from sequential extractions were pooled, dried and stored at -80°C until mass spectrometric analysis. At the moment of use, the peptide mixture was solubilized in 100 μL of 0.1% formic acid (FA) for MS analyses.

LC-MS/MS

All analyses were carried out on an LC-MS (Thermo Finnigan, San Jose, CA, USA) system consisting of a thermostated column oven Surveyor autosampler controlled at 25°C, a quaternary gradient Surveyor MS pump equipped with a diode array detector, and an Linear Trap Quadrupole (LTQ) mass spectrometer with electrospray ionization ion source controlled by Xcalibur software 1.4. Analytes were separated by RP-HPLC on a Jupiter (Phenomenex, Torrance, CA, USA) C_{18} column (150 x 2 mm, 4 μm, 90 Å particle size) using a linear gradient (2–60% solvent B in 60 min) in which solvent A consisted of 0.1% aqueous FA and solvent B consisted of ACN containing 0.1% FA. Flow-rate was 0.2 mL/min. Mass spectra were generated in positive ion mode under constant instrumental conditions: source voltage 5.0 kV, capillary voltage 46 V, sheath gas flow 40 (arbitrary units), auxiliary gas flow 10 (arbitrary units), sweep gas flow 1 (arbitrary units), capillary temperature 200°C, tube lens voltage –105 V. MS/MS spectra, obtained by CID studies in the linear ion trap, were performed with an isolation width of 3 Th *m/z*, the activation amplitude was 35% of ejection RF amplitude that corresponds to 1.58 V.

Data processing was performed using Peaks studio 4.5 software. An ad-hoc database was obtained selecting from the NCBI database all the protein sequences belonging to the following taxonomic groups: *Ixodida* (taxid:6935), *Cervidae* (taxid:9850), *Borrelia* (taxid:138), *Rickettsiales* (taxid:766). The mass lists were searched against the SwissProt and the ad-hoc protein database under combined mode (MS plus MS/MS), with the following parameters: trypsin specificity, five missed cleavages, peptide tolerance at 0.2 Da, MS/MS tolerance at 0.25 Da, peptide charge 1, 2, 3+, and experimental mass values: monoisotopic.

Western Blotting

Western blot analysis was effected starting from 100 micrograms of proteins extracted from the OT and SG pool that exhibited the highest concentrations of *M. mitochondrii* based on *GyrB/cal* gene ratio. Separated proteins were transferred onto nitrocellulose membrane by using a Trans Blot Electrophoresis Transfer Cell (BioRad) and applying a current of 200 mA for 1.20 h in running buffer (25 mM Tris pH 8.3, 192 mM glycine, 20% methanol). To verify the transfer of proteins, the membrane was stained with Ponceau Red and washed with PBS (10 ml) for 10 min. After 1h incubation in 5% milk (10 ml) diluted in PBS and three additional washes with PBST(0,1% Tween (10 ml), the membrane was incubated overnight with the polyclonal antibodies against the *M. mitochondrii* flagellar protein FliD [10] at a dilution 1:5000 in 1% milk. After washing the membrane three times with PBST (10 ml), incubation with the secondary antibody (Dako, Glostrup, Denmark) was carried out for 1 h at room temperature with polyclonal goat anti-rabbit immunoglobulin diluted 1:2000 in 1% milk in PBST. The membrane was finally washed three times with PBS and incubated in ECL Prime solution (GE Healthcare, Uppsala, Sweden). Immunoblots were acquired with the ImageQuant LAS 4000 analyzer (GE Healthcare).

Results

PCR

Concentration of *M. mitochondrii* and presence of tick-borne pathogens was assessed in all the OT and SG pools by performing PCR on the DNA extracted from the samples. Two out of six OT and SG pools were positive to tick-borne pathogens and were thus excluded from subsequent analyses. PCR for the detection of *M. mitochondrii* was performed on the remaining samples and all OT and SG pools resulted, as expected, positive to *M. mitochondrii*. The copy

numbers of *gyrB* and *cal* genes and the *gyrB*/*cal* x1000 ratios are provided in S1 Table of Supporting Information.

Two-dimensional electrophoresis with nonlinear pH 3–10 gradient range

To identify *I. ricinus* proteins differentially expressed between OT and SG, as well as proteins of the *M. mitochondrii* symbiont, parallel 2-DE analyses were performed on the four salivary glands (SG) and ovary tissues (OT) of *I. ricinus* adult ticks that were infected by *M. mitochondrii* that resulted free from other bacterial pathogen presence. Gels were scanned and spots were detected using the spot detection wizard tool, after defining and saving a set of detection parameters. Following spot detection, the original gel scans were filtered and smoothed to clarify spots, remove vertical and horizontal streaks, and remove speckles. Three dimensional Gaussian spots were then created from filtered images. Three images were created from the process: the original raw 2-D scan, the filtered image, and the Gaussian image. A match set for each pool was then created for comparison after the gel images had been aligned and automatically overlaid. If a spot was saturated, irregularly shaped, or otherwise of poor quality, then the Gaussian modeling was unable to accurately determine quantity. In these cases, the spot was defined in the filtered image using the spot boundary tools. Thus, for each pool, a master gel was produced which included protein spots only if present at least in two out of the three gels. The mean spot number in Coomassie stained gels was 235±29 in SG and 221±21 in OT. A set of spots chosen from the two master gels were excised, destained, digested with trypsin, and peptides were submitted to LC-MS/MS. The MS fragmentation data were searched against the SwissProt and the ad-hoc designed protein databases, and the queries were performed using the Peaks studio 4.5 software. A total of 47 proteins were identified, 20 from SG and 27 from OT. A complete list of the identified proteins is presented in S2 Table.

The master gels from both SG and OT pools showed similar patterns of proteins such that they could be matched to each other. This facilitated the correlation of gels and the creation of a virtual image, indicated as high master gel (HMG), comprehensive of all matched spots derived from master gels. The procedure described is summarized in Fig 1.

Differentially expressed proteins

Comparison of 2-DE patterns for SG and OT revealed several qualitative and quantitative differences between the two sets of pools. In terms of presence/absence of spots, qualitative differences are represented in Fig 2. As shown, while the majority of spots were common to both SG and OT (170 ± 25, evidenced in green), some protein spots present in SG profile were absent from the OT one and viceversa. In particular, 81 spots (marked in red) were exclusive of SG and 57 spots (labelled in blue) were detected solely in OT.

Spot quantities of all gels were normalized to remove non expression-related variations in spot intensity, and data were exported as clipboard for further statistical analysis. The raw amount of each protein in a gel was divided by the total quantity of all proteins (spots) that were included in that gel. The results were evaluated in terms of spot optical density (OD). Statistical analysis of PDQuest data allowed to assess differences in protein abundance on a protein-by-protein basis. According to guidelines for differential proteomic research, only spots that showed a change in density at $p < 0.01$ (by Student's t-test) were considered "differentially expressed" in the two pools of samples. This term was used here meaning differential protein abundance determined by several processes, including changes in protein biosynthesis and modification or degradation. Using these criteria, 21 spots differed by the ratio indicated above and were selected by the statistical program as spots having significant differences in the relative abundance between SG and OT. In particular, ten among these spots (indicated by

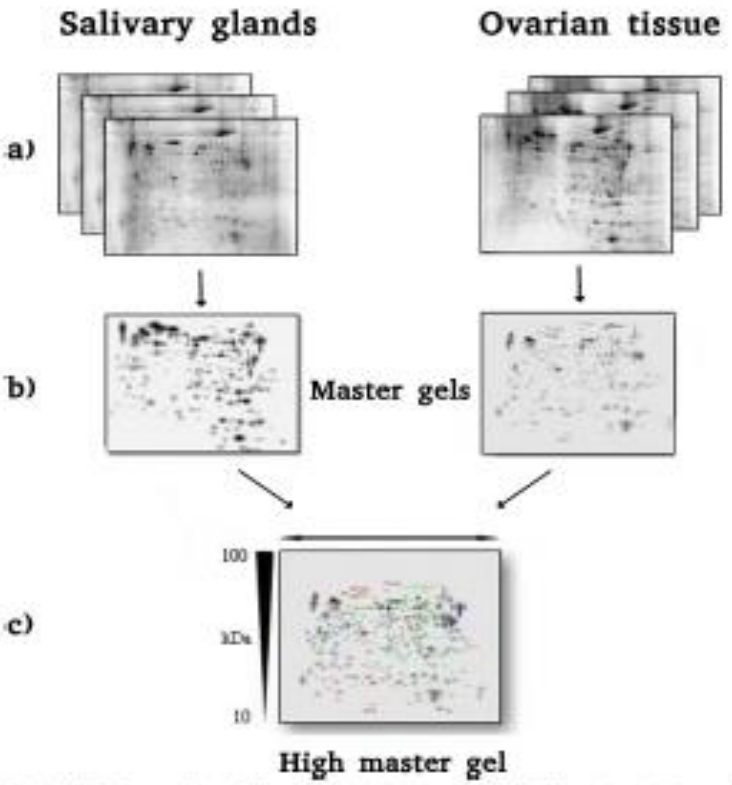

Fig 1. (A) 2-DE maps of three different pools of salivary gland (SG, left) and ovarian tissue (OT, right) of *I. ricinus*, obtained by performing IEF on 7 cm IPG strips with 3–10 NL pH range and SDS-PAGE in the second dimension on 8x6 cm slabs, 12.5% T gels. (B) SG and OT master gels obtained merging the three gels for each sample type. (C) 2-DE High Master Gel created comparing the SG and OT gels.

doi:10.1371/journal.pone.0138842.g001

numbers 1 to 10 in HMG of Fig 2) showed 4- to 18-fold increase/decrease in density. A set of panels, shown in Fig 3, was generated to highlight density variances of these spots between the two sets of pools (i.e. SG and OT).

In these panels the region of stained gel containing the spot of interest was zoomed and up-/downregulation graphically represented. Efforts have been devoted to the identification of these proteins, to investigate whether they might have an involvement in the biological processes characteristic of ovaries and salivary glands, or in the interaction between *M. mitochondrii* and *I. ricinus*.

These spots were thus carefully excised from the gel, destained, digested with trypsin, and peptides were submitted to LC-MS/MS following the procedure detailed in the Materials and Methods section. The MS fragmentation data were searched against the SwissProt and the ad-hoc designed protein databases, and the queries were performed using the Peaks studio 4.5 software. All but two (spots 2 and 9) of the queried proteins were identified. The low abundance of proteins corresponding to spots 2 and 9 most likely determined the poor quality of

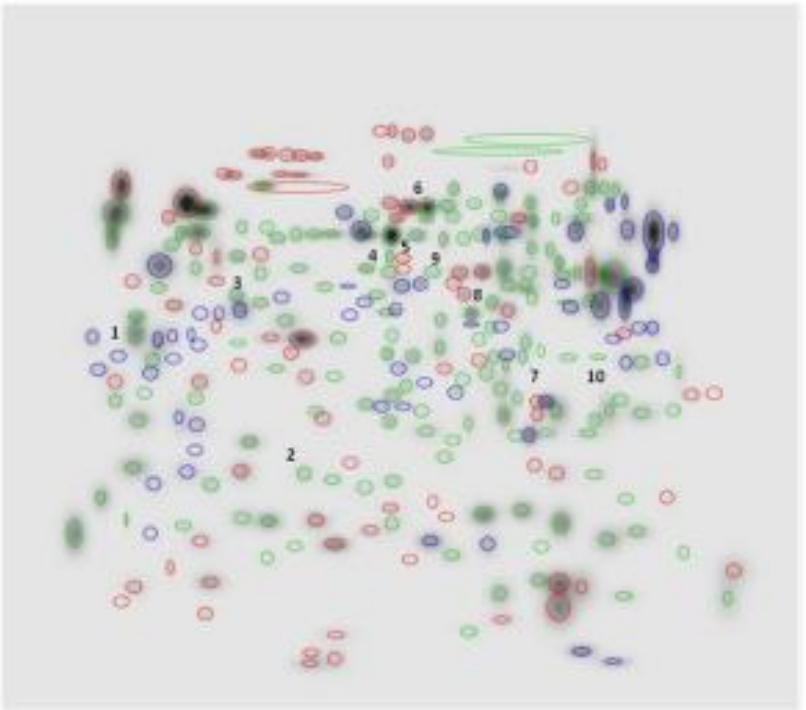

Fig 2. High Master gel, showing qualitative differences between the SG and OT 2-DE master gel patterns (NL, pH3–10 gradient range). Labelled in green: spots (n = 170 ± 25) common to both SG and OT. Labelled in red: spots (n = 81) exclusive of SG. Labelled in blue: spots (n = 57) detected solely in OT.

doi:10.1371/journal.pone.0138842.g002

their MS signals and failure in their identification. The fact that unique proteins were identified for all other analyzed spots suggested that, at least for these spots, spot overlap was minimized.

Detailed identification data, including accession number, theoretical pI, molecular mass, percent of sequence coverage, number of peptides identified, and MOWSE score of each of the nine proteins identified are reported in Table 1.

Additional information concerning the primary sequence of all peptides identified for each protein analyzed was included in S3 Table of Supporting Information.

Western blotting

Given the aim of our study, proteins from SG and OT profiles of the pool that exhibited the highest concentrations of *M. mitochondrii* were transferred onto PVDF membranes and incubated with the polyclonal anti-FliD antibodies, followed by anti-rabbit antibody. Based on: i) its position (pI/Mr) on the PVDF membrane and ii) its recognition by the antibody, the protein spot indicated by an arrow in panel A (OT pool) of Fig 4, was tentatively assigned to FliD. As shown in panel B of Fig 4, despite the appearance of interfering spots, the hypothetical FliD spot was undetectable in the SG profile. This result is expected and the load of *M. mitochondrii* bacteria is much higher in ovaries than in salivary glands (S1 Table) [10, 11].

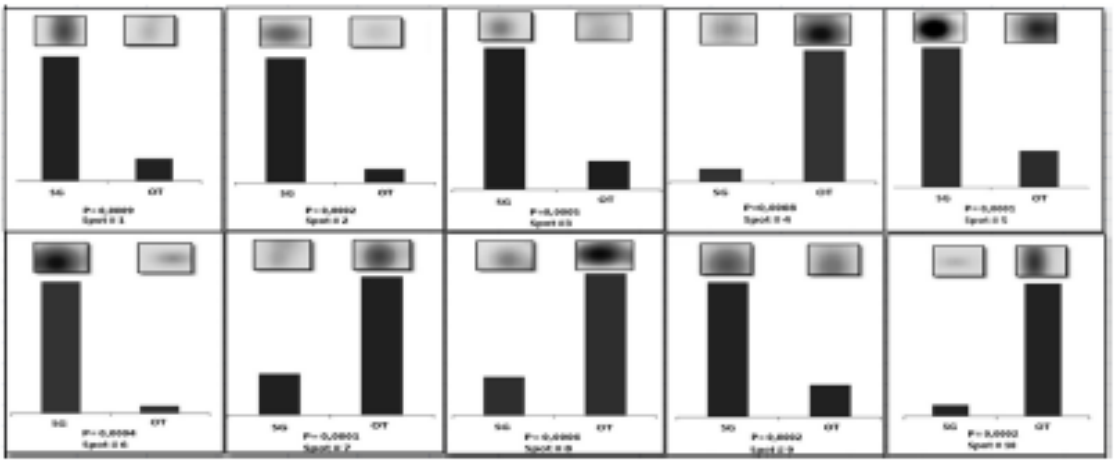

Fig 3. Set of panels showing the density variance between SG and OT pools for spots 1 to 10. In each panel the region of the stained gel containing the spot of interest was magnified (inset) and the up-/down-regulation graphically represented. P value indicating statistically significant density variance (T-test) is reported in each panel.

doi:10.1371/journal.pone.0138862.g003

To achieve identification, the immunoreactive protein spot was thus excised from the original OT gel and submitted to the LC-MS/MS procedure indicated above. The results (shown in Table 2) confirmed what appeared evident from the visual inspection of the gel, i.e. the analyzed spot, rather than comprising a single polypeptide chain, was a mixture of at least three components, i.e. Endoplasmic Reticulum Protein 60, putative actin 2, and an unknown protein

Table 1. Up and downregulated proteins identified by LC-MS/MS.

Spot	Accession	Description	Mass	Score (%)	Coverage (%)	Query matched
1	gi|442756551|gb|JAA70434.1|	Putative heat shock 70 kda protein 5 [Ixodes ricinus]	72,595	99	8,05%	5
2	/	Not detected	/	/	/	/
3	gi|322422107|gb|ADX01224.1|	Beta actin [Ixodes ricinus]	16,038	90	6,94%	1
4	gi|215497327|gb|EEC06821.1|	Enolase, putative [Ixodes scapularis]	21,493	90	4,52%	1
5	gi|442753241|gb|JAA68780.1|	Putative enolase [Ixodes ricinus]	47,145	99	23,79%	6
6	gi|215491972|gb|EEC01613.1|	Protein disulfide isomerase, putative [Ixodes scapularis]	54,929	98	6,38%	4
7	gi|442748259|gb|JAA66289.1|	Putative 3-hydroxy-3-methylglutaryl-coa reductase [Borrelia spp]	10,741	20	22,43%	2
8	gi|597718071|gb|AHN19768.1|	Serum albumin, partial [Cervus nippon]	66,15	75	6,67%	4
9	/	Not detected	/	/	/	/
10	gi|442754645|gb|JAA69482.1|	Putative heat shock protein [Ixodes ricinus]	36,782	82	4,01%	2

doi:10.1371/journal.pone.0138862.t001

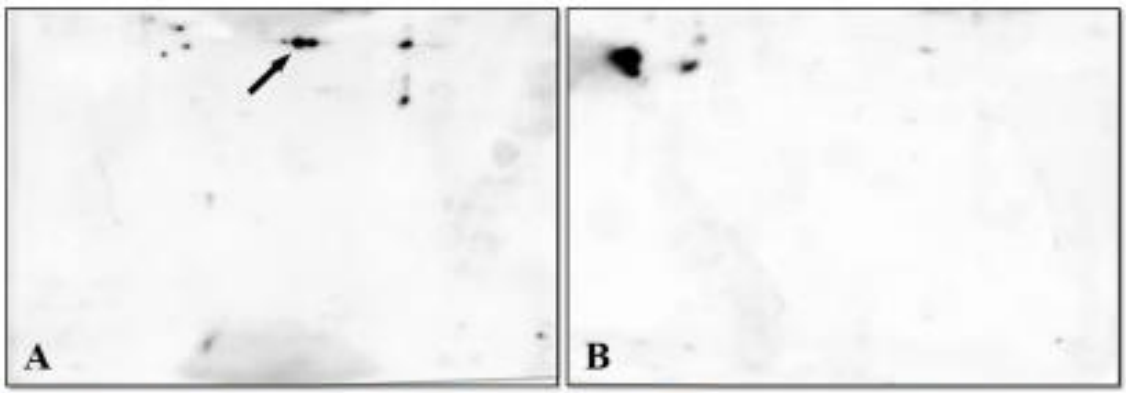

Fig 4. Immunoblotting of proteins from SG and OT profiles generated as indicated in Fig 1. PVDF membranes were incubated with the rabbit polyclonal antibodies anti-FliD of *M. mitochondrii*, followed by anti-rabbit antibody. The protein spot(s) indicated by an arrow in Panel A (OT pool) was tentatively assigned to FliD. Panel B shows the SG profile in which the hypothetical FliD spot is undetectable.

doi:10.1371/journal.pone.0138842.g004

from *Borrelia*. Information concerning the primary sequence of all peptides identified for each protein analyzed have been included in S4 Table of Supporting Information.

We hypothesized that the fact that the putative flagellar protein FliD was, most likely, less abundant compared to the bulk of other proteins present in the spot, prevented its identification. This hypothesis was strengthened by the poor quality of MS sequence data obtained from third spot (or cluster of spots). This indeed made it difficult to define exactly whether the FliD protein of was actually present within the spot(s) considered.

Two-dimensional electrophoresis with pH 4–7 gradient range: identification of FliD

In an effort to overcome the limitations indicated above and to definitively establish (or exclude) the presence of FliD under the spot(s) examined in the OT pool, we worked on the optimization of the electrophoretic conditions. After performing a extensive set of trials with various electrophoretic conditions, the best option was found to be the application of a narrow range pH gradient (linear pH 4–7). This provided a better resolution of proteins, minimizing potential spot overlaps (Fig 5A). The immunoreactive protein spot (indicated by an arrow in PVDF membrane, B) was evidenced in OT profile obtained under the experimental conditions mentioned above.

As a validation of data discussed above, no spot was reactive against the antibody in SG profile (data not shown). After spot excision and tryptic digestion, LC-MS identification confirmed the presence of flagellar protein FliD under this spot (Table 3).

Table 2. List of proteins identified under the immunoreactive spot.

Accession	Description	Mass	Score (%)	Coverage (%)	Query matched
gi|442747457|gb|JAA65693.1|	Putative wpt60 [Ixodes ricinus]	52,115	98	6,46%	3
gi|560650571|gb|JAB75571.1|	putative actin-2 [Ixodes ricinus]	36,27	89	9,79%	2
gi|6841056|gb|AAF28881.1|	unknown [Borrelia hermsii]	29,518	25	3,92%	1

doi:10.1371/journal.pone.0138842.t002

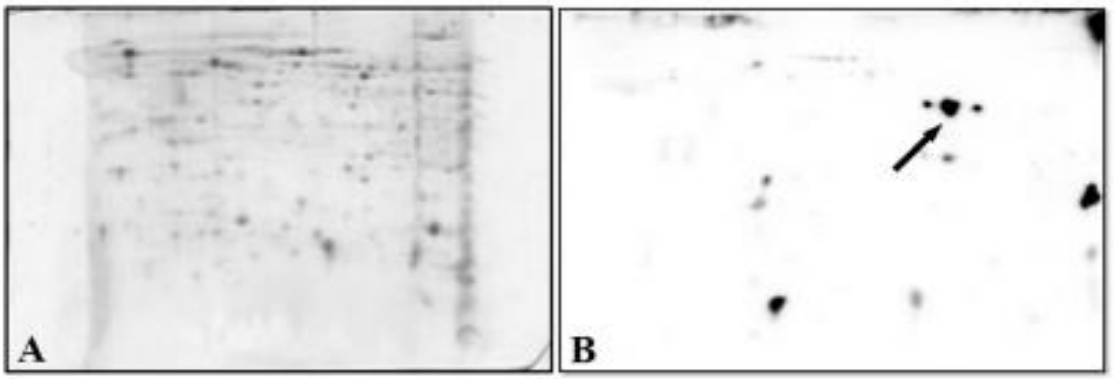

Fig 5. (A) 2-DE map of OT obtained by performing IEF on a 4–7 linear pH range and SDS-PAGE on a constant 12,5% T in the second dimension, to separate proteins clustered in the single spot shown in Fig 4. (B) Immunoblotting of the gel slab indicated in Panel A. Arrowpoints to spot originated from separation and identified as FliD.

doi:10.1371/journal.pone.0138962.g005

The primary sequence of peptides found for identification of protein analyzed was included in S5 Table of Supporting Information.

Discussion

Analysis of common proteins differentially expressed

A recent study presented the identification of hundreds of proteins in salivary glands of *I. ricinus* in the presence of the pathogenic tick-borne spirochete *B. burgdorferi*, demonstrating that the expression of proteins modulated by infection differed as a function of the various strains of *B. burgdorferi* [20]. In the present study, a total of 47 spots, 27 from OT and 20 from SG were selected for sequencing. Our results were fully congruent with those previously published, validating our approach and confirming the high expression level of a number of proteins, such as Heat shock protein, Protein disulfide isomerase, Enolase, Actin, Hemelipoglycoprotein precursor (putative) etc. This sequencing effort detected only proteins that could be readily identified as belonging to the tick proteome, or that could not be identified unambiguously, but did not reveal the presence of proteins belonging to the bacterial symbiont *M. mitochondrii*. To evaluate whether detection of symbiont proteins was possible, we thus designed a specific immunoproteomic approach, described above and discussed below.

To explore qualitative and quantitative differences between SG and OT of *I. ricinus* infected by *M. mitochondrii*, and to identify tissue-specific proteins, as well as proteins involved in the interaction between the bacterium and the tick, we compared the proteomic profiles of these tissues. The reproducible patterns generated for both tissues evidenced 170 ± 25 spots shared between SG and OT. In addition, 81 protein spots were exclusive of SG profile and 57 spots

Table 3. List of proteins that confirmed the presence of FliD.

Accession	Description	Mass	Score (%)	Coverage (%)	Query matched
/	Flagellar protein FLID OS = Midichloria mitochondrii	100,58	84	14,64%	13
gi|442747457|gb|JAA65893.1|	Putative arp60 [Ixodes ricinus]	52,115	98	6,46%	3

doi:10.1371/journal.pone.0138962.t003

were detected solely in OT. In particular, we selected and investigated the 10 proteins that exhibited the largest changes in density (4- to 18-fold increase/decrease, see Fig 2, Fig 3 and Table 1). Proteins under spots 1 and 10, both identified as putative heat shock proteins (HSP), were heavily differentially expressed. Putative HSP70 detected under spot 1 was 6-fold more abundant in SG than in OT. By contrast, the putative HSP identified under spot 10 was 11-fold more abundant in OT than in SG. Heat shock proteins are chaperones that, together with other stress response proteins, are well known to protect cells and organisms from environmental stress. HSP70, is involved in many cellular processes, including folding and refolding of nascent and/or misfolded proteins, protein translocation across membranes, and degradation of terminally misfolded or aggregated proteins [21]. The role played by HSP proteins in the growth and survival of *I. ricinus* is potentially very important. Being involved in the binding and presentation of antigens to the immune system, they constitute candidate molecules that could be involved in tick immune response to pathogen infection. Interestingly, a connection may exist between pathogen infection and tick response to stress conditions. In response to heat and other stress (cold, hunger), nearly all ticks undergo diapause. Indeed HSPs involved in the diapause of multiple species of insects were reported [22], suggesting that they may play key roles in the physiological response to stress of other arthropods, such as ticks. HSP70 is more expressed in salivary glands than in ovarian tissue and midgut and its expression increases with female tick feeding, suggesting a possible role of this protein during blood ingestion and/or digestion [23]. We speculated that this could be ascribed to the great changes in structure that the salivary glands of hard ticks undergo during blood feeding with an increase in size and the acceleration of protein synthesis [24]. However, the fact that HSP70 was found to be down regulated in *Anaplasma phagocytophilum* infected whole *Ixodes scapularis* ticks, guts and salivary glands [23], may suggest that these proteins have a different function during pathogen infection.

The protein identified under spot 3 was β-actin. The reason of its 5-fold higher expression in SG compared to OT is still a matter of speculation. First, we hypothesized that this was a consequence of the importance of SG in tick feeding. Actin is an important structural protein required for exoskeleton rearrangement during tick engorgement [25] and is a common target of many bacterial proteins. It has been shown that the cellular responses induced by a variety of stimuli and pathogens involve changes in cell morphology and the polymerization state of actin [26–27–28]. Studies in prokaryotes and eukaryotes demonstrated that nutrition and stress affect the expression of housekeeping genes [29]. For example the low expression of actin shown in the unfed first instars nymphs of *I. scapularis* is likely due to low nutrition levels since they have not yet taken the blood meal and the nutrients incorporated into the eggs have been depleted by larval development [30]. The significant differences observed during and immediately after feeding in females are likely related to the dynamic changes that occur in the physiology of ticks preparing for reproduction. It has also been shown that silencing the expression of actin in the soft tick *Ornithodoros moubata* resulted in impairment of tick feeding by a global attenuation of tick activity unrelated to specific function associated with engorgement [29]. Finally, further aspects should be taken into consideration. *I. ricinus*, as *I. scapularis*, are vectors of bacterial pathogens including *A. phagocytophilum*, and *B. burgdorferi* [30,31]. To persist in their hosts, obligate intracellular bacteria have evolved a variety of mechanisms including modulating host signaling and the actin cytoskeleton [32]. If this hypothesis proves correct, it may be speculated that the high concentration of actin detected in SG of *I. ricinus* could be the result of a sort of survival strategy developed by the symbiont *M. mitochondrii* to persist in its arthropod vector.

The identification of enolase under spots 4 and 5 attracted our interest. Alpha-enolase, one of the most abundantly expressed proteins in human cytosol, is a key glycolytic enzyme that

converts 2-phosphoglycerate to phosphoenolpyruvate [33]. In blood-feeding arthropods this protein is secreted in saliva and inoculated into the host during feeding. The finding of 4-fold higher expression of enolase in SG compared to OT (spot 5) was not surprising. This result may account for one of the pivotal roles of this enzyme. Enolase, in fact, promotes fibrinolysis and maintains blood fluidity during blood ingestion and distribution in the tick midgut. Fibrinolysis is the natural process of fibrin clot solubilization and, in ticks, this process is essential for dissolving any clot that might be formed during feeding, as well as preventing clotting of the ingested blood meal in its midgut [34]. This said, the higher expression level in OT (10-fold more expressed than in SG) of another putative enolase (spot 4) was a result apparently in contradiction with the previous one. However, the multifunctionality of this protein in both prokaryotes and eukaryotes may probably account for this finding. In fact, it has been shown in *Rhipicephalus microplus* [35] that, to support the energy-intensive processes of embryogenesis, before blastoderm formation, glycogen reserves are preferentially mobilized. As a consequence, protein degradation and gluconeogenesis intensify to supply the embryo with sufficient glucose to allow glycogen re-synthesis. If glycogen is the main energy source during the early stages of *R. microplus* embryogenesis, protein degradation increases during late embryogenesis [35]. Thus, the use of amino acids as a substrate for gluconeogenesis and the subsequent glycogen re-synthesis play an important role during the stages of *R. microplus* embryogenesis. Protein metabolism depends strongly on the substantial expression and activity of carbohydrate metabolism enzymes and alpha-enolase is a key glycolitic enzyme [36].

The protein identified under spot 6 was disulfide isomerase (PDI), a 55 KDa multifunctional protein that participates in protein folding, assembly, and post-translational modification in the endoplasmatic reticulum [37]. The fact that it was 18-fold-more expressed in SG than in OT was not surprising. This protein, together with other saliva enzymes which are putatively associated with antioxidant functions (i.e. glutathion-S-transferase, cytochrome oxidase, oxidoreductase, NADH dehydrogenase), plays an important role in oxidative stress [38]. Tick-feeding, in fact, induces injuries and oxidative stress leading to production of reactive oxygen and nitrogen species (ROS and RNS) as part of the wound healing mechanism and anti-microbial defenses. Several lines of research have shown that many parasites including ticks are susceptible to ROS and RNS, as revealed by high expression of anti-oxidant enzymes in these parasites or improved survival of these parasites when anti-oxidant system of their hosts are impaired [38]. The production of antioxidant enzymes can be considered an evasion mechanism of the immune response used by tick for improving the feeding efficiency, and collaterally enhancing transmission of tick-borne diseases. It is also interesting to note that, given that the tissue destroying effects of oxidative stress products are non-selective, there is a possibility that tick saliva anti-oxidants are protective to host tissue [38].

Identification of FLID

One of the goals of this study was to evaluate whether it is possible to detect proteins from the bacterial symbiont *M. mitochondrii* starting from protein extracts of ovaries and salivary glands of the hard tick *I. ricinus*. Due to the higher symbiont load in OT we expected this to be easier in this tissue, however none of the 2DE gel spots identified resulted to be of *M. mitochondrii*, neither from the OT, nor from the SG. We thus questioned whether this was a result of the low abundance of symbiont proteins or to some kind of technical issue. To investigate this, we performed an immunoproteomic approach based on the detection of a single *M. mitochondrii* protein (FliD) in a blotting experiment after narrow range pH gradient (linear pH 4–7) 2DE separation of OT and SG (see materials and methods). As shown in Fig 5, a spot potentially corresponding to FliD, based on the chemical properties of the protein, was detected in OT

blotting, but not in SG blotting. When analyzing the corresponding region in the original 2DE gel, a cluster of spots was detected. Careful excision of these spots followed by LC/MS-MS allowed the identification of erp60, as well as of the expected *M. mitochondrii* protein FliD. This result indicates that symbiont proteins can indeed be identified using a proteomic approach, but that this is impaired by low protein quantities and by clustering with *I. ricinus* proteins. Specific approaches, such as the use of alternative narrow range pH gradients, immunoproteomic detection are thus needed to investigate the symbiosis between *I. ricinus* and *M. mitochondrii* from a proteomic point of view.

Here we presented a methodological framework that will pave the way for future studies on the proteomics of *I. ricinus*, with the goal of better understanding the biology of this vector and of its symbiont *M. mitochondrii*, but also to be the basis of immunoproteomic approaches that could prove useful for detecting novel antigenic proteins for innovative diagnostic and vaccination approaches.

Supporting Information

S1 Table. PCR results on DNA extracted from ovarian tissue and salivary glands pools. GyrB and Cal gene copy numbers, GyrB Cal gene ratio, PCR positivity to *Borrelia burgdorferi*, *Anaplasma* spp., *Ehrlichia* spp. and *Rickettsia* spp. are indicated.
(DOCX)

S2 Table. Complete list of the 47 identified proteins, 20 from salivary glands and 27 from ovarian tissue.
(DOCX)

S3 Table. List of proteins up and downregulated with additional information such as the primary sequence of peptides.
(DOCX)

S4 Table. List of proteins identified under the immunoreactive spots with additional information such as the primary sequence of peptides.
(DOCX)

S5 Table. Primary sequence of peptides found for identification of analyzed proteins.
(DOCX)

Acknowledgments

The authors thank Maddalena Cagnone and Valentina Serra for technical assistance, as well as Axelle Durand, Cindy Laurence and Claude Rispe (UMR BioEpAR) for their help during tick sampling, Gilles Capron (ONCFS; Office nationale de la Chasse et de la Faune Sauvage) and the ONF (Office National des Forêts) from the "Réserve biologique domaniale intégrale de la Sylve d'Argenson are acknowledged for allowing us to collect ticks on the roe deers captured in the Chizé forest.

Author Contributions

Conceived and designed the experiments: DS AB RS PI. Performed the experiments: ACSE CB MDV MF SV. Analyzed the data: LDM MDV ME. Contributed reagents/materials/analysis tools: OP. Wrote the paper: MDV PI DS OP CB.

References

1. Gubler DJ. Resurgent vector-borne diseases as a global health problem. Emerg Infect Dis. 1998; 4:442–450 PMID: 9716967
2. Parola P, Raoult D. Ticks and tickborne bacterial diseases in humans: an emerging infectious threat. Clin Infect Dis. 2001; 32: 897–928 PMID: 11247714
3. Socolovschi C, Mediannikov O, Raoult D, Parola P. The relationship between spotted fever group Rickettsiae and Ixodid ticks. Vet Res. 2009; 40, 34 doi: 10.1051/vetres/2009017 PMID: 19358804
4. Perrone C. Lyme and associated tick-borne diseases: global challenges in the context of a public health threat. Front Cell Infect Microbiol. 2014; 3: 74. doi: 10.3389/fcimb.2014.00074
5. Rizzoli A, Silaghi C, Obiegala A, Rudolf I, Hubálek Z, Földvári G, et al. Ixodes ricinus and its Transmitted Pathogens in Urban and Peri-Urban Areas in Europe: New Hazards and Relevance for Public Health. Front Public Health. 2014; 2:251. doi: 10.3389/fpubh.2014.00251 PMID: 25520947
6. Sassera D, Beninati T, Bandi C, Bouman EA, Sacchi L, Fabbi M, et al. "Candidatus Midichloria mitochondrii", an endosymbiont of the tick Ixodes ricinus with a unique intramitochondrial lifestyle. Int J Syst Evol Microbiol. 2006; 56: 2535–2540 PMID: 17082386
7. Lo N, Beninati T, Sassera D, Bouman EA, Santagati S, Gern L, et al. Widespread distribution and high prevalence of an alpha-proteobacterial symbiont in the tick Ixodes ricinus. Environ Microbiol. 2006; 8: 1280–1287 PMID: 16817936
8. Sassera D, Lo N, Bouman EA, Epis S, Mortarino M, Bandi C. "Candidatus Midichloria" endosymbionts bloom after the blood meal of the host, the hard tick Ixodes ricinus. Appl Environ Microbiol. 2008; 74: 6138–6140 doi: 10.1128/AEM.00248-08 PMID: 18689506
9. Sacchi L, Bigliardi E, Corona S, Beninati T, Lo N, Franceschi A. A symbiont of the tick Ixodes ricinus invades and consumes mitochondria in a mode similar to that of the parasitic bacterium Bdellovibrio bacteriovorus. Tissue Cell. 2004; 36: 43–53 PMID: 14729462
10. Mariconti M, Epis S, Gaibani P, Dalla Valle C, Sassera D, Tomao P, et al. Humans parasitized by the hard tick Ixodes ricinus are seropositive to Midichloria mitochondrii: is Midichloria a novel pathogen, or just a marker of tick bite? Pathog Glob Health. 2012; 106: 391–396. doi: 10.1179/2047773212Y.0000000060 PMID: 23265610
11. Sazzoachi C, Mariconti M, Sassera D, Rinaldi L, Martin E, Cringoli G, et al. Molecular and serological evidence for the circulation of the tick symbiont Midichloria (Rickettsiales: Midichloriaceae) in different mammalian species. Parasit Vectors. 2013; 12: 350
12. Vu Hai V, Pagès F, Boulanger N, Audebert S, Parola P, Almeras L. Immunoproteomic identification of antigenic salivary biomarkers detected by Ixodes ricinus-exposed rabbit sera. Ticks Tick Borne Dis. 2013; 4: 459–468. doi: 10.1016/j.ttbdis.2013.06.001 PMID: 23890749
13. Schwarz A, Tenzer S, Hackenberg M, Erhart J, Gerhold-Ay A, Mazur J, et al. A systems-level analysis reveals a transcriptomic and proteomic complexity in Ixodes ricinus midgut and salivary glands during early attachment and feeding. Mol Cell Proteomics. 2014; 13: 2725–2735. doi: 10.1074/mcp.M114.038299 PMID: 25048707
14. Michelet L, Delannoy S, Devillers E, Umhang G, Aspan A, et al. High-throughput screening of tick-borne pathogens in Europe. Front Cell Infect Microbiol. 2014; 29: 4–103. doi: 10.3389/fcimb.2014.00103
15. Pistone D, Pajoro M, Fabbi M, Vicari N, Marone P, Genchi C, et al. Lyme borreliosis, Po River Valley, Italy. Emerg Infect Dis. 2010; 16: 1289–1291 doi: 10.3201/eid1608.100152 PMID: 20678327
16. Pesquera C, Portillo A, Palomar AM, Oteo JA. Investigation of tick-borne bacteria (Rickettsia spp., Anaplasma spp., Ehrlichia spp. and Borrelia spp.) in ticks collected from Andean tapirs, cattle and vegetation from a protected area in Ecuador. Parasit Vectors. 2015; 24: 46
17. Smith PK, Krohn RI, Hermanson GT, Mallia AK, Gartner FH, Provenzano MD, et al. Measurement of protein using bicinchoninic acid. Anal Biochem. 1985; 150: 76–85 PMID: 3843705
18. Candiano G, Bruschi M, Musante L, Santucci L, Ghiggeri GM, Carnemolla B, et al. Blue silver: a very sensitive colloidal Coomassie G-250 staining for proteome analysis. Electrophoresis. 2004; 25: 1327–1333 PMID: 15174055
19. Giuliano S, Agnetis AM, De Palma A, Viglio S, Mauri P, Fumagalli M, et al. Proteomic analysis of lymphoblastoid cells from Nasu-Hakola patients: a step forward in our understanding of this neurodegenerative disorder. PLOS ONE. 2014; 9: e100079. doi: 10.1371/journal.pone.0100079 PMID: 25470636
20. Coté V, Sabatier L, Schmelt G, Garmi-Leroy A, Rousselle JC, Arsène-Ploetze F, et al. Differential expression of Ixodes ricinus salivary gland proteins in the presence of the Borrelia burgdorferi sensu lato complex. J Proteomics. 2014; 16: 29–43.

21. Mayer MP, Bukau B. Hsp70 chaperones: cellular functions and molecular mechanism Cell Mol Life Sci. 2005; pp. 670–684 PMID: 15770419

22. Rinehart JP, Li A, Yocum GD, Robich RM, Hayward SA, Denlinger DL. Up-regulation of heat shock proteins is essential for cold survival during insect diapause Proc Natl Acad Sci U S A. 2007; 104: 11130–11137 PMID: 17592124

23. Busby AT, Ayllón N, Kocan KM, Blouin EF, de la Fuente G, Galindo RC, et al. Expression of heat shock proteins and subolesin affects stress responses, Anaplasma phagocytophilum infection and questing behaviour in the tick, Ixodes scapularis. Med Vet Entomol. 2012; 26: 92–102 doi: 10.1111/j.1365-2915.2011.00973.x PMID: 21781141

24. Somershine DE, Hynes WL. Molecular characterization and related aspects of the innate immune response in ticks. Front Biosci. 2008; 13: 7046–7063 PMID: 18508715

25. Narasimhan S1, Montgomery RR, DePonte K, Tschudi C, Marcantonio N, Anderson JF, et al. Disruption of Ixodes scapularis anticoagulation by using RNA interference. Proc Natl Acad Sci U S A. 2004; 101: 1141–1146 PMID: 14745044

26. Cameron LA, Giardini PA, Soo FS, Theriot JA. Secrets of actin-based motility revealed by a bacterial pathogen. Nat Rev Mol Cell Biol. 2000; 1: 110–119 PMID: 11253363

27. Goulin E, Welch MD, Cossart P. Actin-based motility of intracellular pathogens. Curr Opin Microbiol. 2005; 8: 35–45.29. PMID: 15694855

28. Stevens JM, Galyov EE, Stevens MP. Actin-dependent movement of bacterial pathogens. Nat Rev Microbiol. 2006; 4: 91–101 PMID: 16415908

29. Horigane M, Ogihara K, Nakajima Y, Honda H, Taylor D. Identification and expression analysis of an actin gene from the soft tick, Ornithodoros moubata (Acari: Argasidae). Arch Insect Biochem Physiol. 2007; 64: 186–199. PMID: 17366597

30. Schwan TG. Ticks and Borrelia: model systems for investigating pathogen-arthropod interactions. Infect Agents Dis. 1996; 5: 167–181 PMID: 8903079

31. Dumler JS, Choi KS, Garcia-Garcia JC, Barat NS, Scorpio DG, Garyu JW, et al. Human granulocytic anaplasmosis and Anaplasma phagocytophilum. Emerg Infect Dis. 2005; 11: 1828–1834 PMID: 16485466

32. Bhavsar AP, Guttman JA, Finlay BB. Manipulation of host-cell pathways by bacterial pathogens. Nature. 2007; 449: 827–834 PMID: 17943119

33. Pancholi V. Multifunctional alpha-enolase: its role in diseases. Cell Mol Life Sci. 2001; 58: 902–920 PMID: 11497239

34. Maritz-Olivier C, Stutzer C, Jongejan F, Neitz AW, Gaspar AR. Tick anti-hemostatics: targets for future vaccines and therapeutics Trends Parasitol. 2007; 23: 397–407 PMID: 17656153

35. Moraes J, Galina A, Alvarenga P, Rezende G, Masuda A, Vaz IS Jr, Logullo C. Glucose metabolism during embryogenesis of the hard tick Boophilus microplus. Comp Biochem Physiol A Mol Integr Physiol. 2007; 146: 528–533 PMID: 16949322

36. da Silva RM, Nunes BD, Walhero CF, Costa EP, de Abreu LA, Githaka NW, et al. Non-classical gluconeogenesis-dependent glucose metabolism in Rhipicephalus microplus embryonic cell line BME26. Int J Mol Sci. 2015; 14: 1821–39.

37. Liao M, Boldbaatar D, Qiong H, Huang P, Umemiya R, Hammol T, et al. Functional analysis of protein disulfide isomerases in blood feeding, viability and oocyte development in Haemaphysalis longicornis ticks. Insect Biochem Mol Biol. 2008; 38: 285–95. doi: 10.1016/j.ibmb.2007.11.006 PMID: 18252243

38. Radulović ŽM, Kim TK, Porter LM, Sze SH, Lewis L, Mulenga A. A 24–48 h fed Amblyomma americanum tick saliva immuno-proteome. BMC Genomics. 2014; 15:518. doi: 10.1186/1471-2164-15-518 PMID: 24962223